DESIGN OF MICROWAVE BANDPASS FILTERS USING HALF WAVE DIGITAL TEM LINES

A Thesis submitted to the Department of Electrical and Electronic Engineering, Bangladesh University of Engineering and Technology, Dhaka, in partial fulfilment of the requirements for the degree of Master of Science in Engineering (Electrical and Electronic).

MAINUL HASAN

August 1993

DECLARATION

I hereby declare that this work has not been submitted elsewhere for the award of any degree or diploma or for publication.

MAHasan
7/8/93

Mainul Hasan

The Thesis " **DESIGN OF MICROWAVE BANDPASS FILTERS USING HALF WAVE DIGITAL TEM LINES** " submitted by Mainul Hasan, Roll No. 891310P, session 1987-'88 to the Department of Electrical and Electronic Engineering, Bangladesh University of Engineering and Technology, Dhaka, has been accepted as satisfactory in partial fulfilment of the requirements for the degree of Master of Science in Engineering (Electrical and Electronic).

Board of Examiners

1. Dr. Saiful Islam
   Professor and Head — *Supervisor* — Saiful Islam 7/8/93
   EEE Department
   BUET, Dhaka 1000, Bangladesh.

2. Dr. Saiful Islam
   Professor and Head — *Member(Ex-officio)* — Saiful Islam 7/8/93
   EEE Department
   BUET, Dhaka 1000, Bangladesh.

3. Dr. A. B. M. Siddique Hossain
   Professor — *Member* — A B M Siddique Hossain 7/8/93
   EEE Department
   BUET, Dhaka 1000, Bangladesh.

4. Dr. Shamsuddin Ahmed
   Head — *Member(External)* — Ahmed 7/8/93
   EEE Department
   ICTVTR, Gazipur

ACKNOWLEDGEMENT

The author takes the opportunity to express his profound gratitude and indebtedness to Professor Dr. Saiful Islam, Head of the Department of Electrical and Electronic Engineering, BUET for his ceaseless cooperation and meticulous guidance in completing this work. The author thanks him for his expert opinion in designing and fabricating the filter. The author also feels proud to acknowledge him for his important suggestion in improving the performance of the filter.

Thanks are due to Mr. Mollah Ahmed Ali and Mr. Selim Kaiser of Machine Shop and Mr. Zulfiqar Ali Bhuiyan of Welding Shop for their active help and assistance in fabricating the experimental filter.

The author wishes to thank Dr. Mohammad Ali Choudhury, Mr. Md. Sayeed Akmal and Mr. Mohsin Mollah for their support and cooperation. Also thanks are given to friends and colleagues who helped the author completing this work. Finally, the author likes to thank his wife and other family members for their constant inspiration.

CONTENTS

ABSTRACT

A design method is developed for designing a band-pass elliptic function filter using resonators made up of TEM transmission line segments. Each resonating segment of transmission line is of half-wave length long at the center frequency of the band-pass filter. Each of these resonating segment is short circuited at both ends and is stepped in impedance at an electrical distance of $\pi/3$ from one end of the resonator so that the other fraction of length is $(\pi-\pi/3)$. The resonators are coupled along the sides with an arrangement to achieve nearest neighbor interaction only.

This design method starts with a lumped low-pass prototype. A lumped low-pass to distributed band-pass transformation is used to transform to a physically realizable band-pass structure. For physical realization the obtained distributed band-pass filter is modified so that it can be realized with stepped impedance half-wave transmission lines short circuited at both ends. For this purpose, equivalence is established between a segment of resonators of the distributed band-pass filter circuit and a segment of both end short circuited transmission line considering the point of stepping

as the input port. Ultimately the band pass filter has been realized in the form coupled stepped impedance lines. Two transformer elements are needed for coupling at the input and output ports of the filter. The transformer coupling allows to change the impedance levels of the short circuited stepped impedance coupled lines in the middle portion of the filter.

An elliptic function filter has been chosen because it has got an upper hand over the other filter responses namely butterworth and chebychev filter responses. Butterworth response gives maximally flat pass-band, very wide bandwidth and stop-band to pass-band transition is not steep, which makes it unsuitable for narrow-band band-pass filter design. Again chebychev response has steeper transition from stop-band to pass-band but still not suitable for some practical applications. Considering theses points, an elliptic function filter may be designed for narrower bandwidth. It has steeper transition from stop-band to pass-band and the difference between maximum pass-band attenuation and minimum stop-band attenuation is larger compared to other two filter responses.

Based on the developed analytic design method a computer program in FORTRAN has been prepared for designing this type of filters. With the help of this program a five resonator 1% bandwidth elliptic function filter has been designed for 2.0 GHz center frequency. From the line parameters thus obtained, the physical dimensions of the filter are next computed with the help of previously published graphs and analytical expressions. Using these values an experimental filter has been fabricated and measured in the laboratory. The designed parameters and the measured results are presented.

LIST OF PRINCIPAL SYMBOLS

ω	Radian frequency variable for band-pass filter
ω'	Radian frequency variable for low-pass prototype filter
w	Fractional bandwidth
ω_0	Midband radian frequency
γ_t	Propagation constant per unit length
α	Image attenuation constant
β	Image phase constant
P_i	Incident power
P_{LR}	Power loss ratio
ρ	Reflection coefficient
Γ	Input reflection coefficient for lossless network
Γ^*	Conjugate of Γ
L	Insertion loss in dB
M,N	Real and non-negative polynomials
A,B,C,D	Transmission line constants
T_n	Voltage transformation ratio
Y_0	Characteristic admittance
Z_{I1},Z_{I2}	Image impedances
θ_0	Arbitrary stepped impedance plane
Ω_r	Resonant angular velocity
ϵ	Absolute dielectric constant

ϵ_r	Relative dielectric constant
η_0	Intrinsic impedance of free space
w_k	Width of the kth bar
$s_{k,k+1}$	Spacing between kth and (k+1)th lines
t	Thickness of the rectangular bar
b	Ground plate spacing
C_{fe}	Fringing capacitance
C_k	Self capacitance
$C_{k,k+1}$	Mutual capacitance between kth and (k+1)th lines

CHAPTER 1

Introduction

1.1 **Historical Background** : From the beginning of microwave engineering until today, filter design has been a persistent and fruitful field of investigation. According to *Cohn* [1] there are two very good reasons for the continuing attraction of microwave filters. The first is the ever increasing importance of filters to microwave systems, as these systems become more complex and as the spectrum becomes more densely filled with signals. The second reason is a singular appeal of microwave filters for creative study. This appeal results from the amenability of filter circuits to theoretical analysis, the unlimited variety of circuits and structures, and the close experimental agreements that can usually be achieved.

Advances in filter design fortunately are keeping pace with the growing needs. In early days of microwave work, filters were designed by means of hit-or-miss image parameter theory and by analogy to single- and double-tuned IF transformers. Rapid progress led to more sophisticated design yielding maximally flat and equal ripple responses. In most practical cases today filters are designed as

distributed constant approximations to rigorous prototype circuits. Developing formulas, simple to use yet yielding highly accurate approximations has proved to be a fascinating occupation for many engineers leading to a wealth of design information in technical literature.

An exact method of designing microwave filters was based on *Richards'* [2] transformation, which was only for microwave circuits with commensurable line lengths. His [2] transformation mapped the real-frequency axis of the lumped constant prototype onto finite portions of the real-frequency axis of the transmission line circuit and then the response pattern was repeated periodically. Physically the this repetition corresponded to repeated increments of one half wave length in the electrical line lengths of the transmission line circuit as the frequency increased. A remarkably accurate formula for the midband dissipation loss of band-pass filters was given by *Cohn* [3] for well matched filters that are designed from a low-pass prototype. Filters using circular rods were constructed by *Cristal* [4]. Each resonator was one quarter wave length long at band center when the ends of the rods were open circuited. As in the parallel coupled filter, the resonator spacings were not very critical. In addition the resonators commended itself for many applications by its compact form.

A number of structures were analyzed by *Bolljahn* and *Matthaei* [5] which consist of arrays of parallel conductors between ground planes or above a single ground plane. These included interdigital line, meander line, a form of helix, "hairpin line", and reactively loaded combline. They [5] also derived the equations for determining the phase function per section of line in terms of voltage coupling factors K_{1n} which were obtained from the static capacitances per unit length of the conductors. Their results indicated that certain of the structures had special merit for use as filters. They concluded with the construction of an interdigital-line filter using ten conductors which was found to have excellent band pass characteristics and a band width which was in very good agreement with the theory. Interdigital filters are attractive in that they are compact, easily fabricated, free of spurious responses at twice the pass band frequency f_0 (second pass band is at $3f_0$). The interdigital line filter was first built by *Bolljahn* and *Matthaei* [5]. *Matthaei* [6] gave design equations for interdigital filters of prescribed bandwidth and number of cavities N. The low-pass prototype elements were found from tables. He [6] used *Getsinger's* [7] charts of capacitance for coupled rectangular bars between parallel plates for

determination of the widths and spacings of the stripline resonators. Another very compact structure was the combline filter developed also by *Matthaei* [8] which was similar in many ways to the capacitively loaded interdigital-line filter. In this combline filter he [8] placed all the capacitances on the same side. They were necessary to the functioning of the filter, since there was no coupling between quarter wave digital resonators when they were all grounded on one side and all open circuited on the other. The rods were typically one-eighth of a wave length long at midband.

An exact theory of interdigital-line networks and related coupled structures were presented by *Wenzel* [9]. He briefly reviewed the theory of parallel coupled line arrays and the derivation of exact equivalent circuits from the impedance matrix. *Wenzel* [9] introduced a simplified theory of equivalent coupled structures in order to avoid the lengthy analysis required when using the impedance matrix approach. Equivalent networks for the interdigital line were obtained by inspection, using a transformed capacitance matrix associated with the two-dimensional geometry of the conductors and the ground planes. The technique presented by *Wenzel* [9] were simple to apply and allow a given transmission response to be obtained in a variety of line

configurations. He also gave a practical design example and experimental results to illustrate the simplicity of the approach, along with general criteria for the design of practical filter networks with optimum transmission characteristics. His [9] technique can be used to analyze and design a much broader class of microwave networks.

Wenzel [10] described TEM propagation on an array of parallel conductors in terms of the normalized static capacitance matrix. Important properties of capacitance matrices were discussed and a physical and network interpretation was given to a useful linear transformation of the static capacitance matrix. *Wenzel* [10] also used the results of *Getsinger* [7] to obtain the physical dimensions from the matrix of static capacitance.

A design procedure for a practical digital elliptic function filter capable of providing either band pass or band stop characteristics was presented by *Horton* and *Wenzel* [11]. They gave examples to illustrate typical design procedure for both types of filters. *Levy* and *Whiteley* [12] devised a synthesis procedure for distributed elliptic function filters utilizing published tables of lumped constant elliptic function filters. It was dependent upon the application of a new generalized transformation for distributed networks.

A design procedure for narrow-band band pass TEM-line elliptic function filters was presented by *Rhodes* [13]. He proposed the realization in the form of a stepped-impedance digital n-wire line which was one half of a wave length long at midband and short circuited to ground at both ends, where the digital line was stepped in impedance along any arbitrary prescribed plane in the filter. *Rhodes* [13] presented a detailed design procedure for the construction of the two characteristic admittance matrices which described the digital n-wire line from the low pass prototype element values. He also showed that the normalized impedance values of the elements in the filter were all of the order of unity and independent of the actual bandwidth of the filter except for the input and the output transformer elements. *Rhodes* [13] gave a numerical example and experimental results on a seventh degree 1% bandwidth filter with a center frequency of 3.7 GHz. This demonstrated the significant improvements which might be obtained from the half wave stepped digital elliptic filter over most other known form of microwave TEM-line narrow-band band-pass filters, especially for percentage bandwidth of 5% and below. The compactness and inherent physical rigidity also made the filter attractive for applications where size, weight and stability under mechanical vibrations were

important. The only factor which did not compare favorably to conventional forms was that of harmonic rejection. However, the use of a quasi-low-pass filter at the end blocks of the filter through single interdigital sections would attenuate the harmonics without increasing the external size or affecting the other advantages of the filter.

1.2 **Objective of this work**: The objective of this work is to develop a design method for designing narrow-band band-pass elliptic function filter using coupled TEM transmission-lines so that the filter is compact in size. One of the targets of this development is to achieve a design method which is easy to use. The other objectives are to develop a computer program so that one can readily get the normalized capacitance values from the low-pass prototype element values. The last objective is to verify the design method by fabricating a designed band-pass filter and performing necessary measurements.

1.3 **Brief introduction to this thesis**: Some well known methods of filter design are described in chapter 2.

In chapter 3, the method of obtaining band-pass characteristic from low-pass prototype filter specifications has been discussed. The determination of characteristic admittance matrices of two subnetworks has been given in

chapter 4 with elaboration of each step.

Chapter 5 consists of some important information regarding different types of parallel coupled TEM lines between ground planes. Various configurations like coupling with thick rectangular bars, unsymmetrical parallel coupled lines, arrays of parallel coupled lines, etc. have been discussed individually in this chapter.

Chapter six deals with the design procedure of the experimental filter and realization of its physical dimensions using the *Getsinger's* [7] curves and *Saal's* [16] catalogue. In chapter 7 experimental results of the filter response and characteristic curves have been given in detail. The experimental set up with the network analyzer and the discrete frequency generator are also given in this chapter.

In chapter 8, a discussion on the filter characteristics and its future development have been given. Computer program to obtain the static capacitance matrices and some measured values are presented in apppendices.

CHAPTER 2

Some well-known methods of filter design

2.1 Introduction: Most of the low pass, high pass, band pass and band stop filters derive important transmission charaoteristics from those of a low pass prototype filter used in their design. Element values for such low pass prototype filters were originally obtained by network synthesis methods. However, afterwards, concise equations were developed which were convenient for computer programming and were used for the element values of the types of prototype filters of interest. At low frequencies the filters are designed from ideal lumped inductors and capacitors. They have very simple frequency characteristics and also very accurate and complete design procedure has been developed for designing filters using them. Therefore at low frequencies it is possible to design filters directly with a wide variety of prescribed frequency characteristics. But at microwave frequency filter design becomes much more complicated and difficult and at that range of frequencies lumped elements are replaced by distributed parameter elements. In fact no complete

theory or design procedure exists for microwave filter. Microwave filters are realized by replacing all inductors and capacitors by suitable microwave circuit elements that have similar frequency characteristics over the frequency range of interest. In the present chapter two different methods of filter design have been discussed.

2.2 **Different methods of filter design**: There are two filter design techniques at low frequency namely (a) Image parameter method and (b) Insertion loss method. The image impedance and attenuation function of a filter section are defined in terms of an infinite chain of identical filter sections connected together. Using a finite, dissipationless filter network with resistor terminations will permit the image impedances to be matched only at discrete frequencies, and the reflection effects can cause sizeable attenuation in the pass band, as well as distortion of the stop band edges. Proper designing of end sections will reduce these reflection effects. Although such methods will definitely reduce the size of reflections in filters designed by the image method, they give no assurance as to how large the peak reflection loss values may be in the pass band. Thus, though the image method is conceptually simple, it requires

a good deal of cut-and-try or know-how if a precision design with low pass band reflection loss and very accurately defined band edges is required. While the insertion loss method begins with a complete specifications of a physically realizable frequency characteristics, and from this a suitable filter network is designed. That is why the insertion loss method is more preferable than the image parameter method.

2.2.1 **Comparison of image method and network synthesis method**: Network synthesis method of filter design generally starts out by specifying a transfer function, such as the transmission coefficient t as given by,

$$t=2\sqrt{\frac{R_1}{R_2}}\cdot\frac{E_2}{E_g} \qquad (2.1)$$

where R_1 and R_2 are the input and output terminations, and E_g and E_2 are the generator and load voltages respectively of a two port filter network. This transfer function is specified as a function of complex frequency p. From the transfer function the input impedance to the circuit is found as a function of p. Then by various continued-function or partial-fraction expansion procedures, the input impedance is expanded to give the element values of the circuit. The circuit obtained by these procedures

has the same transfer function that was specified at the outset, and all guess work and cut-and-try is eliminated. But image concepts never enter such procedures, and the effects of the terminations are included in the initial specifications of the transfer function. In general, a low pass filter designed by the image method and an analogous filter designed for the same application by the network synthesis method will be quite similar. However, the filter designed by network synthesis method will have somewhat different element values, to give it the specified response.

2.3 Definition of image impedance and image propagation function:

The image viewpoint for the analysis of circuits is a wave viewpoint much the same as the wave viewpoint commonly used for analysis of transmission lines. In fact, for the case of a uniform transmission line the characteristic impedance of the line is also its image impedance, and if γ_t is the propagation constant per unit length then $\gamma_t l$ is the image propagation function for a line of length l. However, the terms image impedance and image propagation function have much more general meaning than their definition with regard to a uniform transmission line alone would suggest.

Let us consider the case of a two port network which can be symmetrical, but for the sake of generality we assume that the network is unsymmetrical with different impedance characteristics at end 1 and end 2. Figure (2.1) shows the case of an infinite number of identical networks of this sort, all connected so that at each junction either end 1s are connected together or end 2s are connected together. Since the chain of network extends to infinity in each direction, the same impedance Z_{I1} is seen looking both left and right at a junction of the two end 1s, while at a junction of two end 2s another impedance Z_{I2} will be seen when looking either left or right. The impedances Z_{I1} and Z_{I2} as shown in figure (2.1) are the image impedances for end 1 and end 2, respectively of the network. For an unsymmetrical network they are generally unequal.

The way the infinite chain of network in figure (2.1) is connected, the impedances seen looking left and right at each junction are always equal, hence there is never any reflection of a wave passing through a junction. Thus from the wave point of view, the networks in figure (2.1) are all perfectly matched. If a wave is set to propagating towards the right, through the chain of networks, it will be attenuated as determined by the

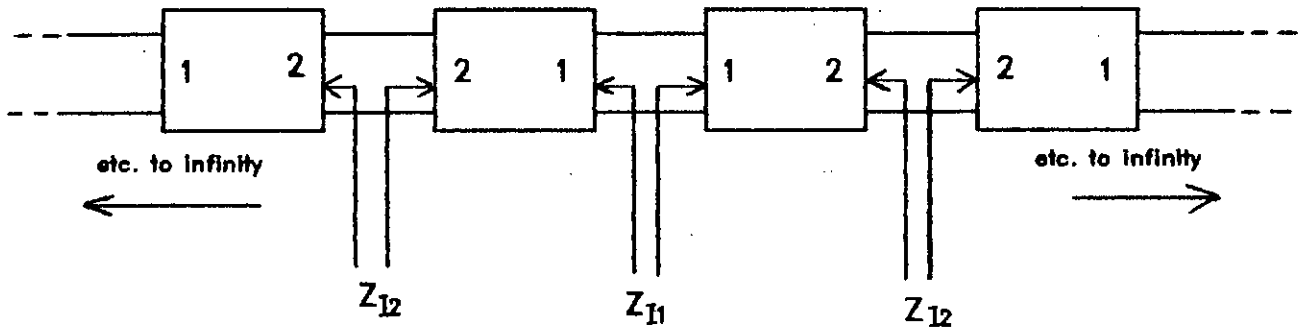

Fig 2.1 Infinite chain of identical networks used for defining image impedances and the image propagation function

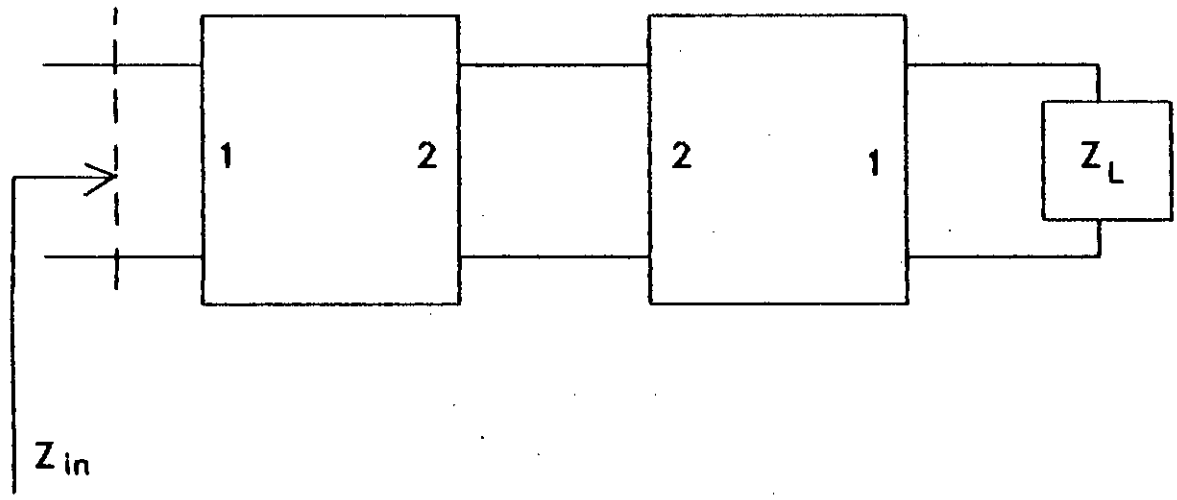

Fig 2.2 A cascade arrangement of two networks

propagation function of each network, but will pass on from network to network without reflection. Here the image impedances Z_{I1} and Z_{I2} are actually the impedance of infinite networks, and as such they should be expected to have a mathematical form different from that of the rational impedance functions that are obtained for finite, lumped element networks. In the cases of lumped element filter structures, the image impedances are usually irrational functions and in the cases of microwave filter structures which involve transmission line elements, the image impedances are usually both irrational and transcendental.

2.4 **Image parameter method**: An equation for the image impedance is easily derived in terms of the circuit in figure (2.2) If Z_L is made to be equal to Z_{I1} then the impedance Z_{in} seen looking in from the left of the circuit will also be equal to Z_{I1}. Now if A, B, C, and D are the general circuit parameters for the box on the left in figure (2.2) assuming that the network is reciprocal, the general circuit parameters A_S, B_S, C_S, and D_S for the two boxes connected as shown can be computed. Therefore,

$$Z_{input} = \frac{A_S Z_L + B_S}{C_S Z_L + D_S} \qquad (2.2)$$

Now setting $Z_{in}=Z_L=Z_{I1}$ and solving for Z_{I1} in terms of A, B, C,

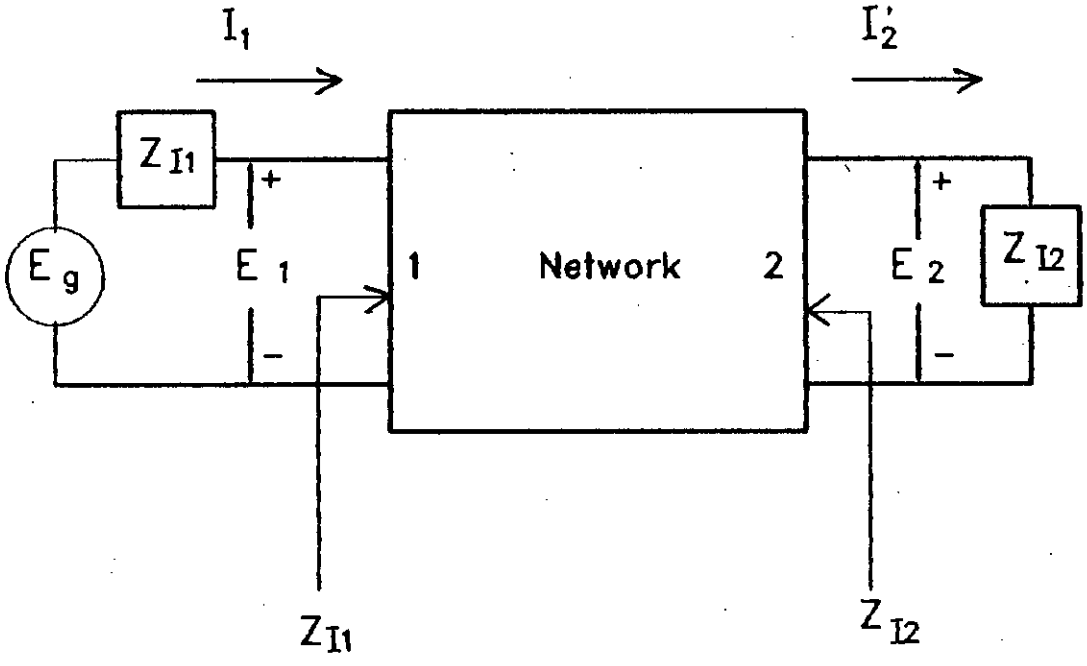

Fig 2.3 Network having terminations which are matched on the image basis

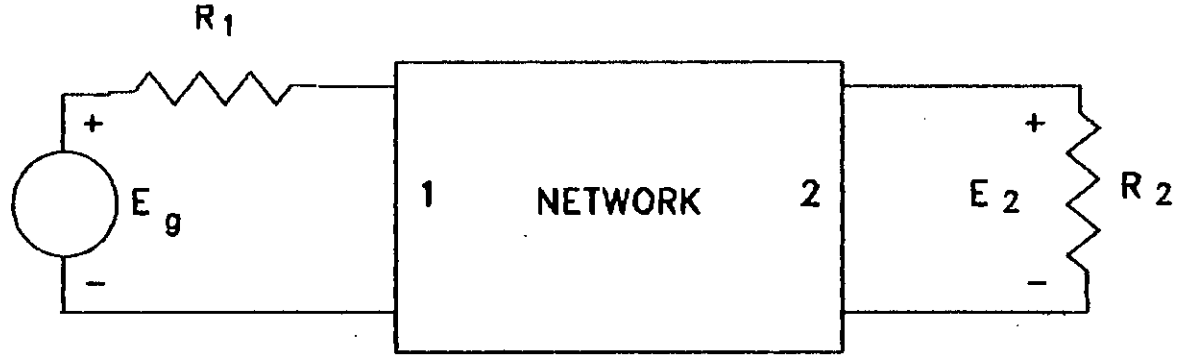

Fig 2.4 Insertion loss calculation for resistive termination

and D, we get,

$$Z_{I1}=\sqrt{\frac{AB}{CD}} \tag{2.3}$$

The same procedure carried out with respect to end 2 gives,

$$Z_{I2}=\sqrt{\frac{DB}{CA}} \tag{2.4}$$

Figure 2.3 shows a network with a generator whose internal impedance is the same as the image impedance at end 1 and with a load impedance on the right equal to the image impedance at end 2. With the terminations matched to the image impedances in this manner it can be shown that,

$$\frac{E_1}{E_2}=\sqrt{\frac{Z_{I1}}{Z_{I2}}}\cdot e^{\gamma} \tag{2.5}$$

or,

$$e^{\gamma}=\frac{E_1}{E_2}\sqrt{\frac{Z_{I2}}{Z_{I1}}} \tag{2.6}$$

The image propagation function is defined as,

$$e^{-\gamma}=\sqrt{AD}-\sqrt{BC} \tag{2.7}$$

from where it is found that,

$$e^{\gamma}=\sqrt{AD}+\sqrt{BC} \tag{2.8}$$

or,

$$\gamma=\alpha+j\beta=\ln(\sqrt{AD}+\sqrt{BC}) \qquad (2.9)$$

where α is the image attenuation in neper and β is the image phase in radian. It is to be noted that the $\sqrt{(Z_{I2}/Z_{I1})}$ factor in eqn. (2.6) has the effect of making γ independent of the relative impedance levels at ends 1 and 2. Eqn. (2.6) can also be written as,

$$\gamma=\alpha j\beta=\ln\sqrt{\frac{E_1 I_1}{E_2 I_2'}} \qquad (2.10)$$

where, $I_1=E_1/Z_{I1}$ and $I_2'=E_2/Z_{I2}$

From eqn. (2.8) it is seen that, $\text{Cosh}\gamma=\sqrt{AD}$ and $\text{Sinh}\gamma=\sqrt{BC}$.

The factor D/A is interpreted as an impedance transformation ratio and may be viewed as an ideal transformer of turns ratio $\sqrt{(D/A)}$.

If the network is lossless, A and D are real and B and C are imaginary for frequencies $j\omega$. In the pass band $\alpha=0$, therefore γ is purely imaginary and equal to $j\beta$ and this occurs for $|AD|<1$. So the phase angle constant β becomes $\text{Cos}^{-1}\sqrt{|AD|}$ or $\text{Sin}^{-1}\sqrt{|BC|}$. Because in the pass band B and C must be of the same sign, so that, $BC=j|B|j|C|=-|BC|$ which will make the second part of eqn. (2.8) imaginary. Thus the solution for Z_{I1} and Z_{I2} will be real and positive since AD must be positive to give a real solution for $\text{Cosh}\gamma$ or $\text{Cos}\beta$. Hence the image impedances are real in a pass

band.

Let N two-port networks are connected in cascade and they have propagation constants γ_n, where n=1,2,3,.....,N and voltage transformation ratios T_n, where n=1,2,3,.....,N. If the output section is terminated in image impedance, the overall voltage transfer ratio will be given by,

$$\frac{V_N}{V_1}=\prod T_n e^{-\gamma_n}, n=1,2,3...N \qquad (2.11)$$

with the assumption that the output image impedance of any section is equal to the input image impedance of the following section. If al the sections in the cascade are properly matched then maximum power will be transferred. Let the generator at the input has an internal impedance of Z_{I1} and Z_{IN} be the image impedance of the Nth section. Therefore an overall impedance ratio change will be given by,

$$\frac{(Z_1)_N}{Z_1}=\prod T_n^2, n=1,2,3....N \qquad (2.12)$$

In the image parameter method of filter design the two port parameters A, B, C, D are chose to provide the required pass bands and stop bands. The image parameters are chosen equal to the terminating impedances at the center of the pass band. The

major disadvantage of this method is the frequency dependency of the image impedances. that is why the impedances do not remain constant and equal to the terminating impedances over the entire pass band. This mismatch results in some loss in the pass band. Moreover this amount of transmission loss can neither be predicted nor can be determined before designing the filter. Also there is no means to control the rate at which the attenuation builds up with frequency beyond the edges of the pass band apart from increasing the number of filter sections.

2.5 **Insertion loss method**: The insertion loss function is defined as the ratio of power delivered directly to the load when connected across the generator without the network and power delivered to the load when the network is inserted. Mathematically the function can be expressed, with reference to figure (2.4) as,

$$\frac{P_{20}}{P_2} = \left(\frac{R_2}{R_1+R_2}\right)^2 \left|\frac{E_g}{E_2}\right|^2 \qquad (2.13)$$

where the quantity P_{20} is the power in R_2 when the network is removed and R_2 is connected directly to R_1 and E_g and P_2 is the power absorbed by R_2 when the network is in place as in figure (2.4). The insertion loss function or the power loss ratio can also

be expressed as,

$$P_{LR}=\frac{P_i}{P_t(1-\rho^2)}=\frac{1}{1-\rho^2}=\frac{1}{1-|\Gamma|^2} \qquad (2.14)$$

where ρ is the reflection coefficient and Γ is the input reflection coefficient for a lossless network terminated in a resistive load. The insertion loss in decibel is given by,

$$L=10\log P_{LR} \qquad (2.15)$$

when the terminating resistive load is equal to the internal impedance of the generator.

The insertion loss method begins by specifying the power loss ratio P_{LR} or the magnitude of the reflection coefficient $|\Gamma|=\rho$ as a function of ω. The network which gives the desired power loss ratio is taken as the design guideline. But a completely arbitrary $\Gamma(\omega)$ can not be chosen since it may not give a physically realizable network. So there are some restrictions on $\Gamma(\omega)$ for physical realizability.

For a passive network it is obvious that the reflected power can not exceed the incident power. So $|\Gamma(\omega)|\leq 1$. If the normalized input impedance is,

$$Z(\omega)=R(\omega)+jX(\omega) \qquad (2.16)$$

we get,

$$\Gamma(\omega)=\frac{Z_{input}-1}{Z_{input}+1}=\frac{R(\omega)-1+jX(\omega)}{R(\omega)+1+jX(\omega)} \qquad (2.17)$$

Since R is an even function of ω and X is an odd function of ω we get,

$$\Gamma(-\omega)=\Gamma^{*}(\omega) \qquad (2.18)$$

Thus,

$$|\Gamma(\omega)|^2=\rho^2(\omega)=\Gamma\Gamma^{*}=\Gamma(\omega)\Gamma(-\omega) \qquad (2.19)$$

From the above relation it is apparent that $\rho^2(\omega)=\rho^2(-\omega)$ is an even function of ω. Now any low frequency impedance function such as impedance of a network made of resistors, capacitors, and inductors can be expressed as the ratio of two polynomials in ω. Therefore $\rho^2(\omega)$ can be expressed as,

$$\rho^2(\omega)=\frac{M(\omega^2)}{[M(\omega^2)+N(\omega^2)]}=\frac{[(R-1)^2+X^2]}{[(R+1)^2+X^2]} \qquad (2.20)$$

where M and N are real and non negative polynomials in ω^2. Now eqn. (2.14) becomes,

$$P_{LR}=1+\frac{M(\omega^2)}{N(\omega^2)}=1+\frac{(R(\omega)-1)^2+X^2(\omega)}{4R(\omega)} \qquad (2.21)$$

In the above equation $N(\omega^2)$ must be an even polynomial of ω because it is equal to $4R(\omega)$. Now writing $N(\omega^2)=Q^2(\omega)$ and $M(\omega^2)=P(\omega^2)$, we get,

$$P_{LR}=1+\frac{P(\omega^2)}{Q^2(\omega)} \qquad (2.22)$$

The conditions specified on P_{LR} upto this point are necessary conditions in order that the network may be physically realizable. The condition that the power loss ratio be expressible in the above form is also a sufficient condition for the network to be realizable.

2.6 **Summary**: The complex frequency behavior of microwave circuits makes it difficult to develop a complete design procedure of microwave filters. Although the two methods of filter design described in this chapter are essentially for low frequency filters, still the study of these design techniques helps one to formulate design procedures for complex microwave filters. The image parameter method describes the pass-band and stop band but does not give any information about the behavior of the circuit in these regions. On the other hand the insertion loss method gives optimum specifications for aphysically realizable filter.

CHAPTER 3

The design of half wave digital TEM line band-pass elliptic function filter

3.1 **Introduction**: In this chapter the design method of half wave digital TEM line band-pass elliptic function filter has been discussed. The design method is based on two step transformation. Firstly, the band pass filter characteristics have been derived from the specifications of the low pass prototype filter. A functional relationship between the low pass cut-off frequency ω_1' and the band pass mid-band frequency ω_0 has been utilized to transform the low pass prototype to the band pass filter. But this transformation only is not sufficient for physical realization of the filter. So, as the second step, two characteristic admittance matrices will be derived and expressed in terms of low-pass element values, which describe the digital n-wire line. In this chapter, only the first step i.e. transformation from low-pass characteristics to band-pass characteristics has been discussed. The second step is covered in the next chapter.

3.2 **Method of transformation from low-pass to band-pass**: The functional relationship is given by,

$$\frac{\omega'}{\omega_1'} = F\left(W, \frac{\omega}{\omega_0}\right) \qquad (3.1)$$

where the primed frequencies refer to the low pass prototype

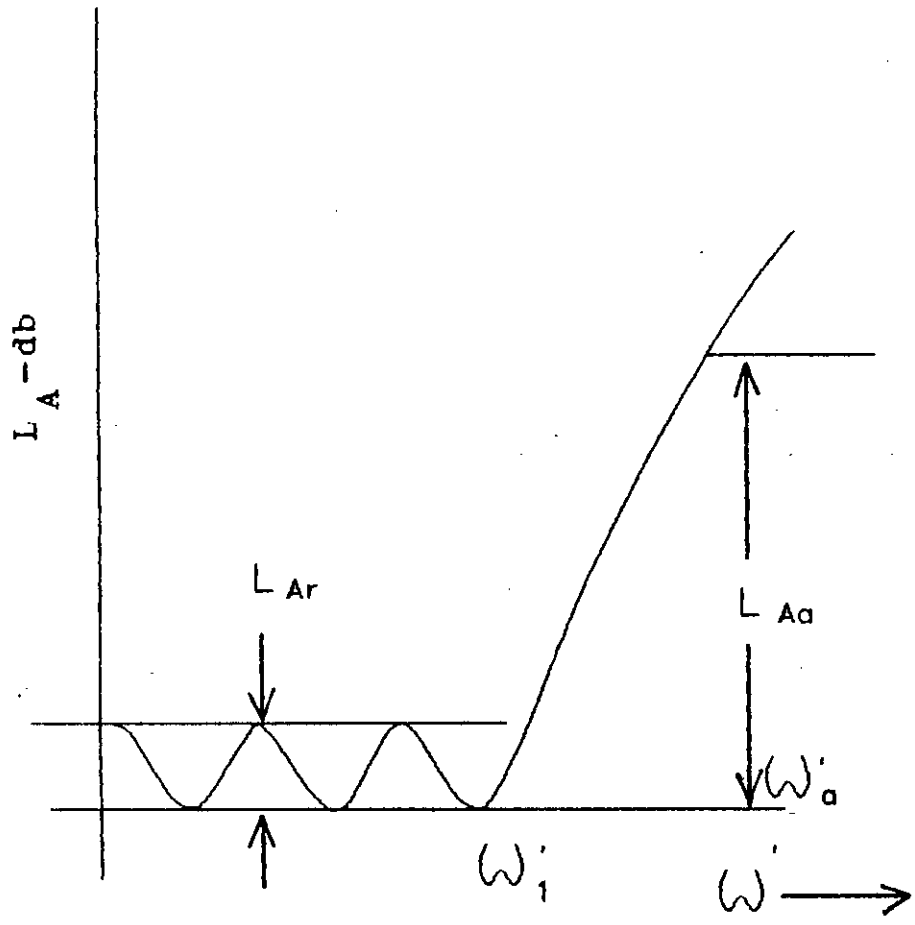

Fig 3.1 Low pass prototype response

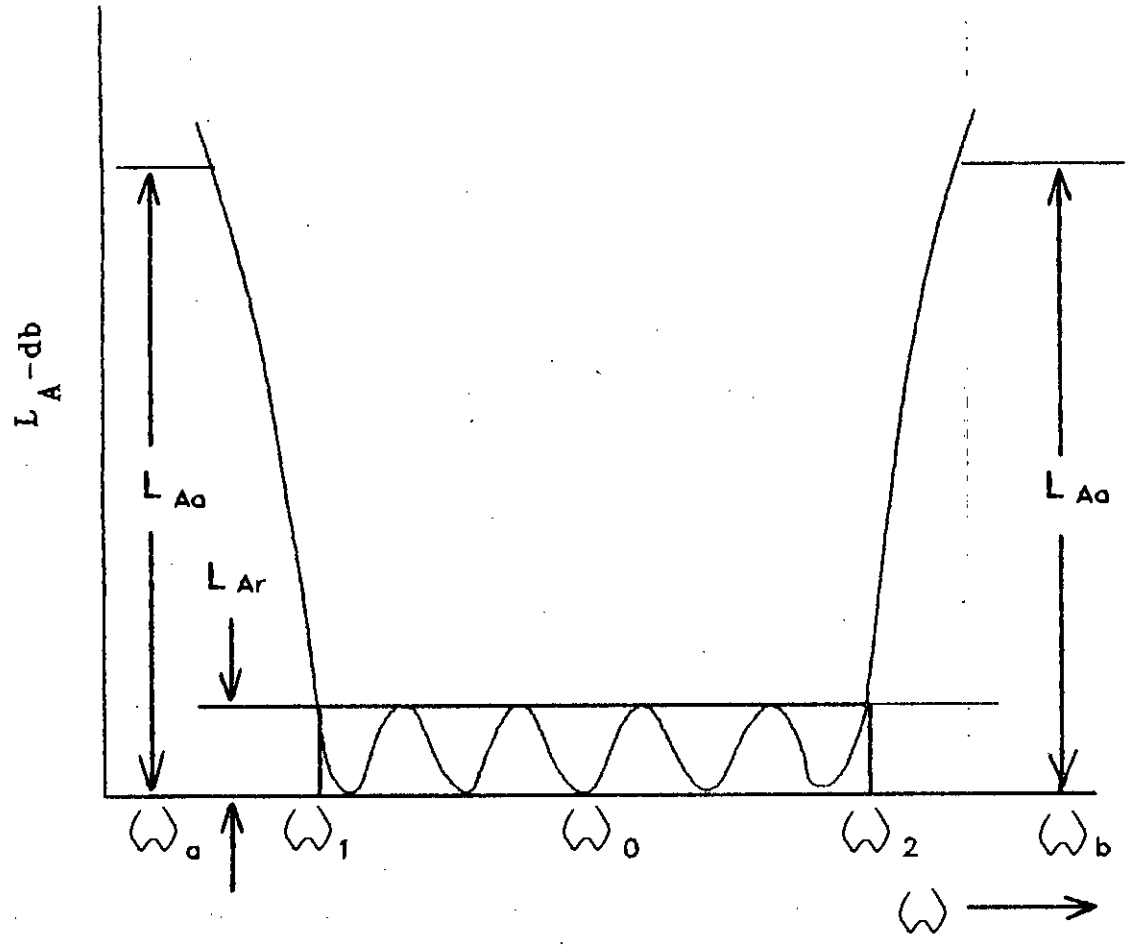

Fig 3.2 Band pass filter response

filter as shown in figure (3.1) and the unprimed frequencies refer to the band pass filter as shown in figure (3.2) ω_1' is the low pass cut-off frequency and ω_0 is the mid band frequency of the band pass filter. w is called the fractional bandwidth of the band pass filter and is denoted by,

$$w=\frac{\omega_2-\omega_1}{\omega_0} \tag{3.2}$$

where ω_1 and ω_2 are the lower cut-off and upper cut-off frequencies of the band pass filter.

For a fixed low pass cut-off frequency eqn. (3.1) can be written as,

$$\frac{\omega'}{\omega_1'}=\left(\frac{\omega_0}{\omega_2-\omega_1}\right)\left(\frac{\omega}{\omega_0}-\frac{\omega_0}{\omega}\right) \tag{3.3}$$

The above equation when solved for ω, gives,

$$\omega=\left(\frac{\omega'}{\omega_1'}\right)\left[\left(\frac{\omega_2-\omega_1}{2}\right)\pm\sqrt{\left(\frac{\omega'}{\omega_1'}\right)^2.\left(\frac{\omega_2-\omega_1}{2}\right)^2+\omega_0^2}\right. \tag{3.4}$$

Now let, $\omega_0^2=\omega_1\omega_2$

Therefore,

$$\omega=\left(\frac{\omega'}{\omega_1'}\right)\left(\frac{\omega_2-\omega_1}{2}\right)\pm\frac{1}{2}\sqrt{\left(\frac{\omega'}{\omega_1'}\right)^2(\omega_2-\omega_1)^2+4\omega_1\omega_2} \tag{3.5}$$

It is found from equation (3.5) that when $(\omega'/\omega_1')=0$, $\omega=\pm\sqrt{\omega_1\omega_2}=\pm\omega_0$ and when $(\omega'/\omega_1')=\pm1$, $\omega=\pm\omega_1,\ \pm\omega_2$.

Therefore the zero frequency of the low pass filter corresponds to a pair of frequencies namely $+\omega_0$ and $-\omega_0$. Again

$(\omega'/\omega_1')=\pm 1$ or the cut-off frequency of the low pass prototype filter corresponds to four points namely $\pm\omega_1$ and $\pm\omega_2$. So the low pass filter characteristics $(\omega'/\omega_1')=0$ and $(\omega'/\omega_1')=\pm 1$ are transformed into a band pass filter of mid-band frequency at $\pm\omega_0$ and cut-off frequencies at $\pm\omega_1$ and $\pm\omega_2$. Figure 3.2 shows only the positive portion of the band pass filter characteristics.

3.3 **Conversion of filter elements**: The series and shunt elements of the required band pass filter will be derived in terms of the series and shunt elements of the low pass prototype filter. From eqn. (3.3) we find,

$$\omega' = \left(\frac{\omega_1'}{w}\right)\left(\frac{\omega}{\omega_0} - \frac{\omega_0}{\omega}\right) \tag{3.6}$$

Now the series element of the low pass prototype filter becomes,

$$\omega' L = \left(\frac{\omega_1'}{w}\right)\left(\frac{\omega}{\omega_0} - \frac{\omega_0}{\omega}\right) L = \omega L' - \frac{1}{\omega C'} \tag{3.7}$$

where $L'=\{\omega_1'/(w\omega_0)\}L$ and $C'=w/(\omega_1'\omega_0 L)$

similarly the shunt element becomes,

$$\omega' C = \left(\frac{\omega_1'}{w}\right)\left(\frac{\omega}{\omega_0} - \frac{\omega_0}{\omega}\right) C = \omega C'' - \frac{1}{\omega L''} \tag{3.8}$$

where $C''=\{\omega_1'/(w\omega_0)\}C$ and $L''=w/(\omega_1'\omega_0 C)$

Therefore it is seen from the above two equations (3.7) and (3.8) that the series element of the low pass prototype filter has become a series combination of L and C and the shunt element has become a parallel combination of L and C in the band pass filter

when the required transformation is used. The specific function $F(w,\omega/\omega_0)$ varies with different filter structures. For two frequencies ω' and ω, which satisfy such a mapping, the attenuation is the same for both the prototype and the band pass filter. Hence the low pass prototype attenuation characteristics can be mapped into corresponding band pass attenuation characteristics by use of such mapping.

3.4 **Summary**: The low pass prototype to band pass transformation has been discussed in this chapter. The lumped low pass prototype filter circuit and its response are used to transform into corresponding band-pass filter circuit and its response. Using the mapping given for the band pass filter radian frequency variable, the attenuation characteristics of the band pass filter can be obtained from the given specifications of the low pass prototype filter since the application of the mapping suggests the same attenuation characteristics for both the prototype and the band pass filter. But this transformation is not sufficient to realize the physical dimensions of the elliptic function band-pass filter. For physical realizability, the characteristic admittance matrices are needed which is described in the next chapter.

CHAPTER 4

Obtaining characteristic admittance matrices

4.1 Introduction : A distributed resonated pi-section is derived upon application of the frequency transformation [12] to the low pass prototype elliptic function filter for n=5. The resonated pi-section is then decomposed in to two subnetworks each consisting of single short circuited transmission line and relating the low pass prototype element values and admittances are derived for both the subnetworks and thus the characteristic admittance matrices are formed.

4.2 Transformation from low pass prototype to resonated pi-section : The input impedance and admittance of a shorted transmission line as shown in figure 4.1 are given by,

$$Z_1 = jZ_0 \tan\theta \qquad (4.1)$$

$$Y_1 = -jY_0 \cot\theta \qquad (4.2)$$

Where Z_0 = Characteristic impedance

Y_0 = Characteristic admittance

$\theta = \omega l/v$

Where ω → angular velocity of propagation

v → velocity of propagation

l → length of the transmission line

Fig 4.2 shows the same for open transmission line. In this figure

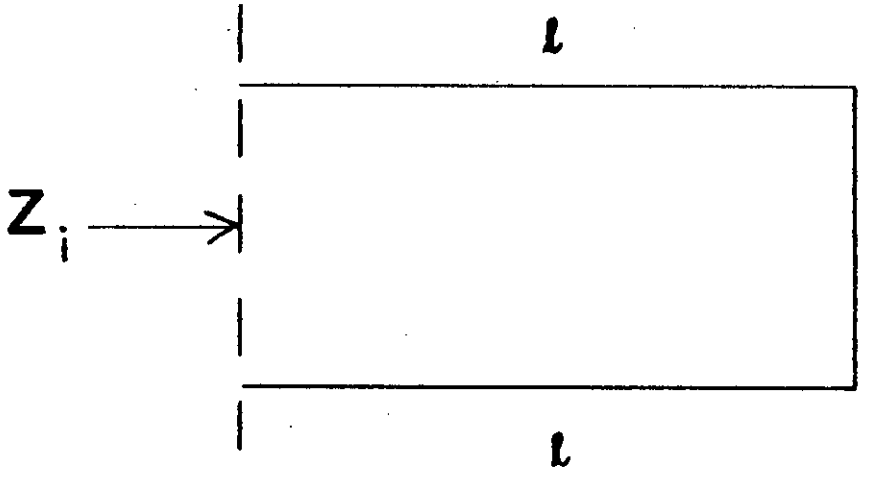

Fig 4.1 Input impedance of a short circuited transmission line

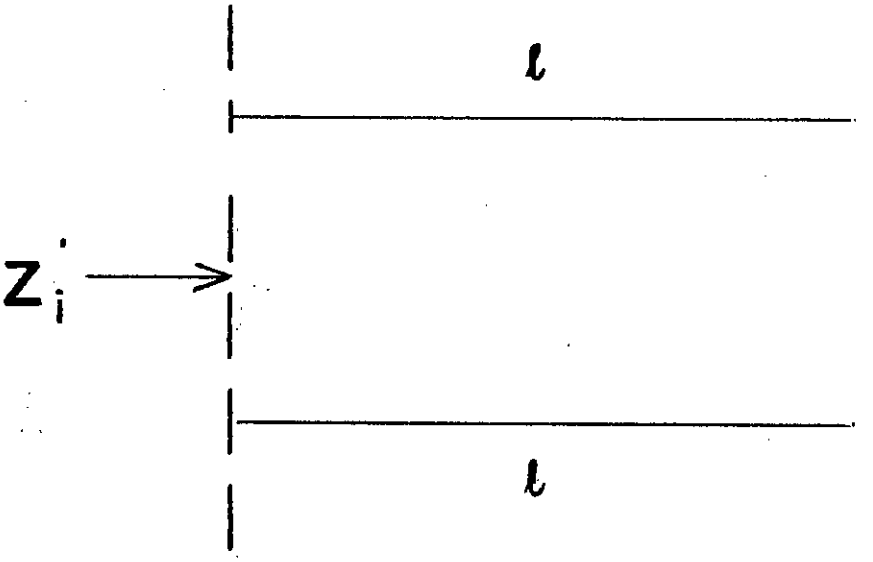

Fig 4.2 Input impedance of an open circuited transmission line

$$Z_1' = -jZ_0 \cot\theta \tag{4.3}$$

$$Y_1' = jY_0 \tan\theta \tag{4.4}$$

The low pass prototype filter for n=5 is shown in figure (4.1). A section of the low pass prototype of the band-pass filter is shown in figure (4.3) which is transformed into resonated pi-section as shown in figure (4.4) by the frequency transformation method given by *Rhodes* [13].

For the shunt element of the resonated pi-section as shown in the figure (4.5),

$$C_1' = \frac{aC_1}{\tan\theta_0}, \quad L_1' = \frac{1}{aC_1 \tan\theta_0}$$

$$Y_{L1}' = \frac{1}{j\omega L_1'} = -jaC_1\left(\frac{\tan\theta_0}{\tan\theta}\right), \quad Y_{C1}' = j\omega C_1' = jaC_1\left(\frac{\tan\theta}{\tan\theta_0}\right)$$

(Conversion from lumped to distributed element is made with the assumption $\omega \rightarrow \tan\theta$)

Similarly, for the series element of the resonated pi-section as shown in the figure (4.6),

$$L_{2+} = \frac{1}{aC_2(1+\lambda_{2+}^2)\tan\theta_0}, \quad L_{2-} = \frac{1}{aC_2(1+\lambda_{2-}^2)\tan\theta_0}$$

$$C_{2+} = \frac{aC_2(1+\lambda_{2-}^2)}{\tan\theta_0'}, \quad C_{2-} = \frac{aC_2(1+\lambda_{2+}^2)}{\tan\theta_0}$$

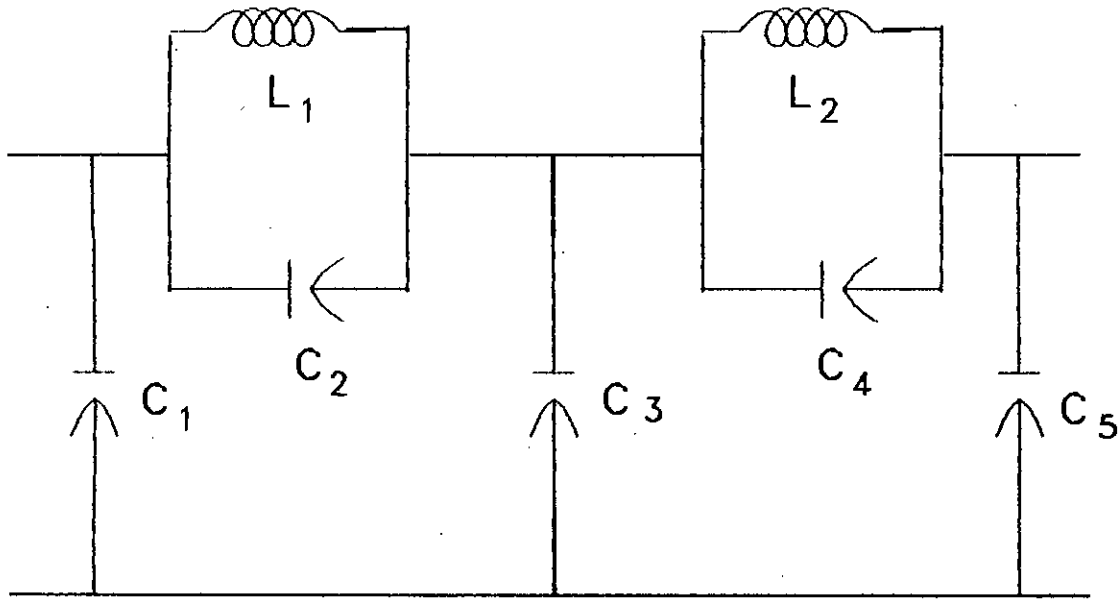

Fig 4.11 Low pass prototype filter for n=5

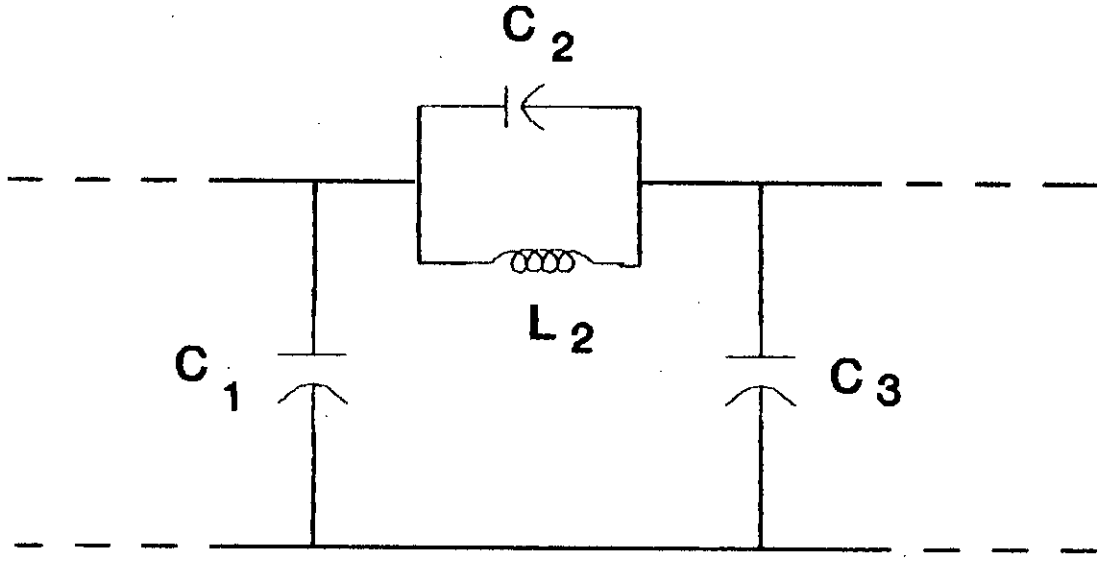

Fig 4.3 Low-pass prototype of the band-pass filter

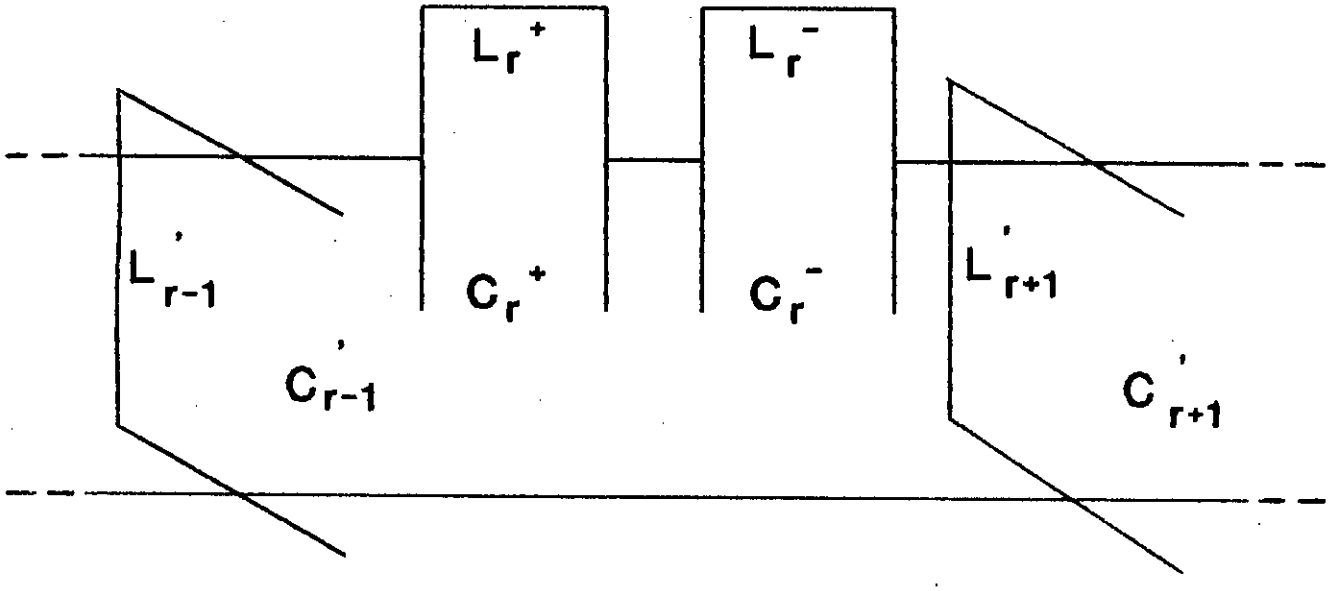

Fig 4.4 Distributed resonated pi-section of the low-pass prototype

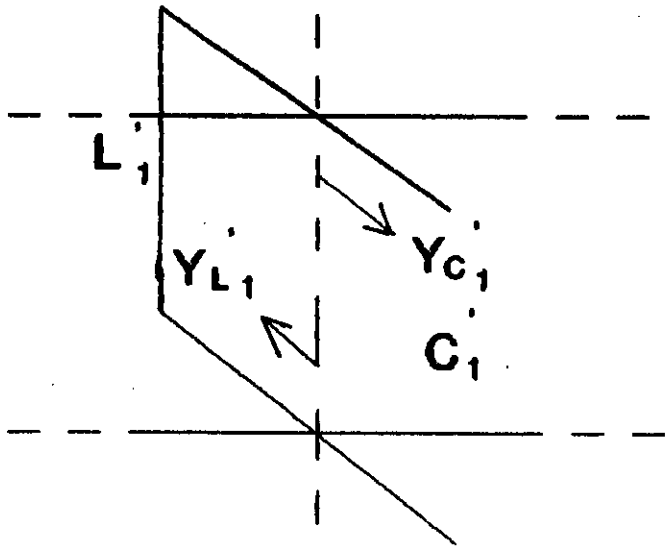

Fig 4.5 Shunt element of the resonated pi–section

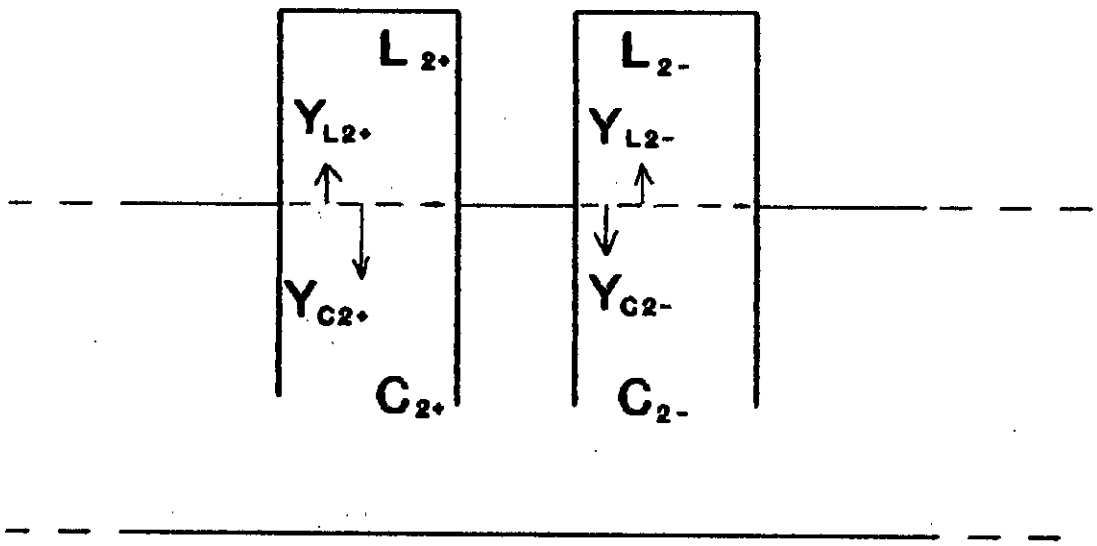

fig 4.6 Series element of the resonated pi–section

$$Y_{L_{2+}}=\frac{1}{j\omega L_{2+}}=-jaC_2(1+\lambda_{2+}^2)\frac{\tan\theta_0}{\tan\theta}$$

$$Y_{L_{2-}}=\frac{1}{j\omega L_{2-}}=-jaC_2(1+\lambda_{2-}^2)\frac{\tan\theta_0}{\tan\theta}$$

$$Y_{C_{2+}}=\frac{1}{-\frac{j}{\omega C_{2+}}}=j\omega C_{2+}=jaC_2(1+\lambda_{2-}^2)\frac{\tan\theta}{\tan\theta_0}$$

$$Y_{C_{2-}}=\frac{1}{-\frac{j}{\omega C_{2-}}}=j\omega C_{2-}=jaC_2(1+\lambda_{2+}^2)\frac{\tan\theta}{\tan\theta_0}$$

Now to determine the distributed element parameters from low pass prototype, we get from figure (4.7),

$$Z_r=\frac{j\omega L_r\cdot\frac{1}{j\omega C_r}}{j\omega L_r+\frac{1}{j\omega C_r}}=\frac{-j\omega L_r}{\omega^2 L_r C_r-1} \qquad (4.5)$$

For distributed pi-section $\omega\rightarrow a[\Omega/\Omega_0-\Omega_0/\Omega]$

Here $\Omega_r=1/\sqrt{L_rC_r}$ is the resonant angular velocity

Therefore,

$$Z_r=-j\frac{a[\frac{\Omega}{\Omega_0}-\frac{\Omega_0}{\Omega}]L_r}{a^2[\frac{\Omega}{\Omega_0}-\frac{\Omega_0}{\Omega}]^2L_rC_r-1}$$

$$=\frac{a[j\frac{\Omega}{\Omega_0}-j\frac{\Omega_0}{\Omega}]L_r}{a^2[j\frac{\Omega}{\Omega_0}-j\frac{\Omega_0}{\Omega}]^2L_rC_r+1}$$

In S-plane $j\Omega\rightarrow s$

$\therefore Z_r=a(s/\Omega_0-\Omega_0/s)L_r/\{a^2(s/\Omega_0-\Omega_0/s)^2L_rC_r+1\}$

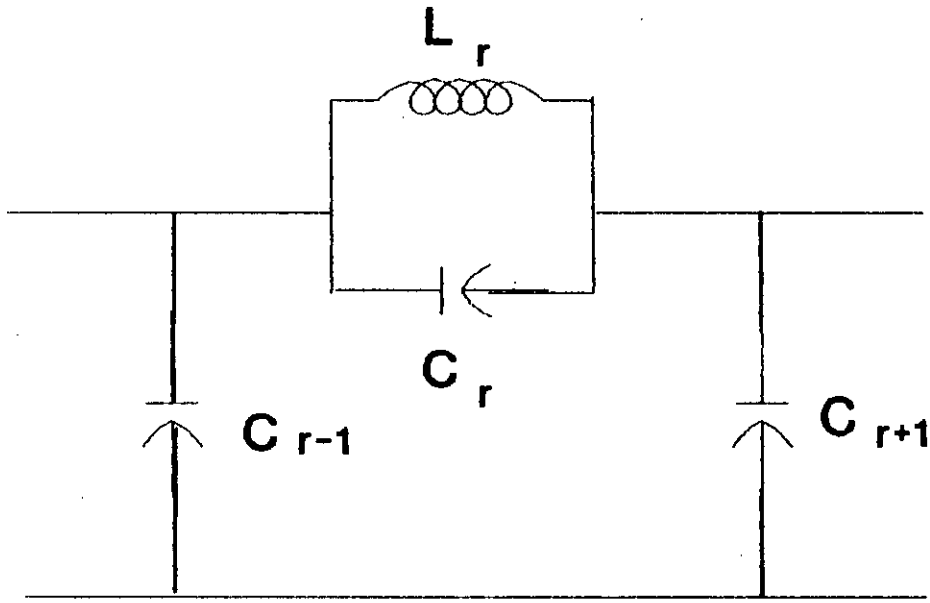

Fig 4.7 A section of the low-pass prototype filter

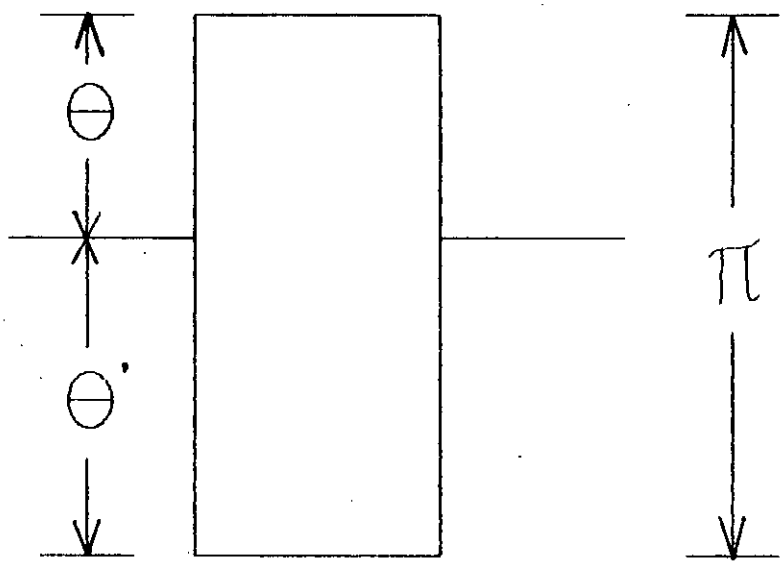

Fig 4.8 Both end shorted approximation of the resonated pi-section

$$= as\Omega_0 L_r (s^2+\Omega_0^2)/\{a^2(s^4+2s^2\Omega_0^2+\Omega_0^4)L_rC_r+s^2\Omega_0^2\}$$

$$= \{as\Omega_0(s^2+\Omega_0^2)/C_r\}/\{a^2(s^4+2s^2\Omega_0^2+\Omega_0^4)+s^2\Omega_0^2/L_rC_r\}$$

$$= \{as\Omega_0(s^2+\Omega_0^2)/C_r\}/\{a^2(s^4+2s^2\Omega_0^2+\Omega_0^4+s^2\Omega_0^2\Omega_r^2/a^2)\}$$

$$= \{\Omega_0 s(s^2+\Omega_0^2)/aC_r\}/\{s^4+(2\Omega_0^2+\Omega_0^2\Omega_r^2/a^2)s^2+\Omega_0^4\} \qquad (4.6)$$

4.2.1 **Calculation of poles** : Auxiliary equation of the characteristic impedance is given by

$$s^4+(2\Omega_0^2+\Omega_0^2\Omega_r^2/a^2)s^2+\Omega_0^4=0$$

$$s^2=[-(2\Omega_0^2+\Omega_0^2\Omega_r^2/a^2)\pm\sqrt{\{(2\Omega_0^2+\Omega_0^2\Omega_r^2/a^2)^2-4\Omega_0^4\}}]/2$$

$$=[-(2\Omega_0^2+\Omega_0^2\Omega_r^2/a^2)\pm\sqrt{(4\Omega_0^4\,\Omega_r^2/a^2+\Omega_0^4\,\Omega_r^4/a^4)}]/2$$

$$=-\Omega_0^2\{\Omega_r^2/(2a^2)+1\}\pm(\Omega_0^2\Omega_r/a)\sqrt{\{1+\Omega_r^2/(4a^2)\}}$$

$$=(\Omega_0^2\Omega_r/a)[-\{(\Omega_r/2a)+a/\Omega_r\}\pm\sqrt{\{1+(\Omega_r^2/4a^2)\}}]$$

Let the roots of the auxiliary equation are Ω_1^2 and Ω_2^2

Therefore,

$$\Omega_1^2=\frac{\Omega_0^2\Omega_r}{a}\left[-\frac{\Omega_r}{2a}-\frac{a}{\Omega_r}+\sqrt{1+\frac{\Omega_r^2}{4a^2}}\right] \qquad (4.7)$$

$$\Omega_2^2=\frac{\Omega_0^2\Omega_r}{a}\left[-\frac{\Omega_r}{2a}-\frac{a}{\Omega_r}-\sqrt{1+\frac{\Omega_r^2}{4a^2}}\right] \qquad (4.8)$$

Let,

$$\lambda_{r+}=\frac{\Omega_r}{2a}+\sqrt{1+\frac{\Omega_r^2}{4a^2}} \qquad (4.9)$$

$$\lambda_{r-}=-\frac{\Omega_r}{2a}+\sqrt{1+\frac{\Omega_r^2}{4a^2}} \qquad (4.10)$$

Therefore,

$$\Omega_1^2 = \frac{\Omega_0^2 \Omega_r}{a}\left(-\frac{a}{\Omega_r} + \lambda_{r-}\right)$$

$$\Omega_2^2 = \frac{\Omega_0^2 \Omega_r}{a}\left(-\frac{a}{\Omega_r} - \lambda_{r-}\right)$$

From the expression of Z_r, we can write,

$Z_r = \{\Omega_0 s(s^2+\Omega_0^2)/aC_r\}/\{(s^2-\Omega_1^2)(s^2-\Omega_2^2)\}$

$= (\Omega_0/aC_r)Z_r'$

$$\text{where,} \quad Z_r' = \frac{s(s^2+\Omega_0^2)}{(s^2-\Omega_1^2)(s^2-\Omega_2^2)} \tag{4.11}$$

Let, $Z_r' = s(s^2+\Omega_0^2)/\{(s^2-\Omega_1^2)(s^2-\Omega_2^2)\}$

$= K_1 s/(s^2-\Omega_1^2) + K_2 s/(s^2-\Omega_2^2)$

$$\text{where,} \quad K_1 = \frac{s^2+\Omega_0^2}{(s^2-\Omega_1^2)(s^2-\Omega_2^2)} \cdot (s^2-\Omega_1^2)\Big|_{s^2=\Omega_1^2}$$

$$= \frac{\Omega_1^2+\Omega_0^2}{\Omega_1^2-\Omega_2^2} = \frac{\lambda_{r-}}{\lambda_{r-}+\lambda_{r+}}$$

$$= \frac{1}{1+\lambda_{r-}^2} \qquad [\ \textit{using}\ \ \lambda_{r+}.\lambda_{r-}=1\ ] \tag{4.12}$$

similarly,

$$K_2 = \frac{\Omega_2^2+\Omega_0^2}{\Omega_2^2-\Omega_1^2} = \frac{\lambda_{r+}}{\lambda_{r-}+\lambda_{r+}} = \frac{1}{1+\lambda_{r-}^2} \tag{4.13}$$

Now, $K_1 s/(s^2-\Omega_1^2) = \{s/(1+\lambda_{r+}^2)\}/\{s^2-(\Omega_0^2\Omega_r/a)(-a/\Omega_r+\lambda_{r-})\}$

$= 1/[s(1+\lambda_{r+}^2) - \{(\Omega_0^2\Omega_r/a)(-a/\Omega_r+\lambda_{r-})(1+\lambda_{r+}^2)\}/s]$

Similarly,

$$K_2 s/(s^2-\Omega_2^2)=\{s/(1+\lambda_{r-}^2)\}/\{s^2+(\Omega_0^2\Omega_r/a)(a/\Omega_r+\lambda_{r-})\}$$

$$=1/[s(1+\lambda_{r-}^2)+\{(\Omega_0^2\Omega_r/a)(a/\Omega_r+\lambda_{r+})(1+\lambda_{r-}^2)\}/s]$$

Therefore,

$$Z_r=(\Omega_0/aC_r)Z_r'=(\Omega_0/aC_r)[K_1 s/(s^2-\Omega_1^2)+K_2 s/(s^2-\Omega_2^2)]$$

$$=(\Omega_0/aC_r)[1/[s(1+\lambda_{r+}^2)-\{(\Omega_0^2\Omega_r/a)(-a/\Omega_r+\lambda_{r-})(1+\lambda_{r+}^2)\}/s]$$

$$+1/[s(1+\lambda_{r-}^2)+\{(\Omega_0^2\Omega_r/a)(a/\Omega_r+\lambda_{r+})(1+\lambda_{r-}^2)\}/s]]$$

From the above equation the following parameters are equated,

$$C_{r-}=\frac{aC_r(1+\lambda_{r+}^2)}{\Omega_0}=\frac{aC_r(1+\lambda_{r+}^2)}{\tan\theta_0} \qquad (4.14)$$

$$L_{r-}=(\Omega_0/aC_r)/\{(\Omega_0^2\Omega_r/a)(a/\Omega_r-\lambda_{r-})(1+\lambda_{r+}^2)\}$$

$$=1/\{C_r\Omega_0\Omega_r(a/\Omega_r+(a/\Omega_r)\lambda_{r+}^2-\lambda_{r-}-\lambda_{r-}\lambda_{r+}^2\}$$

$$=1/[C_r\Omega_0\Omega_r\{a/\Omega_r+(a/\Omega_r)[\Omega_r/2a+\sqrt{\{1+(\Omega_r^2/4a^2)\}}]^2-(\lambda_{r+}+\lambda_{r-})\}]$$

$$=1/[C_r\Omega_0\Omega_r\{2a/\Omega_r+(2a/\Omega_r)(\Omega_r/2a)^2+\sqrt{\{1+(\Omega_r^2/4a^2)\}}$$

$$-2\sqrt{\{1+(\Omega_r^2/4a^2)\}}\}]$$

$$=1/[C_r\Omega_0\Omega_r(a/\Omega_r)\{2+2(\Omega_r/2a)^2-2(\Omega_r/2a)\sqrt{\{1+(\Omega_r^2/4a^2)\}}\}]$$

$$=1/[aC_r\Omega_0\{1+1+(\Omega_r/2a)^2+(\Omega_r/2a)^2-2(\Omega_r/2a)\sqrt{\{1+(\Omega_r^2/4a^2)\}}\}]$$

$$=1/\{aC_r\Omega_0(1+\lambda_{r-}^2)\}$$

$$\therefore\ L_{r-}=\frac{1}{aC_r(1+\lambda_{r-}^2)\tan\theta_0} \qquad (4.15)$$

similarly equating from the second term of the expression of Z_r we get,

$$C_{r+}=\frac{aC_r(1+\lambda_{r-}^2)}{\Omega_0}=\frac{aC_r(1+\lambda_{r-}^2)}{\tan\theta_0} \qquad (4.16)$$

$$L_{r+}=\frac{\frac{\Omega_0}{aC_r}}{\frac{\Omega_0^2\Omega_r}{a}\left(\frac{a}{\Omega_r}+\lambda_{r+}\right)\left(1+\lambda_{r-}^2\right)}=\frac{1}{aC_r(1+\lambda_{r+}^2)\tan\theta_0} \qquad (4.17)$$

4.3 **Both end shorted approximation** : The basic pi-section in the resonated distributed prototype consists of a ladder formation of second order reactance functions whose susceptances may be expressed in the form,

$$Y_2\frac{\tan\theta}{\tan\theta_0}-Y_1\frac{\tan\theta_0}{\tan\theta} \qquad (4.18)$$

This susceptance is now equated to a single stepped impedance half wave cavity at the center frequency $\theta=\theta_0$. The half wave cavity consists of two short circuited transmission lines of characteristic admittance Y_1' and Y_2' connected in parallel at the nodes. The combined length of these stubs is π radian long at $\theta=\theta_0$ with the step in impedance occurring at θ_0 radian from one end as shown in figure (4.8) because,

$$\theta'=\pi\left(\frac{\theta}{\theta_0}\right)-\theta \qquad (4.19)$$

so that at mid band frequency when, $\theta\to\theta_0$, $\theta'\to\pi-\theta_0$

The susceptance of this cavity at the stepped impedance nodes is given by,

$$\frac{-Y_1'}{\tan\theta}-\frac{Y_2'}{\tan\left[\theta\left(\frac{\pi}{\theta_0}-1\right)\right]} \qquad (4.20)$$

Now let, $M=Y_2\tan\theta/\tan\theta_0-Y_1$ (4.21)

and, $$N=-Y_1'/\tan\theta-Y_2'/\tan\{\theta(\pi/\theta_0)-\theta\} \quad (4.22)$$

At $\theta=\theta_0$

$$M=Y_2-Y_1$$

$$N=-Y_1'/\tan\theta_0+Y_2'/\tan\theta_0$$

$$\frac{dM}{d\theta}\Big|_{\theta=\theta_0}=\frac{Y_2\sec^2\theta_0}{\tan\theta_0}+Y_1\tan\theta_0\operatorname{cosec}^2\theta_0 \quad (4.23)$$

$$\frac{dN}{d\theta}\Big|_{\theta=\theta_0}=Y_1'\operatorname{cosec}^2\theta_0+Y_2'\left(\frac{\pi}{\theta_0}-1\right)\operatorname{cosec}^2\left[\theta_0\left(\frac{\pi}{\theta_0}-1\right)\right]$$

$$=Y_1'\operatorname{cosec}^2\theta_0+Y_2'(\pi/\theta_0-1)\operatorname{cosec}^2(\pi-\theta_0)$$

$$=[Y_1'+Y_2'(\pi/\theta_0-1)]\operatorname{cosec}^2\theta_0 \quad (4.24)$$

Equating $M, N, \frac{dM}{d\theta}, \frac{dN}{d\theta}$ *at* $\theta=\theta_0$, *we get*

$$Y_2-Y_1=-Y_1'/\tan\theta_0+Y_2'/\tan\theta_0$$

$$\text{or, } Y_1'=Y_2'+(Y_1-Y_2)\tan\theta_0 \quad (4.25)$$

and,

$$Y_2\sec^2\theta_0/\tan\theta_0+Y_1\tan\theta_0\operatorname{cosec}^2\theta_0=[Y_1'+Y_2'(\pi/\theta_0-1)]\operatorname{cosec}^2\theta_0$$

$$\text{or, } Y_2\sec^2\theta_0/\tan\theta_0+Y_1\tan\theta_0\operatorname{cosec}^2\theta_0$$

$$=[Y_2'+(Y_1-Y_2)\tan\theta_0+Y_2'(\pi/\theta_0-1)]\operatorname{cosec}^2\theta_0$$

$$\text{or, } Y_2(\cos\theta_0/\sin\theta_0)(1/\cos^2\theta_0)+Y_1\tan\theta_0\operatorname{cosec}^2\theta_0$$

$$=Y_2'\operatorname{cosec}^2\theta_0+Y_1\tan\theta_0\operatorname{cosec}^2\theta_0-Y_2\tan\theta_0\operatorname{cosec}^2\theta_0$$

$$+Y_2'(\pi/\theta_0)\operatorname{cosec}^2\theta_0-Y_2'\operatorname{cosec}^2\theta_0$$

$$\text{or, } Y_2(2/\sin\theta_0\cos\theta_0)=Y_2'(\pi/\theta_0)\operatorname{cosec}^2\theta_0$$

$$Y_2'=\frac{2\theta_0}{\pi}|\tan\theta_0|Y_2 \quad (4.26)$$

Again, $$Y_1'=Y_2'+(Y_1-Y_2)\tan\theta_0$$

$$=(2\theta_0/\pi)|\tan\theta_0|Y_2+(Y_1-Y_2)\tan\theta_0$$

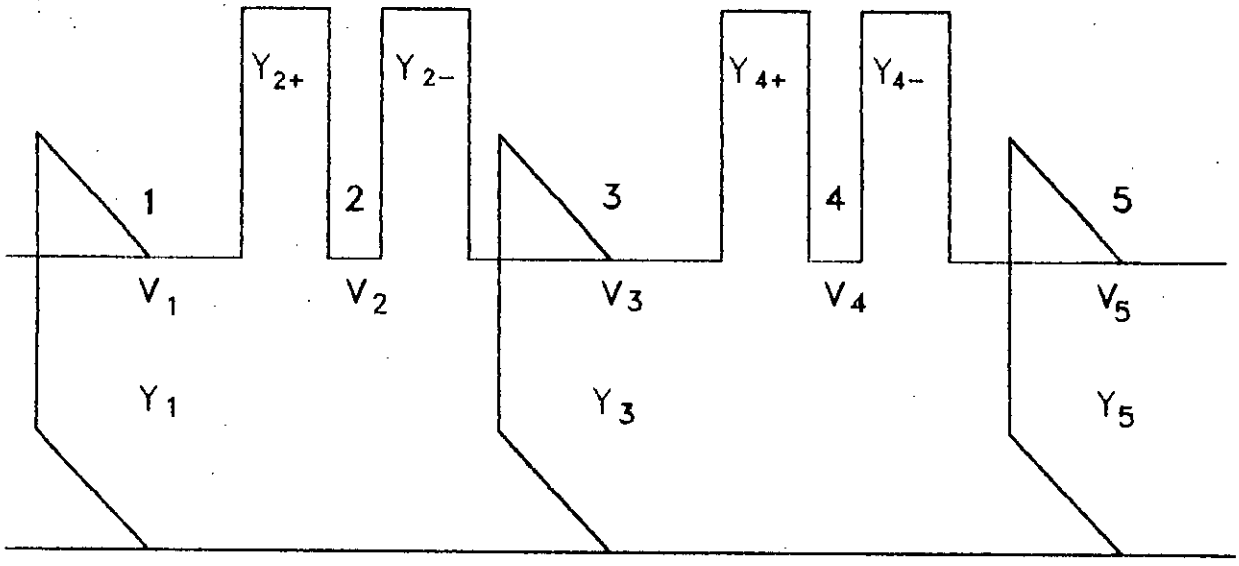

Fig 4.9 Network 1 of the distributed element

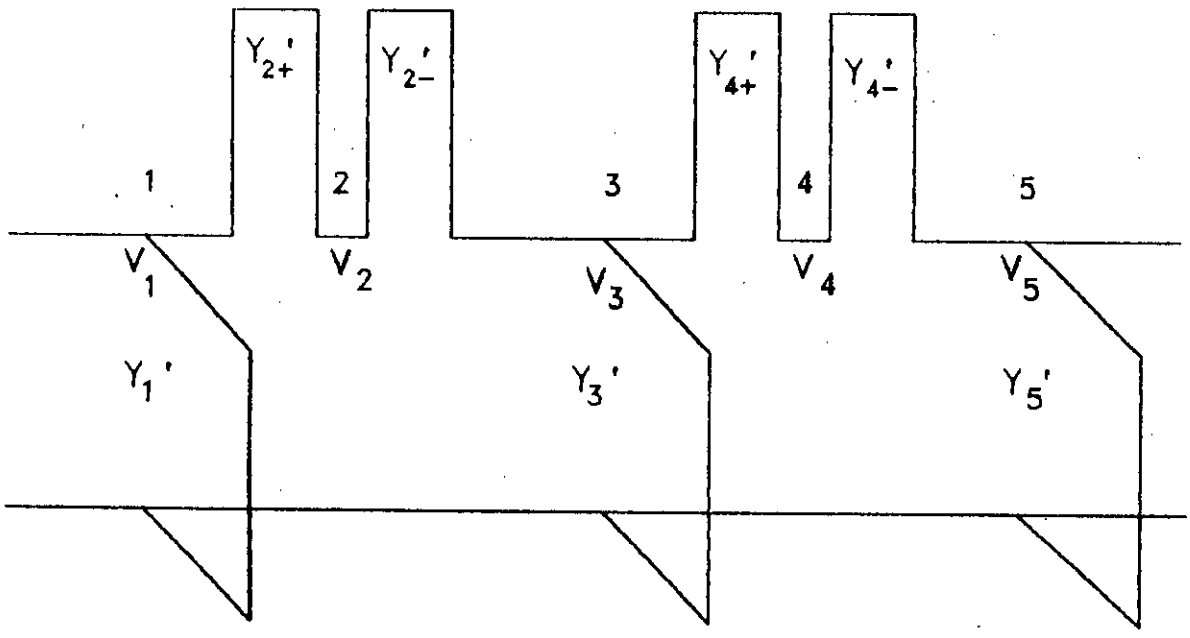

Fig 4.10 Network 2 of the distributed element

$$Y_1' = [Y_1 + (\frac{2\theta_0}{\pi} - 1) Y_2] |\tan\theta_0| \qquad (4.27)$$

4.4 **Characteristic admittance matrix of network 1** : From figure (4.9), one can write the node current equations as,

Node 1:

$$I_1 = Y_1 V_1 + Y_{2+}(V_1 - V_2) = (Y_1 + Y_{2+})V_1 - Y_{2+}V_2 \qquad (4.28)$$

Node 2:

$$I_2 = (V_2 - V_1)Y_{2+} + (V_2 - V_3)Y_{2-} = -Y_{2+}V_1 + (Y_{2+} + Y_{2-})V_2 - Y_{2-}V_3 \qquad (4.29)$$

Node 3:

$$I_3 = (V_3 - V_2)Y_{2-} + Y_3 V_3 + (V_3 - V_4)Y_{4+} = -Y_{2-}V_2 + (Y_{2-} + Y_3 + Y_{4+})V_3 - Y_{4+}V_4 \qquad (4.30)$$

Node 4:

$$I_4 = (V_4 - V_3)Y_{4+} + (V_4 - V_5)Y_{4-} = -Y_{4+}V_3 + (Y_{4+} + Y_{4-})V_4 - Y_{4-}V_5 \qquad (4.31)$$

Node 5:

$$I_5 = Y_5 V_5 + (V_5 - V_4)Y_{4-} = -Y_{4-}V_4 + (Y_{4-} + Y_5)V_5 \qquad (4.32)$$

Now writing the above node equations in matrix form,

$$\begin{bmatrix} I_1 \\ I_2 \\ I_3 \\ I_4 \\ I_5 \end{bmatrix} = \begin{bmatrix} (Y_1+Y_{2+}) & -Y_{2+} & 0 & 0 & 0 \\ -Y_{2+} & (Y_{2+}+Y_{2-}) & -Y_{2-} & 0 & 0 \\ 0 & -Y_{2-} & (Y_{2-}+Y_3+Y_{4+}) & -Y_{4+} & 0 \\ 0 & 0 & -Y_{4+} & (Y_{4+}+Y_{4-}) & -Y_{4-} \\ 0 & 0 & 0 & -Y_{4-} & (Y_{4-}+Y_5) \end{bmatrix} \begin{bmatrix} V_1 \\ V_2 \\ V_3 \\ V_4 \\ V_5 \end{bmatrix} \qquad (4.33)$$

We now make the following substitutions,

$Y_{11} = (Y_1 + Y_{2+})$; $Y_{12} = Y_{2+}$; $Y_{22} = (Y_{2+} + Y_{2-})$; $Y_{23} = Y_{2-}$;

$Y_{33} = (Y_{2-} + Y_3 + Y_{4+})$; $Y_{34} = Y_{4+}$; $Y_{44} = (Y_{4+} + Y_{4-})$; $Y_{45} = Y_{4-}$;

$Y_{55} = (Y_{4-} + Y_5)$

With these substitutions, the characteristic admittance matrix of network 1 may be written as,

$$\begin{bmatrix} Y_{11} & -Y_{12} & 0 & 0 & 0 \\ -Y_{12} & Y_{22} & -Y_{23} & 0 & 0 \\ 0 & -Y_{23} & Y_{33} & -Y_{34} & 0 \\ 0 & 0 & -Y_{34} & Y_{44} & -Y_{45} \\ 0 & 0 & 0 & -Y_{45} & Y_{55} \end{bmatrix} \qquad (4.34)$$

The matrix element values are calculated from the following equations,

$$Y_{11}=Y_1+Y_{2+}$$

$$= |\tan\theta_0| \{aC_1+(2\theta_0/\pi-1)aC_1\}+|\tan\theta_0| \{aC_2(1+\lambda_{2+}^2)$$
$$+(2\theta_0/\pi-1)aC_2(1+\lambda_{2-}^2)\}$$
$$= |\tan\theta_0| (2a\theta_0C_1/\pi)+|\tan\theta_0| \{aC_2(1+\lambda_{2+}^2)-aC_2(1+\lambda_{2-}^2)$$
$$+(2\theta_0/\pi)aC_2(1+\lambda_{2-}^2)\}$$
$$=2a(\theta_0/\pi)|\tan\theta_0| C_1+2a(\theta_0/\pi)|\tan\theta_0| \{(\pi/2\theta_0)C_2(1+\lambda_{2+}^2)$$
$$-(\pi/2\theta_0)C_2(1+\lambda_{2-}^2)+C_2(1+\lambda_{2-}^2)\}$$
$$=2a(\theta_0/\pi)|\tan\theta_0| [C_1+C_2\{1+\lambda_{2-}^2+(\pi/2\theta_0)(\lambda_{2+}^2-\lambda_{2-}^2)\}]$$

$$\therefore Y_{11}=b[C_1+C_2[1+\lambda_{2-}^2+\frac{\pi}{2\theta_0}(\lambda_{2+}^2-\lambda_{2-}^2)]] \qquad (4.35)$$

$$where, \qquad b=2a\frac{\theta_0}{\pi}|\tan\theta_0|$$

$$Y_{12}=Y_{2+}$$

$$= |\tan\theta_0| \{aC_2(1+\lambda_{2+}^2)+(2\theta_0/\pi-1)aC_2(1+\lambda_{2-}^2)\}$$
$$=2a(\theta_0/\pi)|\tan\theta_0| C_2[(\pi/2\theta_0)(\lambda_{2+}^2-\lambda_{2-}^2)+1+\lambda_{2-}^2]$$

$$\therefore Y_{12}=bC_2[1+\lambda_{2-}^2+\frac{\pi}{2\theta_0}(\lambda_{2+}^2-\lambda_{2-}^2)] \qquad (4.36)$$

$$Y_{22}=Y_{2+}+Y_{2-}$$

$$= |\tan\theta_0| \{aC_2(1+\lambda_{2+}^2)+(2\theta_0/\pi-1)aC_2(1+\lambda_{2-}^2)\}$$
$$+|\tan\theta_0| \{aC_2(1+\lambda_{2-}^2)+(2\theta_0/\pi-1)aC_2(1+\lambda_{2+}^2)\}$$

$$=2a(\theta_0/\pi)|\tan\theta_0|\,C_2[1+\lambda_{2-}^2+1+\lambda_{2+}^2]$$

$$\therefore\ Y_{22}=bC_2[2+\lambda_{2+}^2+\lambda_{2-}^2] \tag{4.37}$$

$Y_{23}=Y_{2-}$

$$=|\tan\theta_0|\{aC_2(1+\lambda_{2-}^2)+(2\theta_0/\pi-1)aC_2(1+\lambda_{2+}^2)\}$$

$$=2a(\theta_0/\pi)|\tan\theta_0|\,C_2[1+\lambda_{2+}^2+(\pi/2\theta_0)(\lambda_{2-}^2-\lambda_{2+}^2)]$$

$$\therefore\ Y_{23}=bC_2\left[1+\lambda_{2+}^2+\frac{\pi}{2\theta_0}(\lambda_{2-}^2-\lambda_{2+}^2)\right] \tag{4.38}$$

$Y_{33}=Y_{2-}+Y_3+Y_{4+}$

Here $Y_3=|\tan\theta_0|\{aC_3+(2\theta_0/\pi-1)aC_3\}$

$$=2a(\theta_0/\pi)|\tan\theta_0|\,C_3$$

$$\therefore\ Y_3=bC_3 \tag{4.39}$$

$$Y_{4+}=|\tan\theta_0|\{aC_4(1+\lambda_{4+}^2)+(2\theta_0/\pi-1)aC_4(1+\lambda_{4-}^2)\}$$

$$\therefore\ Y_{4+}=bC_4\left[1+\lambda_{4-}^2+\frac{\pi}{2\theta_0}(\lambda_{4+}^2-\lambda_{4-}^2)\right] \tag{4.40}$$

Therefore

$$Y_{33}=bC_2[1+\lambda_{2+}^2+(\pi/2\theta_0)(\lambda_{2-}^2-\lambda_{2+}^2)]+bC_3$$
$$+bC_4[1+\lambda_{4-}^2+(\pi/2\theta_0)(\lambda_{4+}^2-\lambda_{4-}^2)]$$
$$=b[C_2\{1+\lambda_{2+}^2+(\pi/2\theta_0)(\lambda_{2-}^2-\lambda_{2+}^2)\}+C_3$$

$$\therefore\ Y_{33}=b\left[C_2\left[1+\lambda_{2+}^2+\frac{\pi}{2\theta_0}(\lambda_{2-}^2-\lambda_{2+}^2)\right]+C_3+C_4\left[1+\lambda_{4-}^2+\frac{\pi}{2\theta_0}(\lambda_{4+}^2-\lambda_{4-}^2)\right]\right] \tag{4.41}$$

$Y_{34}=Y_{4+}$

$$\therefore\ Y_{34}=bC_4\left[1+\lambda_{4-}^2+\frac{\pi}{2\theta_0}(\lambda_{4+}^2-\lambda_{4-}^2)\right] \tag{4.42}$$

$Y_{44}=Y_{4+}+Y_{4-}$

$$=bC_4[1+\lambda_{4-}^2+(\pi/2\theta_0)(\lambda_{4+}^2-\lambda_{4-}^2)]+bC_4[1+\lambda_{4+}^2+(\pi/2\theta_0)(\lambda_{4-}^2-\lambda_{4+}^2)]$$

$$\therefore\ Y_{44}=bC_4[2+\lambda_{4+}^2+\lambda_{4-}^2] \qquad (4.43)$$

$Y_{45}=Y_{4-}'$

$$\therefore\ Y_{45}=bC_4\left[1+\lambda_{4+}^2+\frac{\pi}{2\theta_0}(\lambda_{4-}^2-\lambda_{4+}^2)\right] \qquad (4.44)$$

$Y_{55}=Y_{4-}+Y_5$

$=bC_4[1+\lambda_{4+}{}^2+(\pi/2\theta_0)(\lambda_{4-}{}^2-\lambda_{4+}{}^2)]+|\tan\theta_0|\{aC_5+(2\theta_0/\pi-1)aC_5\}$

$=bC_4[1+\lambda_{4+}{}^2+(\pi/2\theta_0)(\lambda_{4-}{}^2-\lambda_{4+}{}^2)]+bC_5$

$$\therefore\ Y_{55}=b\left[C_5+C_4\left[1+\lambda_{4+}^2+\frac{\pi}{2\theta_0}(\lambda_{4-}^2-\lambda_{4+}^2)\right]\right] \qquad (4.45)$$

4.5 **Characteristic admittance matrix of network 2** : From figure (4.10), one can write the current node equations as,

Node 1:

$$I_1'=Y_1'V_1'+Y_{2+}'(V_1'-V_2')=(Y_1'+Y_{2+}')V_1'-Y_{2+}'V_2' \qquad (4.46)$$

Node 2:

$$I_2'=(V_2'-V_1')Y_{2+}'+(V_2'-V_3')Y_{2-}'=-Y_{2+}'V_1'+(Y_{2+}'+Y_{2-}')V_2'-Y_{2-}'V_3' \qquad (4.47)$$

Node 3:

$$I_3'=(V_3'-V_2')Y_{2-}'+Y_3'V_3'+(V_3'-V_4')Y_{4+}'$$

$$=-Y_{2-}'V_2'+(Y_{2-}'+Y_3'+Y_{4+}')V_3'-Y_{4+}'V_4' \qquad (4.48)$$

Node 4:

$$I_4'=(V_4'-V_3')Y_{4+}'+(V_4'-V_5')Y_{4-}'=-Y_{4+}'V_3'+(Y_{4+}'+Y_{4-}')V_4'-Y_{4-}'V_5' \qquad (4.49)$$

Node 5:

$$I_5'=Y_5'V_5'+(V_5'-V_4')Y_{4-}'=-Y_{4-}'V_4'+(Y_{4-}'+Y_5')V_5' \qquad (4.50)$$

Now writing the above node equations in matrix form,

$$\begin{bmatrix} I_1' \\ I_2' \\ I_3' \\ I_4' \\ I_5' \end{bmatrix} = \begin{bmatrix} (Y_1'+Y_{2+}') & -Y_{2+}' & 0 & 0 & 0 \\ -Y_{2+}' & (Y_{2+}'+Y_{2-}') & -Y_{2-}' & 0 & 0 \\ 0 & -Y_{2-}' & (Y_{2-}'+Y_3'+Y_{4+}') & -Y_{4+}' & 0 \\ 0 & 0 & -Y_{4+}' & (Y_{4+}'+Y_{4-}') & -Y_{4-}' \\ 0 & 0 & 0 & -Y_{4-}' & (Y_{4-}'+Y_5') \end{bmatrix} \begin{bmatrix} V_1' \\ V_2' \\ V_3' \\ V_4' \\ V_5' \end{bmatrix} \quad (4.51)$$

We now make the following substitutions,

$Y_{11}=(Y_1'+Y_{2+}')$; $Y_{12}=Y_{2+}'$; $Y_{22}=(Y_{2+}'+Y_{2-}')$; $Y_{23}=Y_{2-}'$;

$Y_{33}=(Y_{2-}'+Y_3'+Y_{4+}')$; $Y_{34}=Y_{4+}'$; $Y_{44}=(Y_{4+}'+Y_{4-}')$; $Y_{45}=Y_{4-}'$;

$Y_{55}=(Y_{4-}'+Y_5')$

With these substitutions, the characteristic admittance of network 2 may be written as,

$$\begin{bmatrix} Y_{11} & -Y_{12} & 0 & 0 & 0 \\ -Y_{12} & Y_{22} & -Y_{23} & 0 & 0 \\ 0 & -Y_{23} & Y_{33} & -Y_{34} & 0 \\ 0 & 0 & -Y_{34} & Y_{44} & -Y_{45} \\ 0 & 0 & 0 & -Y_{45} & Y_{55} \end{bmatrix} \quad (4.52)$$

The matrix element values are calculated from the following equations,

$Y_{11}=(Y_1'+Y_{2+}')$

$=(2\theta_0/\pi)\,|\tan\theta_0|\,aC_1+(2\theta_0/\pi)\,|\tan\theta_0|\,aC_2(1+\lambda_{2-}^2)$

$=2a(\theta_0/\pi)\,|\tan\theta_0|\,[C_1+C_2(1+\lambda_{2-}^2)]$

$$\therefore Y_{11}=b[C_1+C_2(1+\lambda_{2-}^2)] \quad (4.53)$$

$Y_{12}=Y_{2+}'$

$$\therefore Y_{12}=bC_2(1+\lambda_{2-}^2) \quad (4.54)$$

$Y_{22}=(Y_{2+}'+Y_{2-}')$

$=bC_2(1+\lambda_{2-}^2)+bC_2(1+\lambda_{2+}^2)$

$$\therefore\ Y_{22}=bC_2[2+\lambda_{2+}^2+\lambda_{2-}^2] \tag{4.55}$$

$Y_{23}=Y_{2-}'$

$$\therefore\ Y_{23}=bC_2(1+\lambda_{2+}^2) \tag{4.56}$$

$Y_{33}=(Y_{2-}'+Y_3'+Y_{4+}')$

$=bC_2(1+\lambda_{2+}{}^2)+bC_3+bC_4(1+\lambda_{4-}{}^2)$

$$\therefore\ Y_{33}=b[C_2(1+\lambda_{2+}^2)+C_3+C_4(1+\lambda_{4-}^2)] \tag{4.57}$$

$Y_{34}=Y_{4+}'$

$$\therefore\ Y_{34}=bC_4(1+\lambda_{4-}^2) \tag{4.58}$$

$Y_{44}=(Y_{4+}'+Y_{4-}')$

$=bC_4(1+\lambda_{4-}{}^2)+bC_4(1+\lambda_{4+}{}^2)$

$$\therefore\ Y_{44}=bC_4[2+\lambda_{4+}^2+\lambda_{4-}^2] \tag{4.59}$$

$Y_{45}=Y_{4-}'$

$$\therefore\ Y_{45}=bC_4(1+\lambda_{4+}^2) \tag{4.60}$$

$Y_{55}=(Y_{4-}'+Y_5')$

$=bC_4(1+\lambda_{4+}{}^2)+bC_5$

$$\therefore\ Y_{55}=b[C_5+C_4(1+\lambda_{4+}^2)] \tag{4.61}$$

4.6 **Summary**: The distributed resonated pi-section has been formed from the low pass prototype elliptic function filter. The resonated pi-section has been converted to a half wave cavity which is stepped in impedance and has two short circuited transmission lines connected in parallel at the nodes. The transformation equations from prototype element values to characteristic admittance values

have been deduced in detail and the characteristic admittance matrices for both the networks have been formed using the calculated admittance values.

CHAPTER 5

Parallel coupled lines between ground planes

5.1 **Introduction**: A number of strip line components utilize the natural coupling existing between parallel conductors between ground plates. Examples of such components are directional couplers, filters, baluns, and delay lines such as interdigital lines. The present chapter describes elaborately the nature of various types of parallel coupled lines between ground plates.

5.2 **Different types of parallel coupled lines**: A number of examples of parallel coupled lines are shown in figure 5.1. The configurations (a), (b) and (c) are primarily useful in applications where weak coupling between the lines desired. The configurations (d), (e), (f) and (g) are useful where strong coupling between lines is desired. The characteristic of these coupled lines can be specified in terms of Z_{oe} and Z_{oo} i.e. their even and odd impedances [14] respectively. Z_{oe} is defined as the characteristic impedance of one line to ground when equal currents are flowing in the two lines in the same direction. Z_{oo} is defined as the characteristic impedance of one line to ground when equal and opposite currents are flowing in the two lines. The even and odd mode characteristic impedances shown in figure 5.1(a), (d) and (e) are modified slightly when the strips have a finite thickness. Correction terms that account for the effects of finite thickness have been derived by *Cohn* [15].

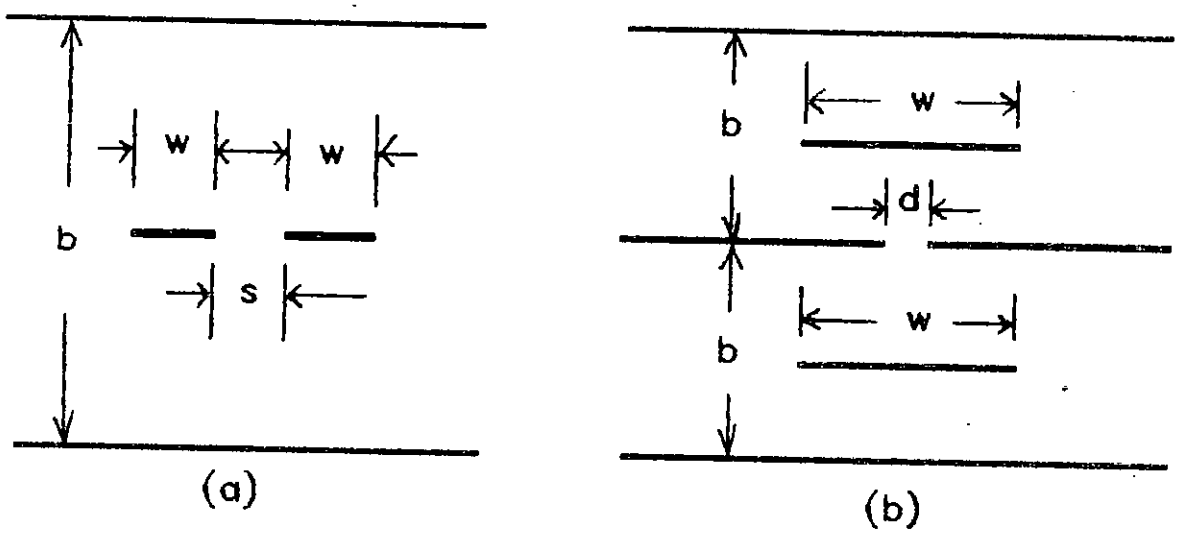

Fig 5.1 Cross sections of various coupled transmission line configurations

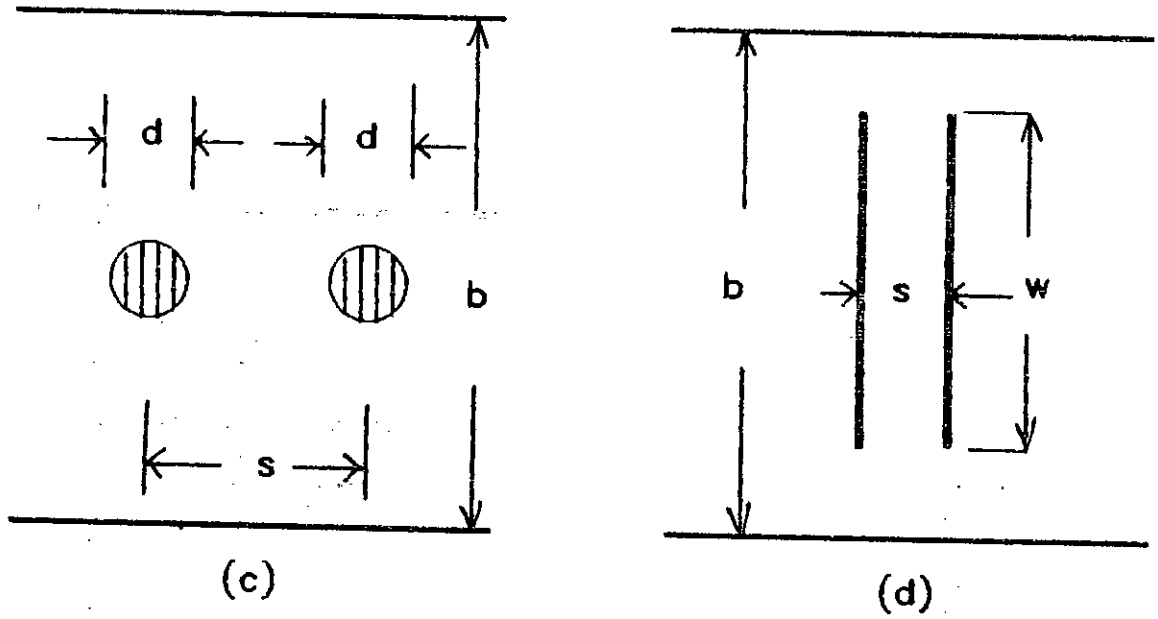

Fig 5.1 Cross sections of various coupled transmission line configurations

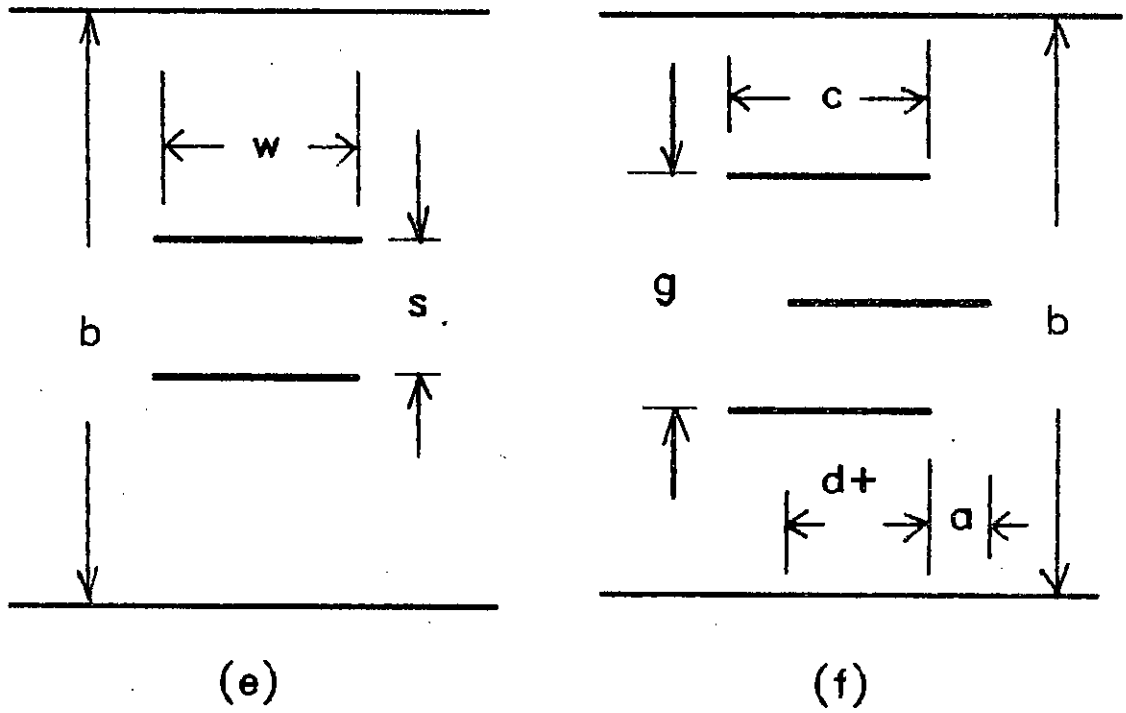

fig 5.1 Cross sections of various coupled transmission line configurations

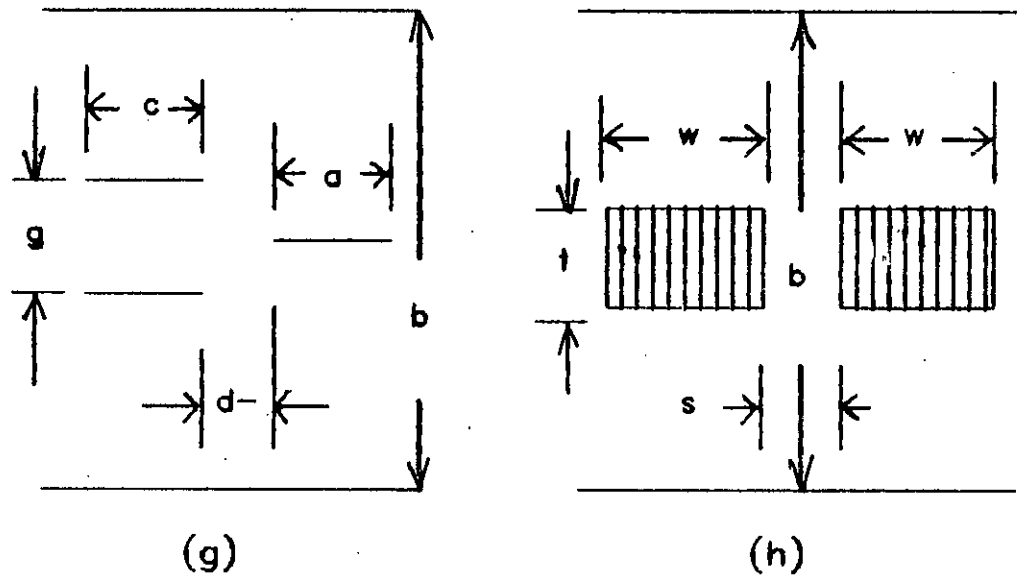

Fig 5.1 Cross sections of various coupled transmission line configurations

5.3 **Coupling with interleaved thin lines**: The configuration of coupled strip lines illustrated in figure (5.1)(f) in which the two lines of width c are always operated at the same potential, is particularly useful when it is desired to obtain tight coupling with thin strips that are supported by a homogeneous dielectric of relative dielectric constant ϵ_r that completely fills the region between the ground planes. The dimensions of the strips for particular values of Z_{oe} and Z_{oo} can be determined from graphs. For this purpose one needs the definitions that,

$$\sqrt{\epsilon_r} Z_{oe} = \frac{376.6\epsilon}{C_{oe}} \tag{5.1}$$

$$\sqrt{\epsilon_r} Z_{oo} = \frac{376.6\epsilon}{C_{oo}} \tag{5.2}$$

where C_{oe} and C_{oo} are the total capacities to ground per unit length of the strips of width c or the strip width a, when the lines are excited in the even and odd modes respectively. The absolute dielectric constant ϵ is equal to $0.225\epsilon_r$ pf per inch. Using the values of Z_{oe} and Z_{oo} which are assumed to be known one then computes $\Delta C/\epsilon$ from,

$$\frac{\Delta C}{\epsilon} = \frac{188.3}{\sqrt{\epsilon_r}} \left[\frac{1}{Z_{oo}} - \frac{1}{Z_{oe}}\right] = \frac{1}{2}\left[\frac{C_{oo}}{\epsilon} - \frac{C_{oe}}{\epsilon}\right] \tag{5.3}$$

Values of g/b are then selected and d/g is determined from the graph. Next, values of $C_{c\omega}'/\epsilon$ and C_{ce}'/ϵ are read from the graphs. These quantities together with the value of C_{oe}/ϵ from

eqn. (5.1) are then substituted in the following equation to get c/b,

$$\frac{c}{b}=\frac{1-\frac{g}{b}}{2}\left[\frac{C_{oe}}{2\epsilon}-\frac{C'_{om}}{\epsilon}-\frac{C'_{ce}}{\epsilon}\right] \qquad (5.4)$$

Finally C_{ae}'/ϵ is found from the graph and substituted in the following equation to get a/b

$$\frac{a}{b}=\frac{1}{2}\left[\frac{C_{oe}}{2\epsilon}-\frac{C'_{ae}}{\epsilon}-0.441\right] \qquad (5.5)$$

In this way all the physical dimensions are determined for coupling with interleaved thin lines. These formulas are exact in the limit of a and $c \gg b$ so that fringing fields at opposite edges of the strips do not interact.

5.4 **Coupling with thick rectangular bars**: The thick rectangular bar configuration of coupled transmission lines as shown in figure (5.1)(h) can also be conveniently used where tight coupling between lines is desired [7]. the dimensions of the strips for particular values of Z_{oe} and Z_{oo} can be determined with the aid of Getsinger's [7] curves in figure (5.2) figure (5.3) and figure (5.4) The above curves are used in the following way. First, $\Delta C/\epsilon$ is determined from eqn. (5.3) using the specified values of Z_{oe} and Z_{oo}. Next a convenient value of t/b is selected and the value of s/b is determined from figure (5.2) The value of w/b is then determined from,

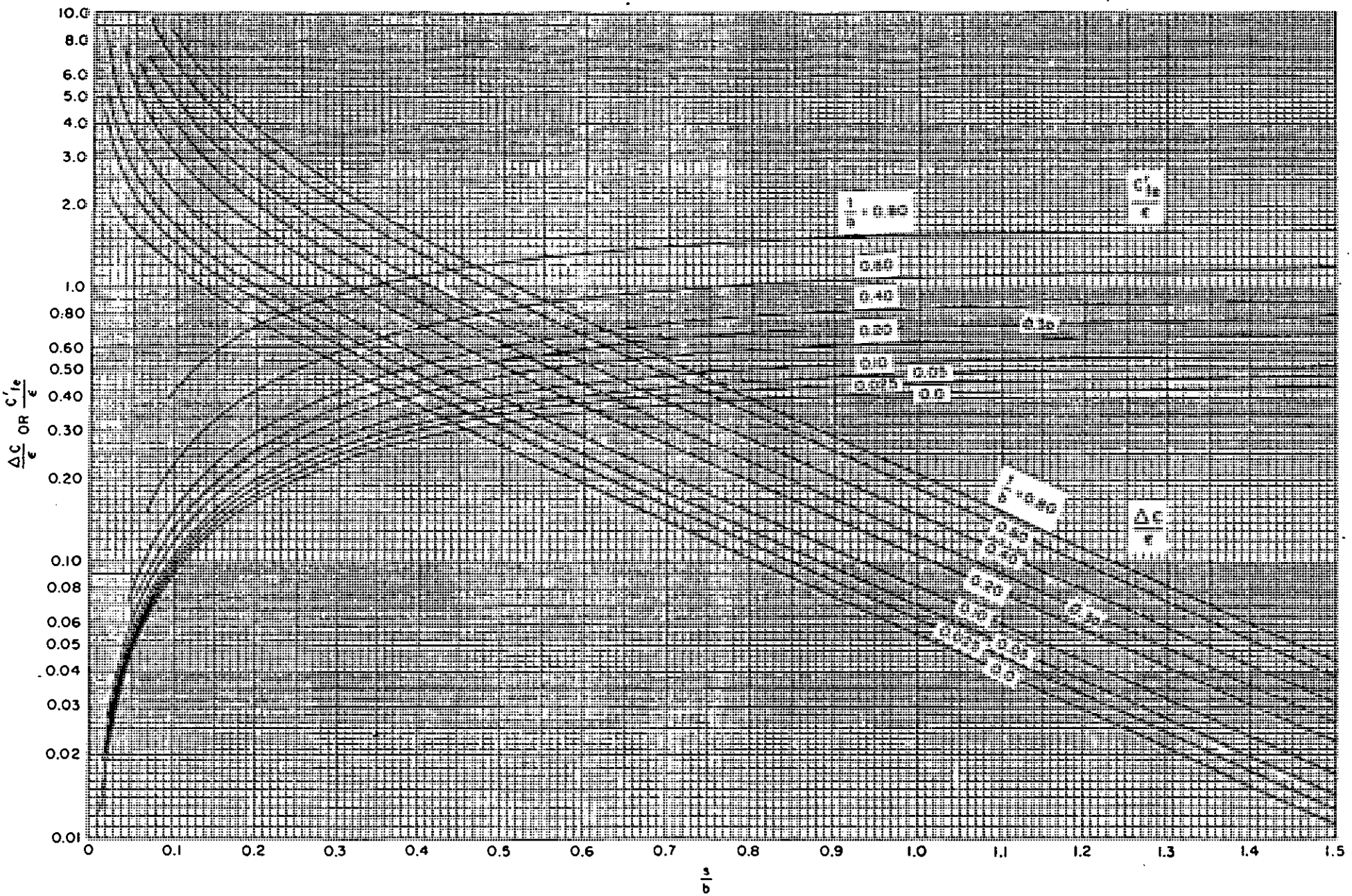

Fig 5.2 Normalized even mode fringing capacitance and interbar capacitance for coupled rectangular bars.[7]

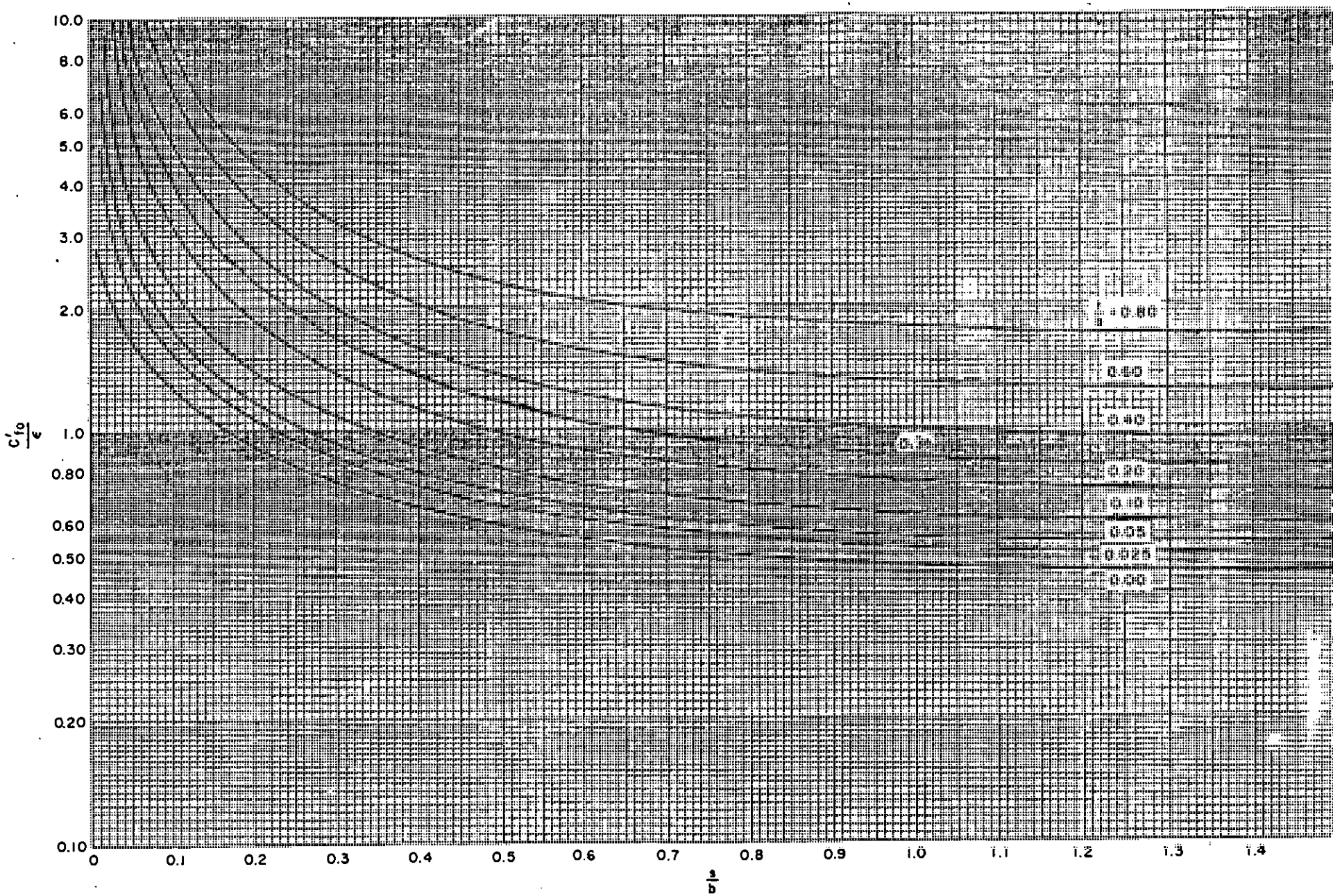

Fig 5.3 Normalized odd mode fringing capacitance for coupled rectangular bars [7]

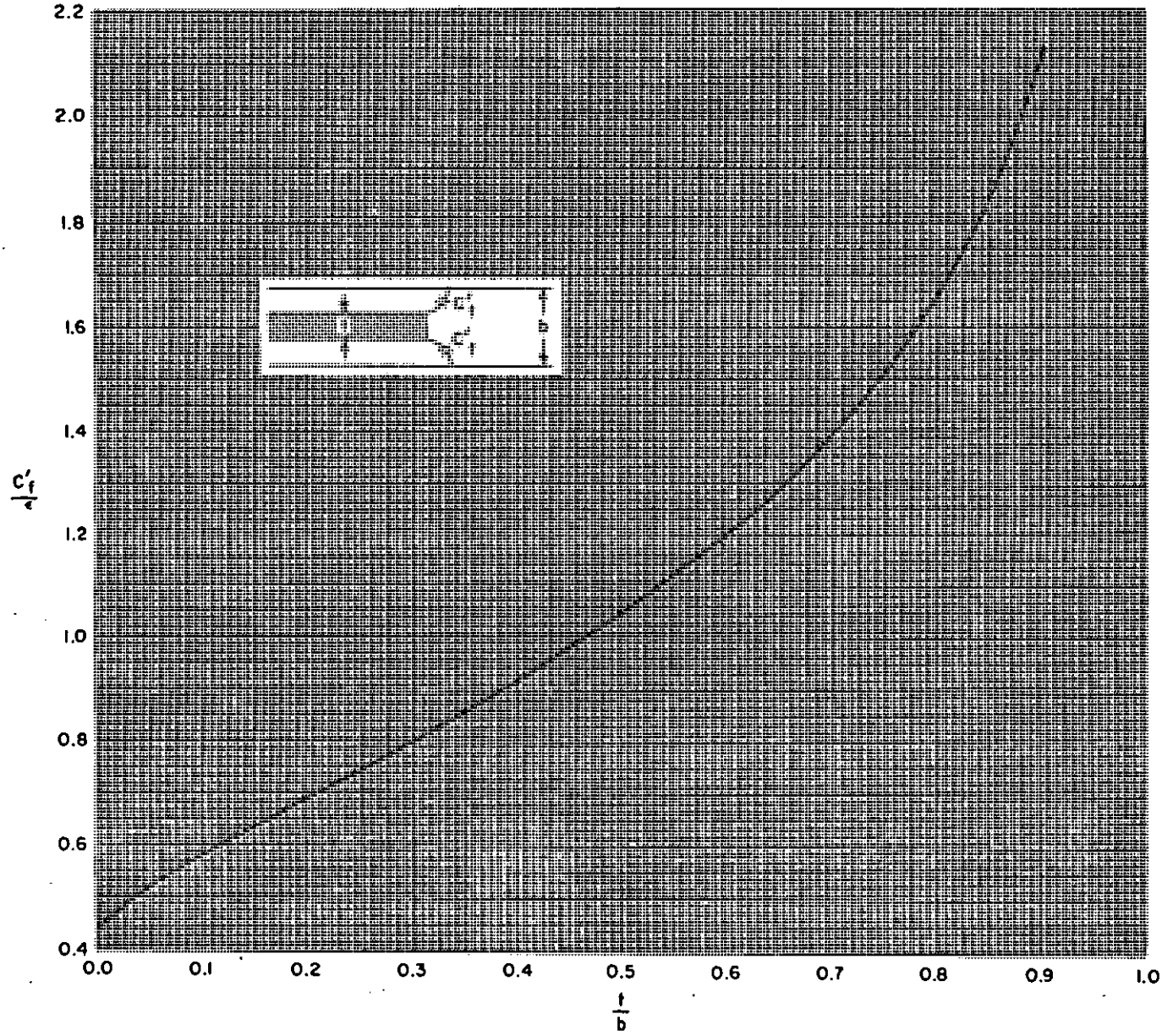

Fig 5.4 Normalized fringing capacitance for an isolated rectangular bar [7]

$$\frac{w}{b}=\frac{1}{2}\left(1-\frac{t}{b}\right)\left[\frac{C_{oe}}{2\epsilon}-\frac{C'_{fe}}{\epsilon}-\frac{C'_{f}}{\epsilon}\right] \qquad (5.6)$$

The value of C_{oe} is determined from the specified value of Z_{oe} using eqn. (5.1) The fringing capacitance C_{fe}' for the even mode can be read from figure (5.2) and C_f' can be determined from figure (5.4) The curves in figure (5.3) give the value of C_{fo}' directly.

The various fringing and parallel plate capacitances are shown in figure (5.5) The odd mode fringing capacitances C_{fo}' correspond to the fringing capacitances between the inner edges of the bars and a metallic wall halfway between the bars. The total odd mode capacitance of a bar is given by the following equation,

$$\frac{C_{oo}}{\epsilon}=2\left[\frac{C_p}{\epsilon}+\frac{C'_{fo}}{\epsilon}+\frac{C'_{f}}{\epsilon}\right] \qquad (5.7)$$

and the total even mode capacitances of a bar is given by,

$$\frac{C_{oe}}{\epsilon}=2\left[\frac{C_p}{\epsilon}+\frac{C'_{fe}}{\epsilon}+\frac{C'_{f}}{\epsilon}\right] \qquad (5.8)$$

The normalized per unit length parallel plate capacitance $C_p/\epsilon=2w/(b-t)$ and $\epsilon=0.225\epsilon_r$ pf per inch. The even and odd mode fringing capacitances are derived by conformal mapping techniques and are exact in limits of $[w/b/(1-t/b)]\to\infty$. It is believed that when $[w/b/(1-t/b)]>0.35$ the interaction between the fringing fields is small enough so that the values of C_{oo}/ϵ and C_{oe}/ϵ determined from eqns. (5.7) and (5.8) are reduced by a maximum of 1.24% of their true values.

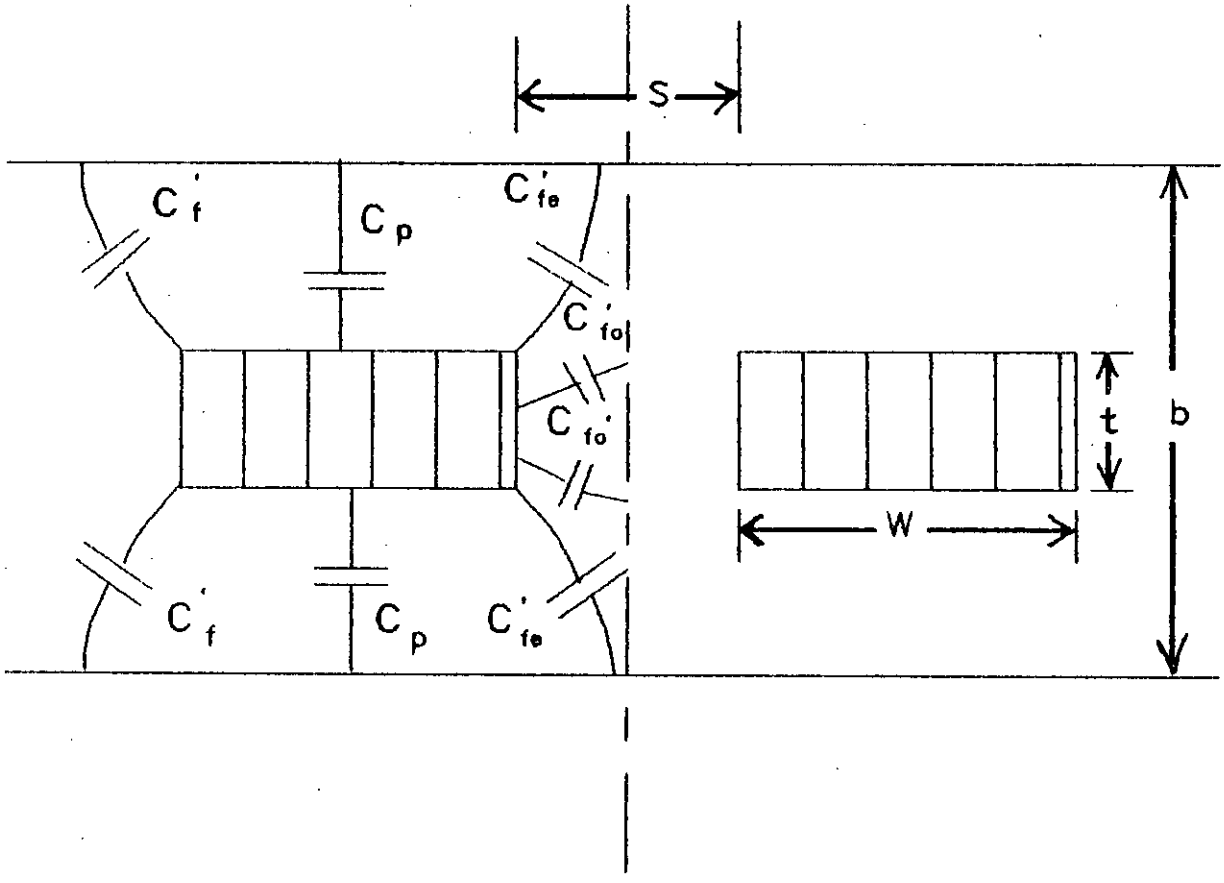

Fig 5.5 Coupled rectangular bars centered between parallel plates illustrating the various fringing and parallel plate capacities

In situations where an initial value, w/b is found from eqn. (5.6) to be less than $0.35[1-(t/b)]$ so that the fringing fields interact, a new value of w'/b can be used where,

$$\frac{w'}{b}=\frac{(0.07[1-\frac{t}{b}]+\frac{w}{b})}{1.2} \qquad (5.9)$$

provided $0.1<(w'/b)/[1-(t/b)]<0.35$

5.5 **Coupling with unsymmetrical parallel coupled lines**: Figure (5.6) shows an unsymmetrical pair of parallel coupled lines and various line capacitances. C_a is the capacitance per unit length between line a and ground, C_{ab} is that between line a and b, while C_b is the capacitance per unit length between line b and ground. When C_a is not equal to C_b the two lines will have different odd and even mode admittances. In terms of odd and even mode capacitances, for line a,

$$(C_{oo})_a=C_a+2C_{ab},\ (C_{oe})_a=C_a \qquad 5.10$$

while for line b,

$$(C_{oo})_b=C_b+2C_{ab},\ (C_{oe})_b=C_b \qquad 5.11$$

For symmetrical parallel coupled lines the odd mode impedances are simply the reciprocals of the odd mode admittances and analogously for the even mode impedances and admittances. However this is not the case for unsymmetrical parallel coupled lines. For unsymmetrical lines the odd and even mode impedances are not simply the reciprocals of the odd and even mode

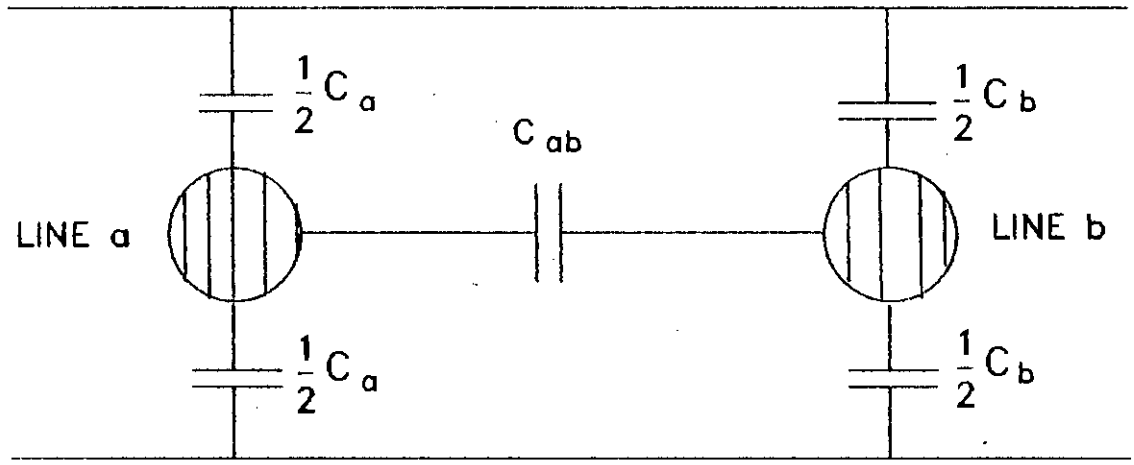

Fig 5.6 An unsymmetrical pair of parallel coupled lines

admittances. The reason for this lies in the fact that when the odd and even mode admittances are computed the basic definition of these admittances assumes that the lines are being driven with voltages of identical magnitude with equal or opposite phase, while the current in the lines may be of different magnitudes. While for the case of odd and even mode impedances it is the other way round. These two different sets of boundary conditions can be seen to lead to different voltage-current ratios if the lines are unsymmetrical.

Some unsymmetrical parallel coupled lines which are quite easy to design are shown in figure (5.7). Both bars have the same height and both are assumed to be wide enough so that the interactions between the fringing fields at the right and left sides of each bar are negligible or at least small enough to be corrected. On this basis the fringing fields are same for both bars and their different capacitances C_a and C_b are due entirely to different parallel plate capacitances $(C_p)_a$ and $(C_p)_b$. For the structure shown in figure (5.7),

$$C_a = 2\left((C_p)_a + C'_f + C'_{fe}\right)$$

$$C_{ab} = (C'_{fo} - C'_{fe}) \qquad (5.12)$$

$$C_b = 2\left((C_p)_b + C'_f + C'_{fe}\right)$$

To design a pair of lines such as those in figure (5.7) to have specified odd and even mode admittances or impedances, first the values of C_a/ϵ, C_{ab}/ϵ and C_b/ϵ are computed from the following equations,

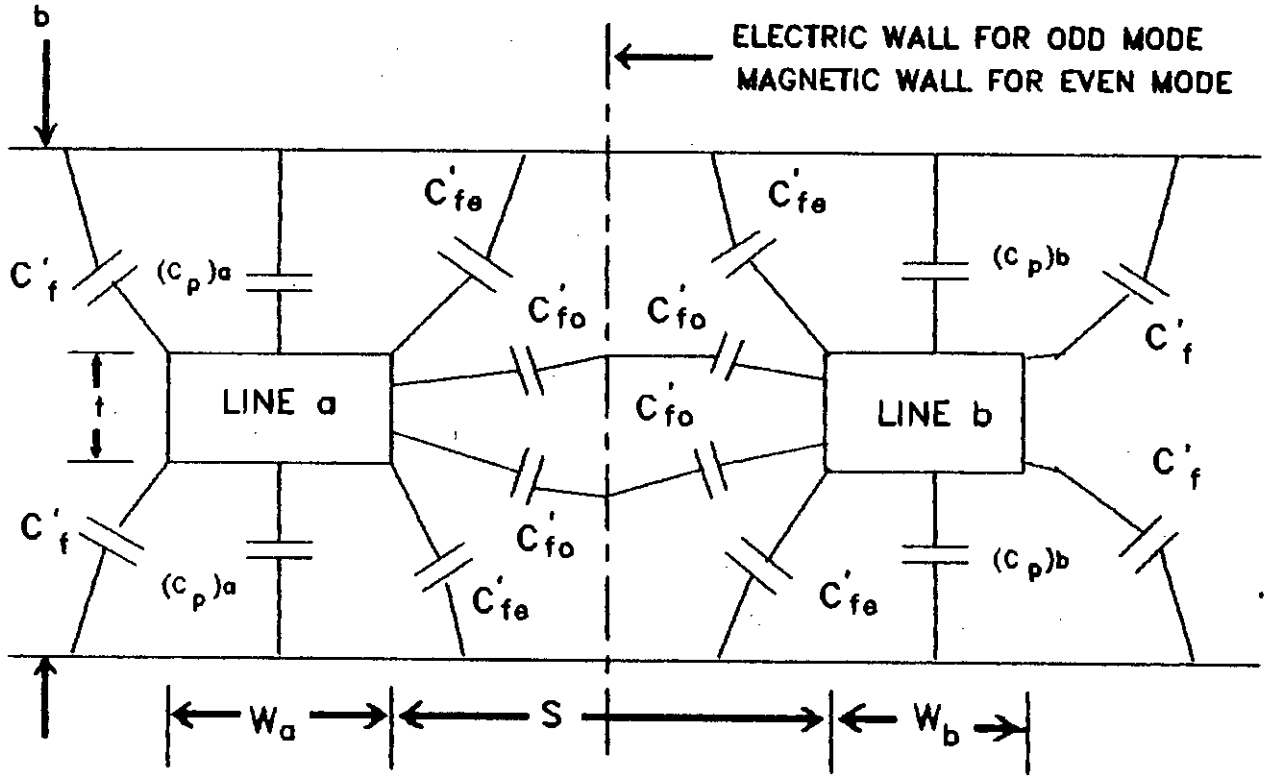

Fig 5.7 Cross section of a pair of coupled rectangular-bar parallel coupled lines. The two lines 'a' and 'b' are unsymmetrical in width

$$\frac{C_a}{e}=\frac{\eta_0(Y_{oo})_a}{\sqrt{\epsilon_r}},\ \frac{C_{ab}}{e}=\frac{\eta_0}{\sqrt{\epsilon_r}}\left(\frac{(Y_{oo})_a-(Y_{oe})_a}{2}\right) \qquad [5.13(a)]$$

$$\frac{C_b}{e}=\frac{\eta_0(Y_{oo})_b}{\sqrt{\epsilon_r}},\ \frac{C_{ab}}{e}=\frac{\eta_0}{\sqrt{\epsilon_r}}\left(\frac{(Y_{oo})_b-(Y_{oe})_b}{2}\right) \qquad [5.13(b)]$$

Next a convenient value of t/b is selected and using figure (5.2) both s/b and C_{fe}'/ϵ are calculated. Lastly the value of C_f'/ϵ is determined from the selected value of t/b and figure (5.4). Then the width of the bars are calculated from the following equations,

$$\frac{w_a}{b}=\frac{1}{2}\left(1-\frac{t}{b}\right)\left[\frac{C_a}{2e}-\frac{C_{fe}'}{e}-\frac{C_f'}{e}\right] \qquad (5.14)$$

$$\frac{w_b}{b}=\frac{1}{2}\left(1-\frac{t}{b}\right)\left[\frac{C_b}{2e}-\frac{C_{fe}'}{e}-\frac{C_f'}{e}\right] \qquad (5.15)$$

This procedure also works for the thin strip case where $t/b\approx 0$. If either w_a/b or w_b/b is less than $0.35[1-t/b]$, eqn. (5.9) should be applied to obtain corrected values.

5.6 **An array of parallel coupled lines**: Figure (5.8) shows an array of parallel coupled lines which is used in the interdigital line filters. In the structure shown all of the bars have the same t/b ratio and the other dimensions of the bars are easily obtained by generalizing the procedure described in designing the unsymmetrical parallel coupled lines. In the structure of figure (5.8) the electrical properties of the structure are characterized in terms of self capacitances C_k per unit length of each bar with

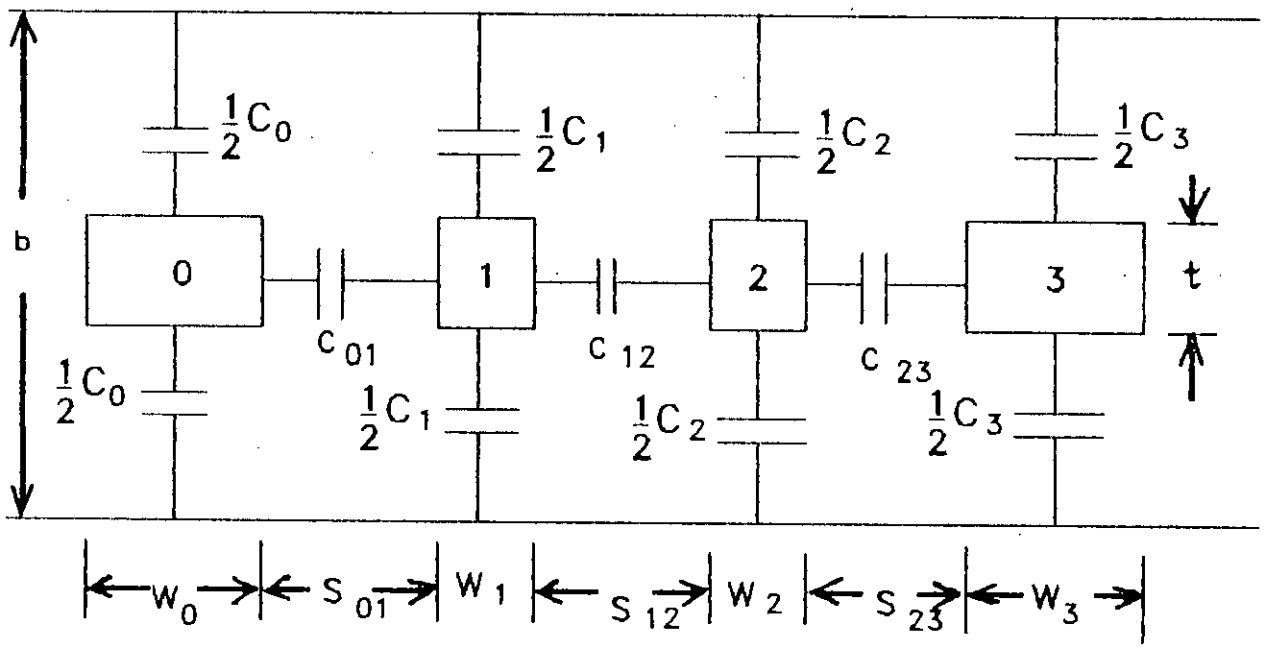

Fig 5.8 Cross section of an array of parallel -coupled lines between ground planes

unit length of each bar with respect to ground and the mutual capacitances $C_{k,k+1}$ per unit length between adjacent bars k and k+1. This representation is not necessarily always highly accurate because there can conceivably be a significant amount of fringing capacitance in some cases between a given line element, and for example, the line element beyond the nearest neighbor. However, at least for geometries, experiment has shown this representation to have satisfactory accuracy for applications such as interdigital filter design.

Equations are given for the normalized self and mutual capacitances C_k/ϵ and $C_{k,k+1}/\epsilon$ per unit length for all the lines in the structure for design of the parallel coupled array of rectangular bars between ground planes. The cross sectional dimensions of the bars and spacings between them are determined by first, choosing values for t and b and then since,

$$\frac{(\Delta C)_{k,k+1}}{\epsilon} = \frac{C_{k,k+1}}{\epsilon} \qquad (5.16)$$

figure (5.2) can be used to determine $s_{k,k+1}/b$. In this way the spacings $s_{k,k+1}$ between all the bars are obtained. Also, using figure (5.2) the normalized fringing capacitances $(C_{fe}')_{k,k+1}/\epsilon$ associated with the gaps $s_{k,k+1}$ between bars are obtained. Then the normalized width of the kth bar is,

$$\frac{w_k}{b} = \frac{1}{2}\left(1-\frac{t}{b}\right)\left[\frac{C_k}{2\epsilon} - \frac{(C_{fo}')_{k-1,k}}{\epsilon} - \frac{(C_{fo}')_{k,k+1}}{\epsilon}\right] \qquad (5.17)$$

In the case of the bar at the end of the array i.e. the bar

at the far left in figure (5.8) C_{fe}'/ϵ for the edge of the bar which has no neighbor must be replaced by C_f'/ϵ which is to be determined from figure (5.4) As for example, for bar '0' eqn. (5.17) will become,

$$\frac{w_0}{b}=\frac{1}{2}\left(1-\frac{t}{b}\right)\left[\frac{C_0}{2\epsilon}-\frac{C_f'}{\epsilon}-\frac{(C_{fe}')_{0,1}}{\epsilon}\right] \qquad (5.18)$$

If $w_k/b<0.35[1-t/b]$ for any of the bars, the width correction given in eqn. (5.9) should be applied to those bars where this condition exists.

5.7 **Summary**: Coupling between a pair of parallel coupled TEM lines between ground plates have been described in terms of even and odd mode impedances and admittances. The procedure of calculating the widths of coupled rectangular bars and the interline spacings of the rectangular bars from self and interline capacitance are presented following *Getsinger's* [7] chart analysis.

CHAPTER 6

Designing a filter and obtaining its physical dimensions

6.1 **Introduction**: This chapter deals in detail with the design procedure of the band pass filter and calculation of its physical dimensions. In determining the widths and spacings of the rectangular bars, the curves by *Getsinger* [7] and the low pass prototype values from the catalogue by *Saal* [16] are used.

6.2 **Design of the experimental filter**: The filter to be designed should have the following specifications : The stop band attenuation level (A_S[dB]) is 60.1 dB or a_S[N]=6.91 Neper. Pass band VSWR (Voltage Standing Wave Ratio) is less than 1.222. The percentage bandwidth is 1.0. The center frequency is 2000 MHz. From the given VSWR the reflection coefficient is found to be equal to 0.1 i.e. ρ=10%. Also the maximum attenuation in the pass band is found to be 0.044 dB for a VSWR=1.222. The bandwidth scaling factor calculated from the following equation is 41.35,

$$a=\frac{f_0|\sin 2\theta_0|}{4\theta_0(f_2-f_1)} \qquad (6.1)$$

where $f_0=(f_1+f_2)/2$ is the center frequency of the filter and f_1 and f_2 are the pass band edge frequencies which are 1990 MHz and 2010 MHz respectively. θ_0 is the arbitrary stepped impedance plane and equals to $\pi/3$.

6.2.1 **Low pass prototype element values**: The following low pass prototype element values are obtained from the 'filter katalog' by *Saal*. The values are given for n=5, ρ=10%, A_s=60.1 dB, Ω_s=2.202689, θ=27°.

C_1=0.9265 C_2=0.05866 C_3=1.6660

C_4=0.1607 C_5=0.8363

Ω_2=3.611883 Ω_4=2.303827

By using the equations 4.9 and 4.10 the following transmission zeros are calculated,

λ_{2+}=1.045 λ_{2-}=0.957 λ_{4+}=1.028

λ_{4-}=0.973

6.3 **Length of the networks**: If the center frequency is f_0, the wave length of the signal can be calculated from the relation $\lambda_0=c/f_0$, where c is the velocity of light and equals to 3×10^{10} cm/sec. Therefore the length of the rectangular bars of network 1 will be $\lambda_0/(6\times2.54)$ inch and that of the network 2 will be $\{\lambda_0/(2\times2.54)-\lambda_0/(6\times2.54)\}$ inch. From the above relation the length l_1 of network 1 is **0.9842** and l_2 of network 2 is **1.9685**.

6.4 **Characteristic admittance matrices of two networks**: All the elements of the matrices are calculated using the equations given in chapter 4. Now putting the values of the elements in the matrices, the following two characteristic admittance matrices are formed for network 1 and 2 respectively,

NETWORK 1

1	2	3	4	5
50.3392	-6.1021	0.0000	0.0000	0.0000
-6.1021	11.2246	-5.1225	0.0000	0.0000
0.0000	-5.1225	100.8811	-16.2130	0.0000
0.0000	0.0000	-16.2130	30.7153	-14.5023
0.0000	0.0000	0.0000	-14.5023	54.4327

(6.2)

NETWORK 2

1	2	3	4	5
49.6045	-5.3674	0.0000	0.0000	0.0000
-5.3674	11.2246	-5.8572	0.0000	0.0000
0.0000	-5.8572	100.3328	-14.9300	0.0000
0.0000	0.0000	-14.9300	30.7153	-15.7853
0.0000	0.0000	0.0000	-15.7853	55.7157

(6.3)

6.4.1 **Input and output transformer elements**: The input and output terminals of the filter are shown in figure (6.1) Direct connection of the input and output terminals to the external ports will lower the impedance of the internal elements. To overcome this problem, two transformers are used at input and output between the external ports and the corresponding internal elements as shown in figure (6.2) The transformer elements have unity characteristic impedances and one sixth of a wavelength long at the center frequency. After adding the unit elements at input and output the characteristic admittance matrix of network 1 becomes,

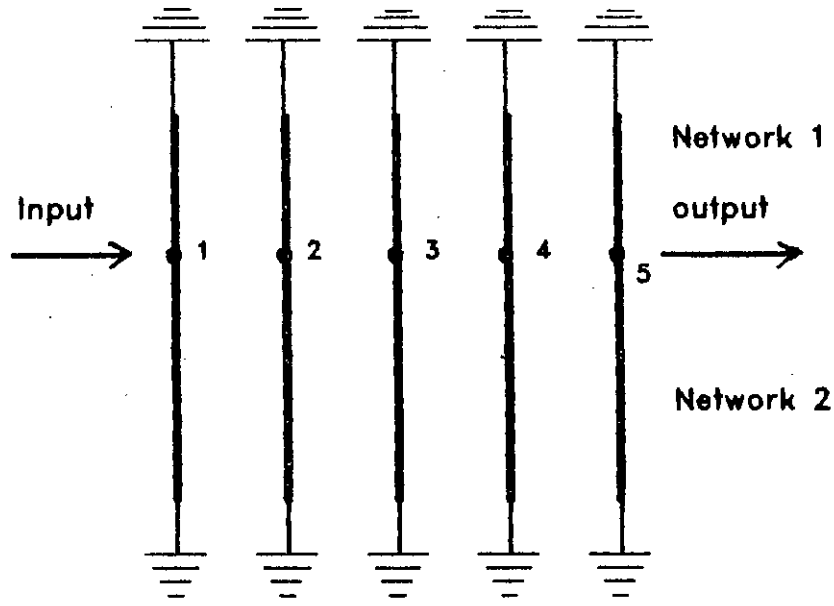

Fig 6.1 Realization of the two networks of a filter using TEM lines short circuited at one endfor n=5. The open ends of the coupled lines of the two networks are joined together

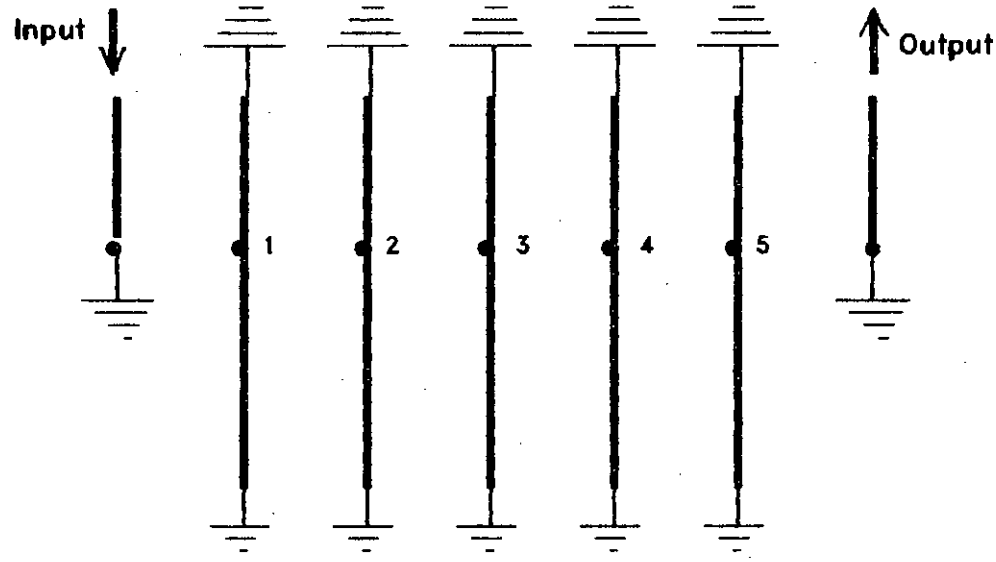

Fig 6.2 The complete filter with the input and output transformer elements

$$
\begin{array}{c}
\begin{array}{ccccccc} 0 & 1 & 2 & 3 & 4 & 5 & 6 \end{array} \\
\begin{bmatrix}
1.0000 & -1.0000 & 0.0000 & 0.0000 & 0.0000 & 0.0000 & 0.0000 \\
-1.0000 & 51.3392 & -6.1021 & 0.0000 & 0.0000 & 0.0000 & 0.0000 \\
0.0000 & -6.1021 & 11.2246 & -5.1225 & 0.0000 & 0.0000 & 0.0000 \\
0.0000 & 0.0000 & -5.1225 & 100.8811 & -16.2130 & 0.0000 & 0.0000 \\
0.0000 & 0.0000 & 0.0000 & -16.2130 & 30.7153 & -14.5023 & 0.0000 \\
0.0000 & 0.0000 & 0.0000 & 0.0000 & -14.5023 & 55.4327 & -1.0000 \\
0.0000 & 0.0000 & 0.0000 & 0.0000 & 0.0000 & -1.0000 & 1.0000
\end{bmatrix}
\end{array} \qquad (6.4)
$$

The characteristic admittance matrix of network 2 remains same because the unit element is not connected with network 2.

6.4.2 **Admittance scaling factor**: Admittance scaling factor is necessary for physical realizability of the filter. This factor is chosen in such a way so that capacitances from line to ground for all lines except the input and output lines are almost same. Generally, at first, all the lines except the lines on which the input and output ports are connected are scaled by a factor $1/\sqrt{b}$ where,

$$b=\frac{2a(\frac{\theta_0}{\pi})}{|\tan\theta_0|} \qquad (6.5)$$

and a is given by eqn. (6.1)

In the present case, firstly, the modification of the networks is made in lines 1 and 5 (because line 0 and 6 are the input and output port connection). After scaling of the lines 1 and 5 of both the networks by the factor $1/\sqrt{b}$ the resultant admittance matrices become,

NETWORK 1

0	1	2	3	4	5	6
1.0000	-0.1447	0.0000	0.0000	0.0000	0.0000	0.0000
-0.1447	1.0752	-0.8831	0.0000	0.0000	0.0000	0.0000
0.0000	-0.8831	11.2246	-5.1225	0.0000	0.0000	0.0000
0.0000	0.0000	-5.1225	100.8811	-16.2130	0.0000	0.0000
0.0000	0.0000	0.0000	-16.2130	30.7153	-2.0988	0.0000
0.0000	0.0000	0.0000	0.0000	-2.0988	1.1610	-0.1447
0.0000	0.0000	0.0000	0.0000	0.0000	-0.1447	1.0000

(6.6)

NETWORK 2

1	2	3	4	5
1.0389	-0.7768	0.0000	0.0000	0.0000
-0.7768	11.2246	-5.8572	0.0000	0.0000
0.0000	-5.8572	100.3328	-14.9300	0.0000
0.0000	0.0000	-14.9300	30.7153	-2.2845
0.0000	0.0000	0.0000	-2.2845	1.1669

(6.7)

After scaling line 1 and 5 of both the networks, the remaining lines are scaled in such a way that the difference among the diagonal elements of the matrices is not too large. In doing so, the following procedure is followed.

In network 1, the second diagonal element i.e. Y_{11} (1.0752) is multiplied by 1.2 and the product is treated as the new value of third diagonal element i.e. Y_{22} (which was previously 11.2246). Similarly the new value of fifth diagonal element Y_{44} (which was previously 30.7153) is found by multiplying Y_{55} (1.1610) by 1.2. Finally the center diagonal element Y_{33} (which was previously 100.8811) is found from the product of 1.2 and the new value of Y_{22} (1.2903). While multiplying the diagonal elements by 1.2 the corresponding row and column elements are multiplied by $\sqrt{1.2}$ which is demonstrated by a simple example in

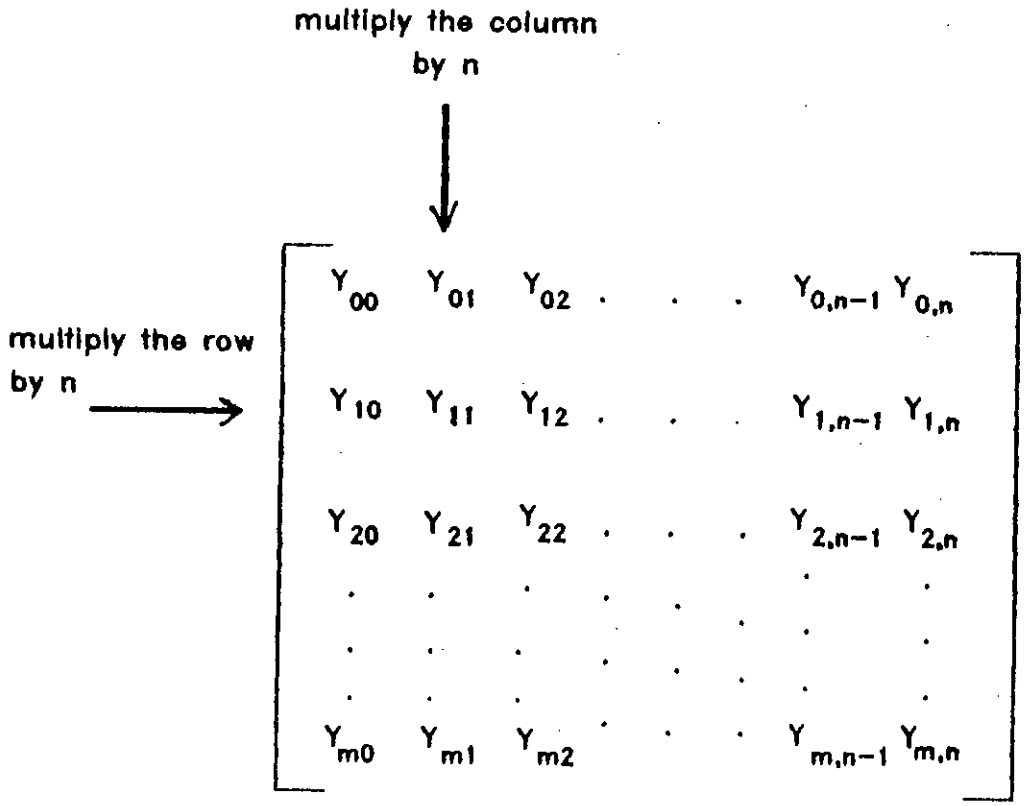

Fig 6.3 Modification of different elements of an admittance matrix by multiplying with a factor n

figure (6.3) The same procedure is applied to network 2, where, $(Y_{22})_{new}=1.2\times(Y_{11})_{old}$, $(Y_{44})_{new}=1.2\times(Y_{55})_{old}$ and, $(Y_{33})_{new}=1.2\times(Y_{22})_{new}$. After this scaling the admittance matrices take the following shape,

NETWORK 1

0	1	2	3	4	5	6
1.0000	-0.1447	0.0000	0.0000	0.0000	0.0000	0.0000
-0.1447	1.0752	-0.2994	0.0000	0.0000	0.0000	0.0000
0.0000	-0.2994	1.2903	-0.2152	0.0000	0.0000	0.0000
0.0000	0.0000	-0.2152	1.5484	-0.4278	0.0000	0.0000
0.0000	0.0000	0.0000	-0.4278	1.3932	-0.4470	0.0000
0.0000	0.0000	0.0000	0.0000	-0.4470	1.1610	-0.1447
0.0000	0.0000	0.0000	0.0000	0.0000	-0.1447	1.0000

(6.8)

NETWORK 2

1	2	3	4	5
1.0389	-0.2589	0.0000	0.0000	0.0000
-0.2589	1.2476	-0.2384	0.0000	0.0000
0.0000	-0.2384	1.4960	-0.3893	0.0000
0.0000	0.0000	-0.3893	1.4003	-0.4878
0.0000	0.0000	0.0000	-0.4878	1.1669

(6.9)

6.5 **Static capacitance matrices**: Now eqn. (6.8) and eqn. (6.9) give the characteristic admittance matrices of network 1 and 2 respectively after the required scaling and changing of level. In order to get the static capacitance matrices all the elements of both the characteristic admittance matrices are multiplied by η_0. Finally to convert the values to a 50 Ω termination impedance the elements are divided by 50. So, to convert the characteristic admittance matrices to static capacitance matrices all the elements of the former are multiplied by η_0/Z_0 or 376.7/50=7.534.

Now multiplying all the elements of the two networks by

7.534 the following static capacitance matrices are formed,

NETWORK 1

0	1	2	3	4	5	6
7.5540	-1.0932	0.0000	0.0000	0.0000	0.0000	0.0000
-1.0932	8.1224	-2.2617	0.0000	0.0000	0.0000	0.0000
0.0000	-2.2617	9.7469	-1.6254	0.0000	0.0000	0.0000
0.0000	0.0000	-1.6254	11.6963	-3.2314	0.0000	0.0000
0.0000	0.0000	0.0000	-3.2314	10.5240	-3.3765	0.0000
0.0000	0.0000	0.0000	0.0000	-3.3765	8.7700	-1.0932
0.0000	0.0000	0.0000	0.0000	0.0000	-1.0932	7.5540

(6.10)

NETWORK 2

1	2	3	4	5
7.8480	-1.9555	0.0000	0.0000	0.0000
-1.9555	9.4176	-1.8006	0.0000	0.0000
0.0000	-1.8006	11.3011	-2.9405	0.0000
0.0000	0.0000	-2.9405	10.5778	-3.6846
0.0000	0.0000	0.0000	-3.6846	8.8148

(6.11)

From the above two matrices the physical dimensions of the filter are now calculated. The procedure described in section (5.6) of chapter 5 is applied to find the mutual capacitance i.e. capacitance between line to line and self capacitance i.e. capacitance between line to ground of the coupled rectangular bars. The mutual capacitances can be easily calculated from the static capacitance matrices. For example, the mutual capacitance between line 1 and 2 of network 1 will simply be Y_{12} or Y_{21} which is 2.2617 as seen from eqn. (6.10). On the other hand the self capacitance of any line to ground can be calculated by adding up the respective row or column elements. For example, the self capacitance of line 2 of network 1 will be the addition of -2.2617, 9.7469 and -1.6254 which is equal to 5.8598 as seen from

eqn. (6.10). This capacitance value is same for either the row or the column addition. After calculating the normalized capacitance values of both the networks, eqns. (5.17), (5.18) and *Getsinger's* [7] curves in figures (5.2), (5.3) and (5.4) are used, as described in section (5.6) of chapter 5, to find the physical dimensions of the filter.

6.6 **Calculation of physical dimensions**: After calculating all the widths and spacings of the rectangular bars the following table is constructed.

TABLE 6.1 Calculation of widths and spacings of Network 1

k	C_k/ϵ	$C_{k,k+1}/\epsilon$	$(C_{fe}')_{k,k+1}/\epsilon$	w_k/b	w_k	$s_{k,k+1}/b$	$s_{k,k+1}$
0	6.4608			0.6651	0.4430		
0,1		1.0932	0.5300			0.3350	0.2230
1	4.7674			0.5704	0.3800		
1,2		2.2617	0.2240			0.1700	0.1130
2	5.8598			0.8386	0.5580		
2,3		1.6254	0.3100			0.2450	0.1630
3	6.8395			1.034	0.6880		
3,4		3.2314	0.1560			0.1170	0.0780
4	3.9161			0.5782	0.3850		
4,5		3.3765	0.1500			0.1120	0.0750
5	4.3003			0.5145	0.3430		
5,6		1.0932	0.5300			0.3350	0.2230
6	6.4608			0.6651	0.4430		

In the above table,

k → line number

C_k/ϵ → normalized static capacitance of kth line to ground

$C_{k,k+1}/\epsilon$ → normalized static capacitance between kth and (k+1)th line

$(C_{fe}')_{k,k+1}/\epsilon$ → normalized even mode fringing capacitance between kth and (k+1)th line

w_k → width of kth line in inches

$s_{k,k+1}$ → spacing between kth and (k+1)th line in inches

In the k column of the above table 0,1 ; 1,2 etc. means between the lines 0 and 1, 1 and 2 etc.

The center plate of the designed filter is shown in figure (6.4). The vertical cross section of two networks of the filter is shown in figure (6.5)(a) and (b). From figure (6.5) it is seen that the thickness of the center plate is t=0.2 inch and the spacing between the two ground plates is b=0.666 inch, so that t/b=0.3. The widths of all the coupled lines of network 1 except the input and output unit elements are calculated using eqn. (5.17) and figure (5.2). For width calculation of two unit elements eqn. (5.18), figure (5.2) and figure (5.4) are used. The width calculation of line 1 and one of the unit elements line 0 are shown below.

For line 1, C_1/ϵ=4.7674, $(C_{fe}')_{0,1}/\epsilon$=0.5300, and $(C_{fe}')_{1,2}/\epsilon$=0.2240. The self capacitance is found from table (6.1) and the fringing capacitances are found from figure (5.2) corresponding to the given values of t/b and the mutual capacitance $C_{k,k+1}/\epsilon$ or $(\Delta C)_{k,k+1}/\epsilon$ of table (6.1). Now putting these values in eqn (5.17),

$$\frac{w_1}{b}=\frac{1}{2}(1-0.3)\left[\frac{1}{2}(4.7674)-0.5300-0.2240\right]$$

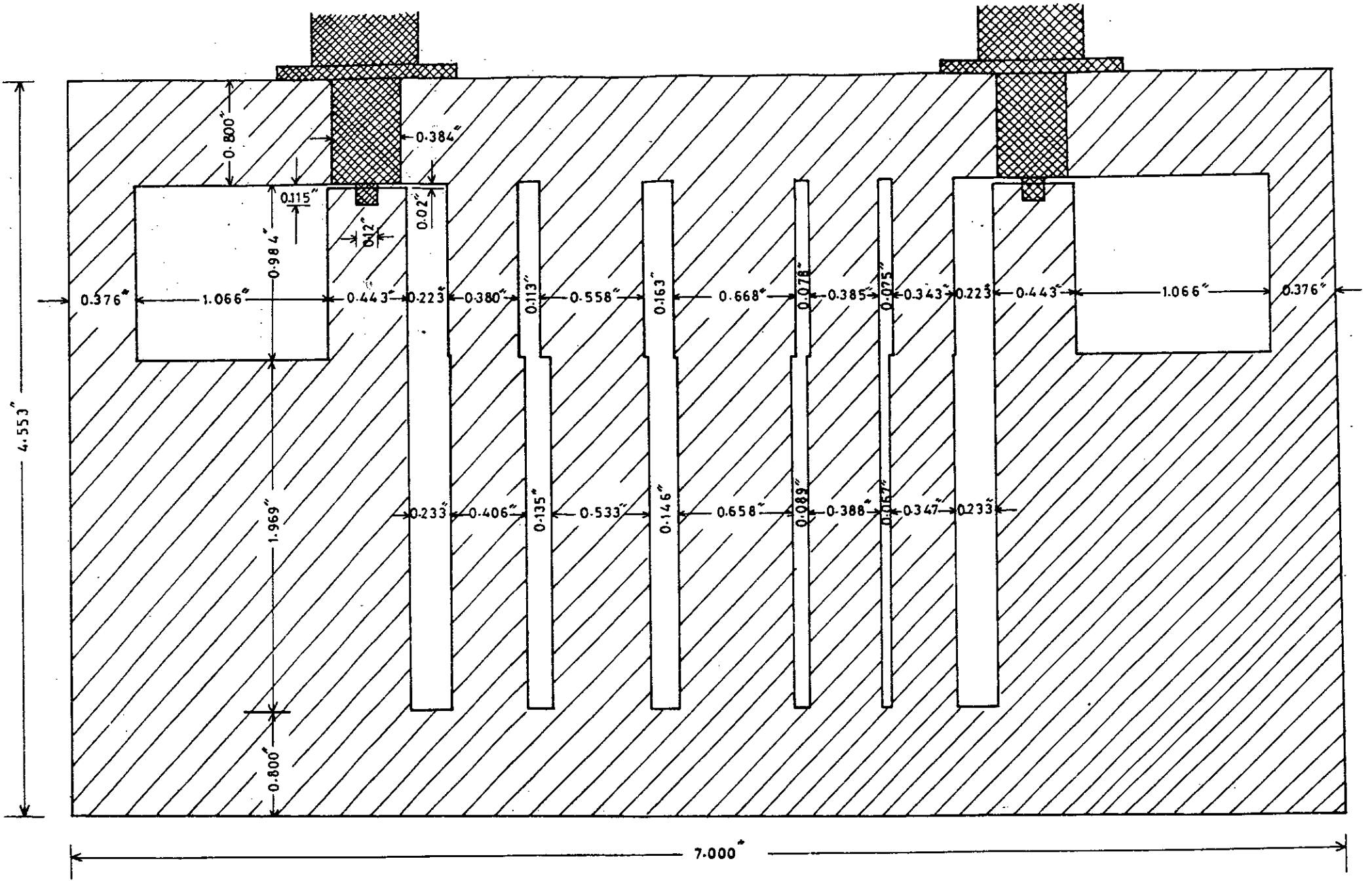

Fig. 6.4 : The cross section of the centre plate of the designed filter.

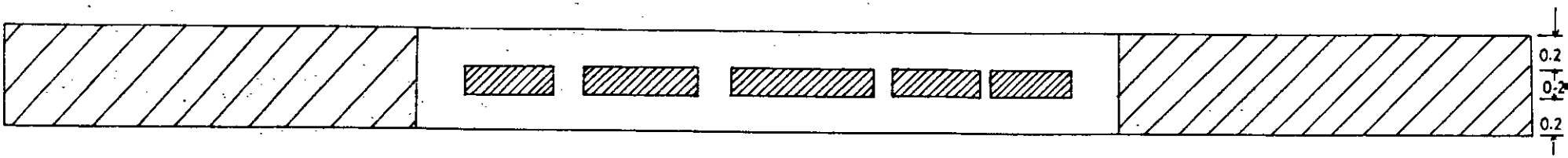

Fig. 6.5(a): Vertical cross section of network 2

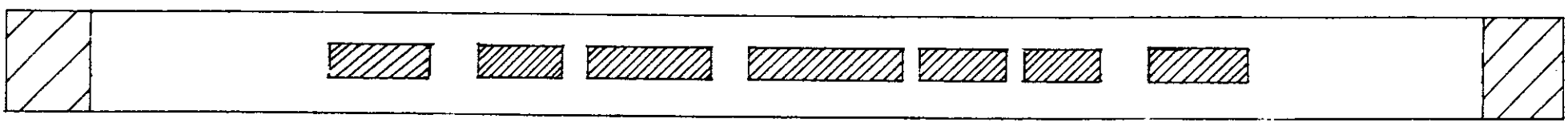

Fig. 6.5(b): Vertical cross section of network 1

$\therefore w_1 = 0.3800$ inch

But for line 0, eqn. (5.18) will be used instead of (5.17) because this line has no neighbor and that is why $(C_{fe}')_{k-1,k}/\epsilon$ in eqn. (5.17) is replaced by C_f'/ϵ in eqn. (5.18). For line 0, C_f'/ϵ is found, from figure (5.4) to be equal to 0.8000 and this is same for both the unit elements. From table (6.1) $C_0/\epsilon = 6.4608$, and $(C_{fe}')_{0,1}/\epsilon = 0.5300$. Now putting these values in eqn. (5.18),

$$\frac{w_0}{b} = \frac{1}{2}(1-0.3)\left[\frac{1}{2}(6.4608) - 0.8000 - 0.5300\right]$$

$\therefore w_0 = 0.4430$ inch.

A similar table is formed for network 2 under the same symbols which is given below. Only in the k column G means ground and G,1 5,G etc. means between ground and 1, 5 and ground etc.

TABLE 6.2 Calculation of widths and spacings of Network 2

k	C_k/ϵ	$C_{k,k+1}/\epsilon$	$(C_{fe}')_{k,k+1}/\epsilon$	w_k/b	w_k	$s_{k,k+1}/$	$s_{k,k+1}$
G,1							
1	5.8924			0.6590	0.4390		
1,2		1.9555	0.2630			0.2027	0.1350
2	5.6614			0.8010	0.5330		
2,3		1.8006	0.2800			0.2192	0.1460
3	6.5600			0.9880	0.6580		
3,4		2.9405	0.1780			0.1336	0.0890
4	3.9527			0.5820	0.3880		
4,5		3.6846	0.1350			0.1006	0.0670
5	5.1302			0.5710	0.3800		
5,G							

6.7 **Correction of widths of network 2**: It is seen from table (6.2) that spacings between ground and line 1 and that between line 5 and ground of network 2 are not given. In network 1 the widths of the unit elements as well as their spacings with the nearest neighbor lines are identical at both ends thus making the network symmetrical at both ends. To restore the symmetry in network 2 i.e. to modify the widths of line 1 and 5 in such a way that their spacings with ground at both ends are identical, the following iterations are carried out without affecting the widths and spacings of rest of the lines.

It is seen from table (6.2) that w_1=0.439". If the ground spacing of line 1 is assumed to be 0.2" i.e. $s_{G,1}$=0.2", w_1 and $s_{G,1}$ adds up to 0.639". The objective is to modify the width w_1 and to find a new value of $s_{G,1}$ in such a way that the sum of w_1 and $s_{G,1}$ remains 0.639". The iterations are carried out until two successive iterations give same result. All the values and calculations refer to eqn. (5.17) and figure (5.2)

Iteration 1: $s_{G,1}$=0.2" (assumed) $s_{G,1}/b$=0.3

$(C_{fe}')_{G,1}/\epsilon$=0.365 (from fig. (5.2)) $(\Delta C)_{k,k+1}/\epsilon$=1.27 (fig. (5.2))

$(C_k)_{new}$=7.8480-1.9555-1.27=4.6225 (from eqn. (6.11))

$\therefore$ $\mathbf{(w_1)_{new}=0.392"}$ and $\mathbf{(s_{G,1})_{new}=0.247"}$

Iteration 2: $s_{G,1}$=0.247" (from previous iteration) $s_{G,1}/b$=0.371

$(C_{fe}')_{G,1}/\epsilon$=0.430 (from fig. (5.2)) $(\Delta C)_{k,k+1}/\epsilon$=0.96 (fig. (5.2))

$(C_k)_{new}$=7.8480-1.9555-0.96=4.9325 (from eqn. (6.11))

$\therefore$ $\mathbf{(w_1)_{new}=0.413"}$ and $\mathbf{(s_{G,1})_{new}=0.226"}$

Iteration 3: $s_{G,1}$=0.226" (from previous iteration) $s_{G,1}/b$=0.340

$(C_{fe}')_{G,1}/\epsilon$=0.410 (from fig. 5.2) $(\Delta C)_{k,k+1}/\epsilon$=1.08 (fig. 5.2)

$(C_k)_{new}$=7.8480-1.9555-1.08=4.8125 (from eqn. 6.1)

$\therefore$ $(w_1)_{new}$=0.404" and $(s_{G,1})_{new}$=0.235"

Iteration 4: $s_{G,1}$=0.235" (from previous iteration) $s_{G,1}/b$=0.353

$(C_{fe}')_{G,1}/\epsilon$=0.420 (from fig. 5.2) $(\Delta C)_{k,k+1}/\epsilon$=1.03 (fig. 5.2)

$(C_k)_{new}$=7.8480-1.9555-1.03=4.8625 (from eqn. 6.1)

$\therefore$ $(w_1)_{new}$=0.407" and $(s_{G,1})_{new}$=0.232"

Iteration 5: $s_{G,1}$=0.232" (from previous iteration) $s_{G,1}/b$=0.348

$(C_{fe}')_{G,1}/\epsilon$=0.418 (from fig. 5.2) $(\Delta C)_{k,k+1}/\epsilon$=1.05 (fig. 5.2)

$(C_k)_{new}$=7.8480-1.9555-1.05=4.8425 (from eqn. 6.1)

$\therefore$ $(w_1)_{new}$=0.406" and $(s_{G,1})_{new}$=0.233"

Iteration 6: $s_{G,1}$=0.233" (from previous iteration) $s_{G,1}/b$=0.350

$(C_{fe}')_{G,1}/\epsilon$=0.418 (from fig. 5.2) $(\Delta C)_{k,k+1}/\epsilon$=1.05 (fig. 5.2)

$(C_k)_{new}$=7.8480-1.9555-1.05=4.8425 (from eqn. 6.1)

$\therefore$ $(w_1)_{new}$=0.406" and $(s_{G,1})_{new}$=0.233"

So the final value of w_1 and $s_{G,1}$ are 0.406" and 0.233" respectively. An exactly similar procedure of iteration is carried out at the other end of the network 2. Here $s_{5,G}$ is assumed to be 0.2" which gives the summation of w_5 and $s_{5,G}$ to be (0.380"+0.2")=0.580". Now the following iterations are carried out.

Iteration 1: $s_{5,G}$=0.2" (assumed) $s_{5,G}/b$=0.3

$(C_{fe}')_{5,G}/\epsilon$=0.365 (from fig. 5.2) $(\Delta C)_{k,k+1}/\epsilon$=1.27 (fig. 5.2)

$(C_k)_{new}$=8.8148-3.6846-1.27=3.8602 (from eqn. 6.1)

$\therefore$ $(w_5)_{new}$=0.333" and $(s_{5,G})_{new}$=0.247"

Iteration 2: $s_{5,G}$=0.247" (from previous iteration) $s_{5,G}/b$=0.371

$(C_{fe}')_{5,G}/\epsilon$=0.430 (from fig. 5.2) $(\Delta C)_{k,k+1}/\epsilon$=0.96 (fig. 5.2)

$(C_k)_{new}$=8.8148-3.6846-0.96=4.1702 (from eqn. 6.11)

$\therefore$ **$(w_5)_{new}$=0.354"** and **$(s_{5,G})_{new}$=0.226"**

Iteration 3: $s_{5,G}$=0.226" (from previous iteration) $s_{5,G}/b$=0.340

$(C_{fe}')_{5,G}/\epsilon$=0.410 (from fig. 5.2) $(\Delta C)_{k,k+1}/\epsilon$=1.08 (fig. 5.2)

$(C_k)_{new}$=8.8148-3.6846-1.08=4.0502 (from eqn. 6.11)

$\therefore$ **$(w_5)_{new}$=0.345"** and **$(s_{5,G})_{new}$=0.235"**

Iteration 4: $s_{5,G}$=0.235" (from previous iteration) $s_{5,G}/b$=0.353

$(C_{fe}')_{5,G}/\epsilon$=0.420 (from fig. 5.2) $(\Delta C)_{k,k+1}/\epsilon$=1.03 (fig. 5.2)

$(C_k)_{new}$=8.8148-3.6846-1.03=4.1002 (from eqn. 6.11)

$\therefore$ **$(w_5)_{new}$=0.348"** and **$(s_{5,G})_{new}$=0.232"**

Iteration 5: $s_{5,G}$=0.232" (from previous iteration) $s_{5,G}/b$=0.348

$(C_{fe}')_{5,G}/\epsilon$=0.418 (from fig. 5.2) $(\Delta C)_{k,k+1}/\epsilon$=1.05 (fig. 5.2)

$(C_k)_{new}$=8.8148-3.6846-1.05=4.0802 (from eqn. 6.11)

$\therefore$ **$(w_5)_{new}$=0.347"** and **$(s_{5,G})_{new}$=0.233"**

Iteration 6: $s_{5,G}$=0.233" (from previous iteration) $s_{5,G}/b$=0.350

$(C_{fe}')_{5,G}/\epsilon$=0.418 (from fig. 5.2) $(\Delta C)_{k,k+1}/\epsilon$=1.05 (fig. 5.2)

$(C_k)_{new}$=8.8148-3.6846-1.05=4.0802 (from eqn. 6.11)

$\therefore$ **$(w_5)_{new}$=0.347"** and **$(s_{5,G})_{new}$=0.233"**

Thus the final value of w_5 and $s_{5,G}$ are 0.347" and 0.233" respectively. The interesting point to be noted is that assumption of any value for $s_{G,1}$ or $s_{5,G}$ leads to the same result after the required iterations. Now the new entries are made to table 6.2 to form the following table for network 2 which is finally used to realize the physical dimensions.

TABLE 6.2 Calculation of widths and spacings of Network 2 (Modified)

k	C_k/ϵ	$C_{k,k+1}/\epsilon$	$(C_{fe}')_{k,k+1}/\epsilon$	w_k/b	w_k	$s_{k,k+1}/$	$s_{k,k+1}$
G,1						0.3498	0.2330
1	5.8824			0.6590	0.4060		
1,2		1.9555	0.2630			0.2027	0.1350
2	5.6614			0.8010	0.5330		
2,3		1.8006	0.2800			0.2192	0.1460
3	6.5600			0.9880	0.6580		
3,4		2.9405	0.1780			0.1336	0.0890
4	3.9527			0.5820	0.3880		
4,5		3.6846	0.1350			0.1006	0.0670
5	5.1302			0.5710	0.3470		
5,G						0.3498	0.2330

6.8 **Summary**: In this chapter the physical dimensions of the parallel coupled lines of both the networks of the filter are calculated using some specified expressions for width and spacing calculation and the curves of *Getsinger* [7]. Also for network 2 modifications in width and spacing are made at the two ends to keep the symmetry of the netwo that are used for modification are also given at the end.

CHAPTER 7

Fabrication of the designed filter and measurement of insertion loss

7.1 **Introduction**: In this chapter, the fabrication technique of the designed filter has been presented in details. After construction, the filter has been tested by measuring the insertion loss characteristics directly from the network analyzer and also with the help of Microwave signal generator and microwave power meter. The experimental results are presented and discussed in this chapter.

7.2 **Fabrication of the designed filter**: A neat drawing of the designed filter with all dimensions has been given in figures (6.4) (6.5(a)) and (6.5(b)) of chapter 6. The experimental filter has been constructed by cutting and machining brass plates. From figures (6.5(a)) and (6.5(b)) it is clear that the resonator elements are supported by two cover plates which actually act as the ground plates. These ground plates were made by cutting and machining brass plates with less hardship because the dimensions were large enough to maintain precision. But the cutting and machining of the resonator elements and the small pieces in between them were very much difficult because of their precise dimension upto the third decimal of an inch.

Five resonator elements and two transformer elements of thickness 0.233 inch , as shown figure (6.5)(a), were cut and machined very carefully from a brass plate of thickness 0.25 inch. Each of the cover plates were also made of brass plates and placed 0.2 inch away from the center plate of the filter. The center plate or the resonator elements along with the transformer elements were first assembled together by light welding. After welding, the resonator elements and the small pieces were screwed tightly in between two spacers of thickness 0.2 inch. After this the two ground plates were screwed to the center plate. In order to connect the filter to the measuring instruments, two Flange Mount Jack Receptacles (Captured Center Contact Straight Terminal, Part Number 3052-1201-10) were mounted on the input and output transformer elements as shown in figure (6.4) Some photographs of the constructed filter are shown in figures (7.8)(a) and (b).

7.3 **Measurement of insertion loss characteristics**: The diagram of the arrangement for measuring the insertion loss of a filter by means of a power meter and thermistor mount is shown in figures (7.1) and (7.2) The arrangement consists of a hp-430C microwave power meter, a hp-477B coaxial thermistor mount and hp-616B UHF signal generator. The thermistor is a resistive device capable of dissipating radio frequency power and can change resistance using the thermal energy absorbed. It has a

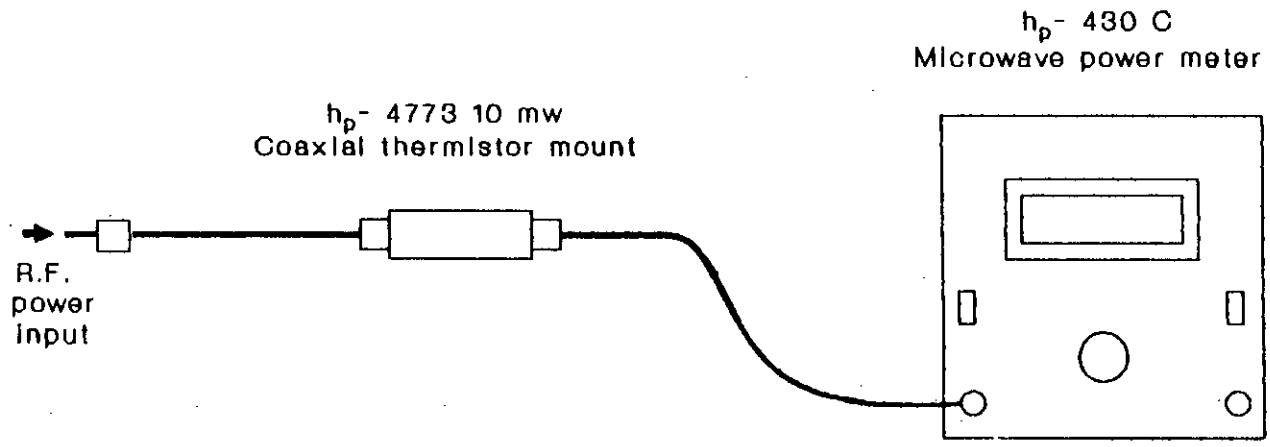

Fig. 7.1 Measurement of microwave power of a microwave source at discrete frequency points with the help of a microwave power meter.

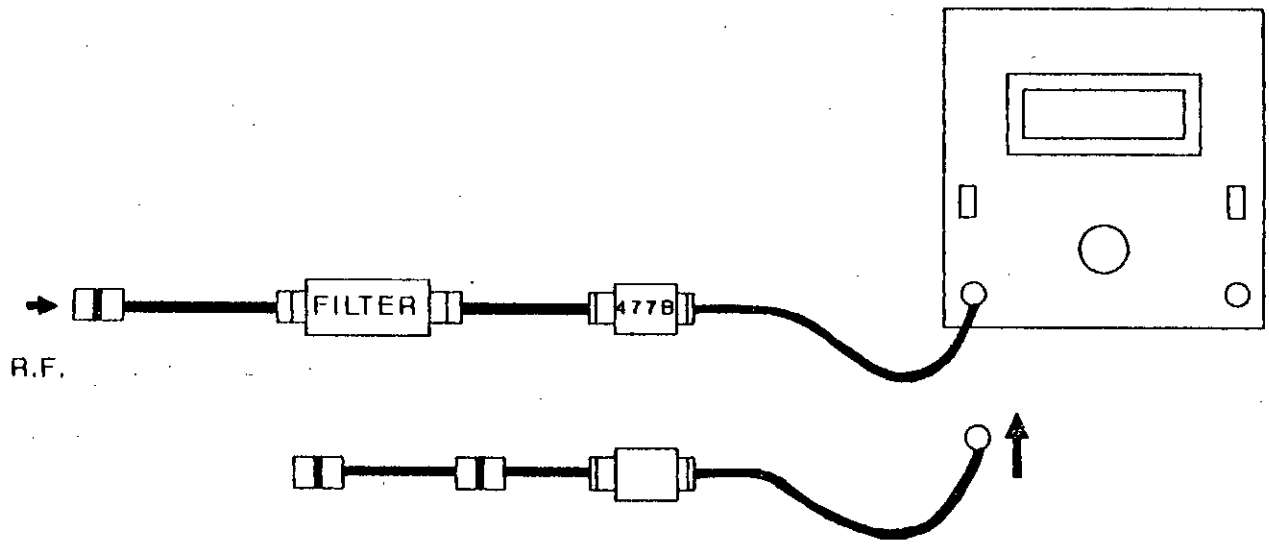

Fig. 7.2 Measurement of input and output power of a microwave filter for obtaining power loss ratio at a particular frequency.

negative temperature co-efficient and is designed to operate at 200 ohm resistance.

In this measuring arrangement, the thermistor mount forms one leg of a self balancing bridge of the power meter. The power meter contains such a bridge, a 10.8 KHz oscillator, a dc bias circuit and a meter circuit. Initially the thermistor element is connected to the instrument bridge circuit keeping the bias off but is not connected to the r.f. power source. The thermistor mount bridge is balanced when the element changes its cold resistance state to its operating resistance state. The change takes place as the element absorbs power from the oscillator and dc power from the bias circuit of the power meter.

The input and output power of the filter were measured at different frequencies within the pass band using the UHF signal generator as the input power source, the power meter as the output power measuring device and the thermistor mount. The following procedure was followed to take the readings. First, the indicator of the power meter is set at zero position by the 'zero set' knobs. The power range indicator is set at 1 mW position. The r.f. power source (UHF signal generator) is then connected to the thermistor mount. The thermistor element absorbs the external r.f. power, gets heated and changes its resistance which unbalances the bridge.

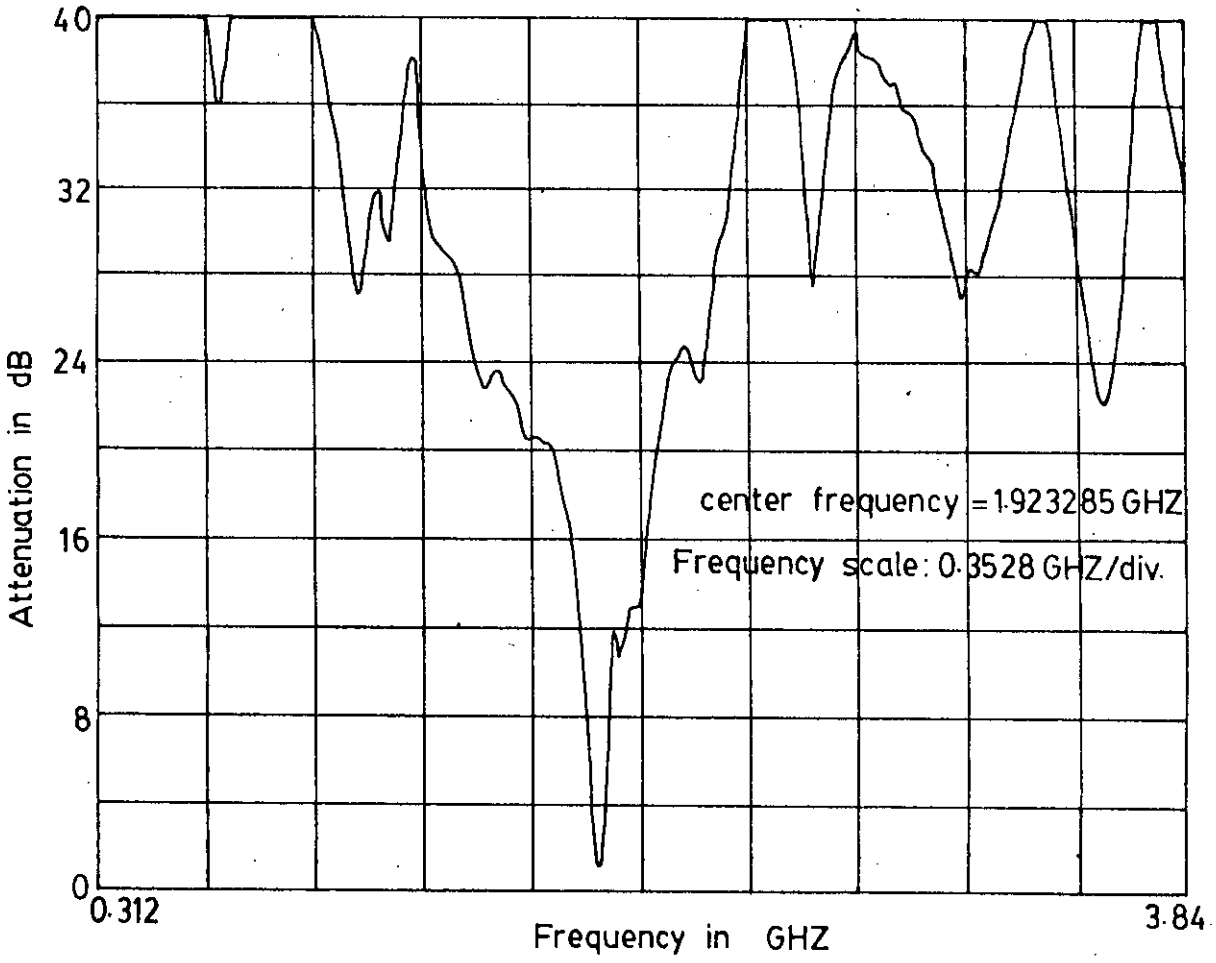

Fig. 7.3(a) Insertion loss characteristics of the designed filter obtained from the network analyzer.

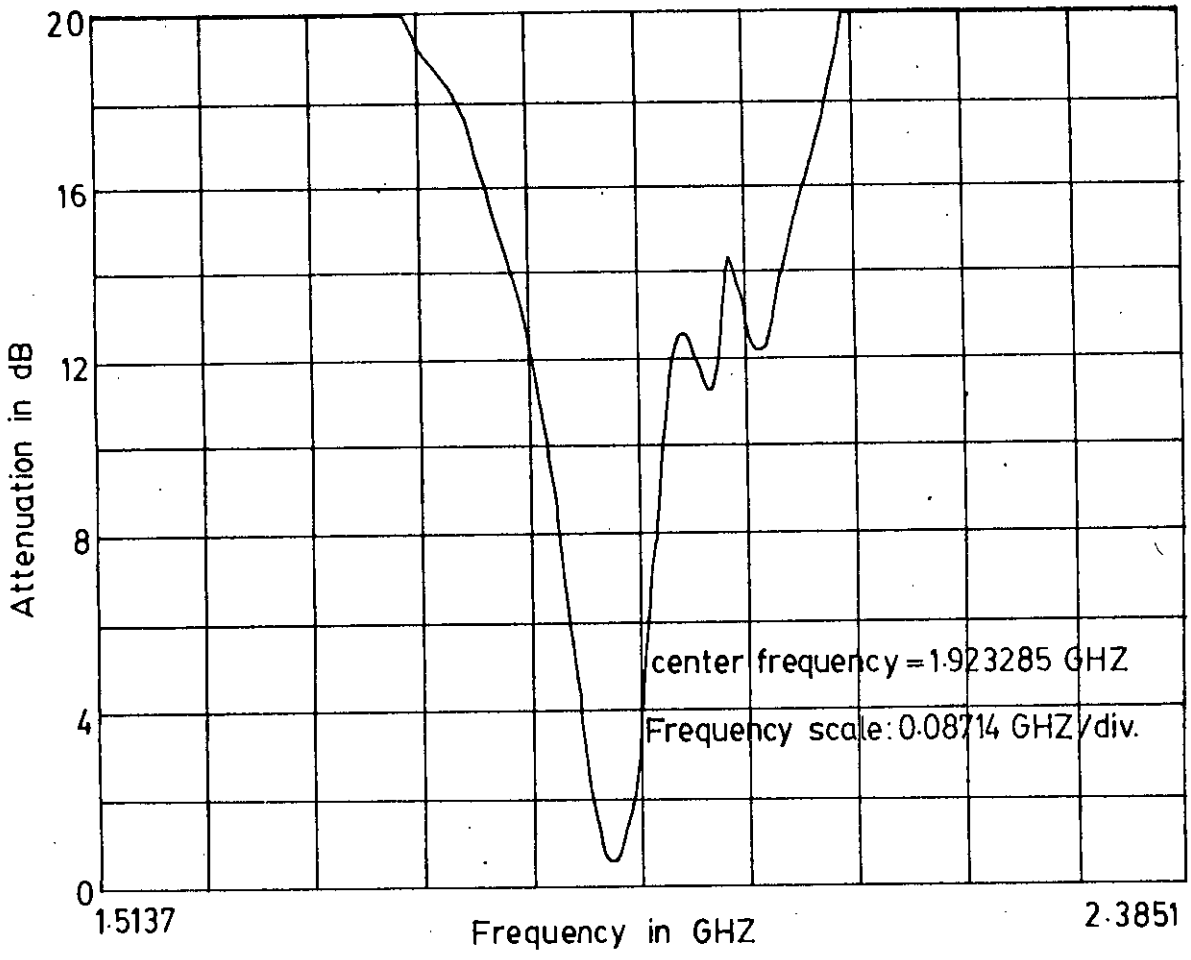

Fig. 7.3(b) Insertion loss characteristics of the designed filter within a short span of frequency.

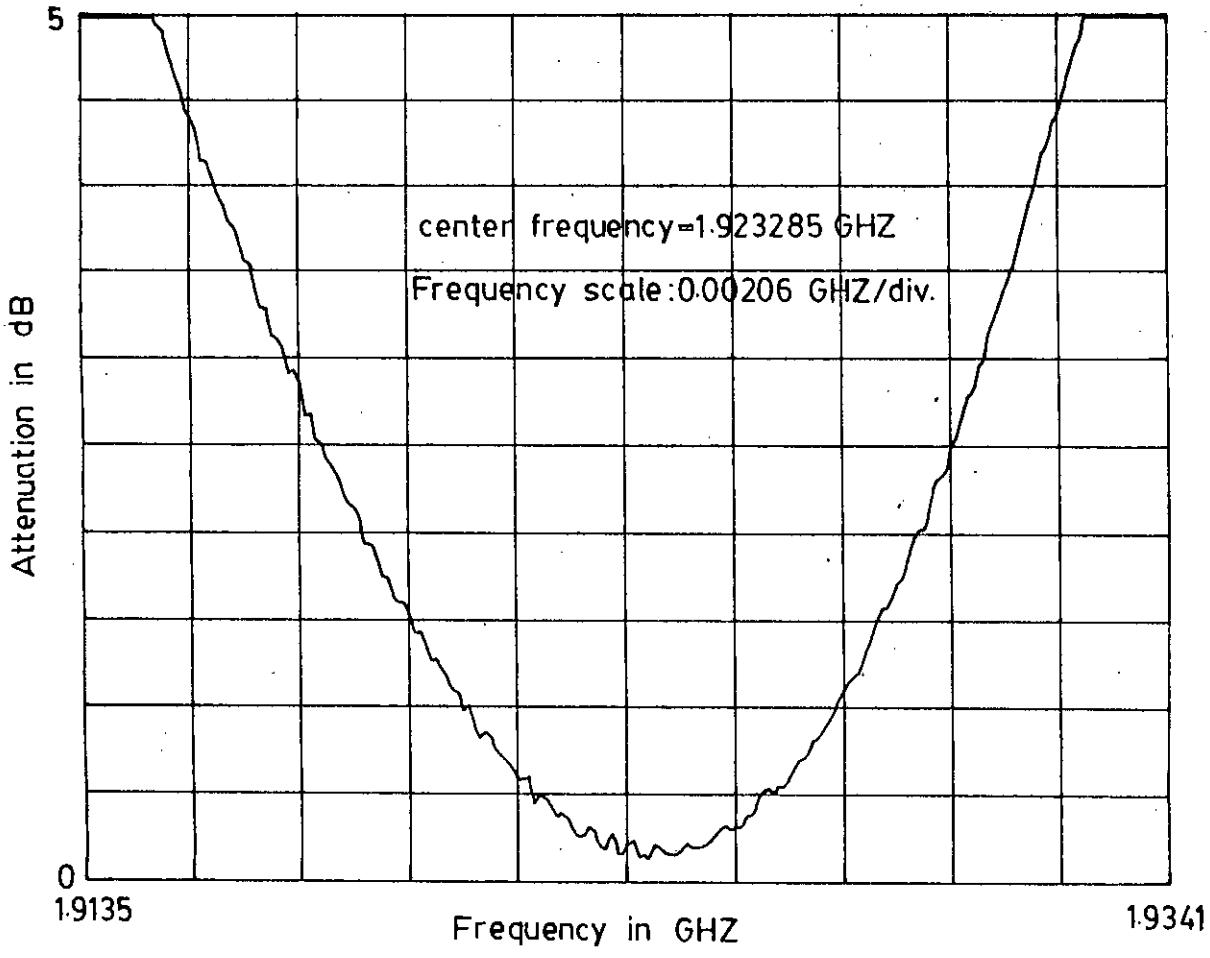

Fig. 7.4 An extended plot of the pass band of the designed filter obtained from the network analyzer.

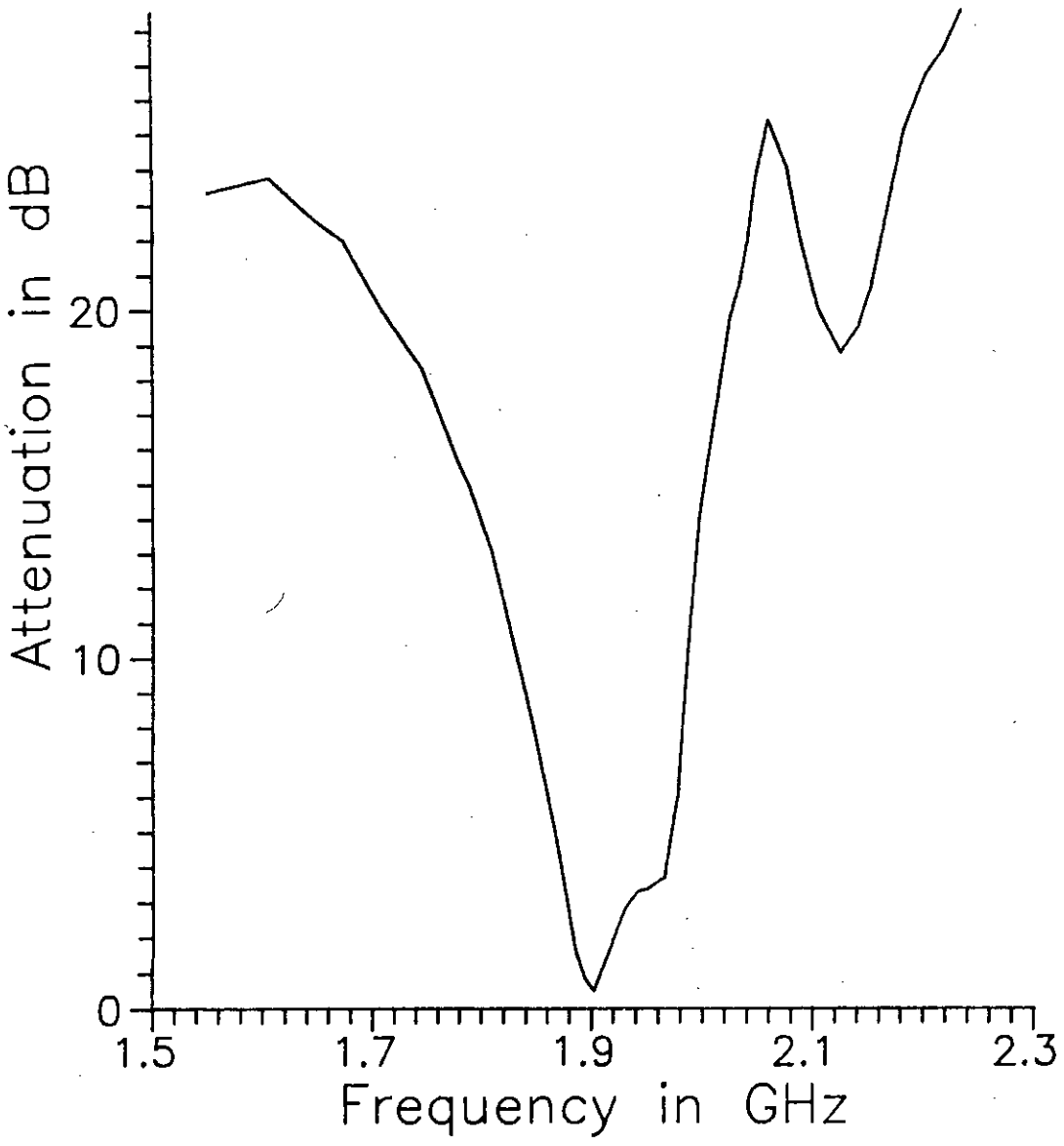

Fig 7.5 Insertion loss characteristics of the filter for a particular adjustment of ground plates

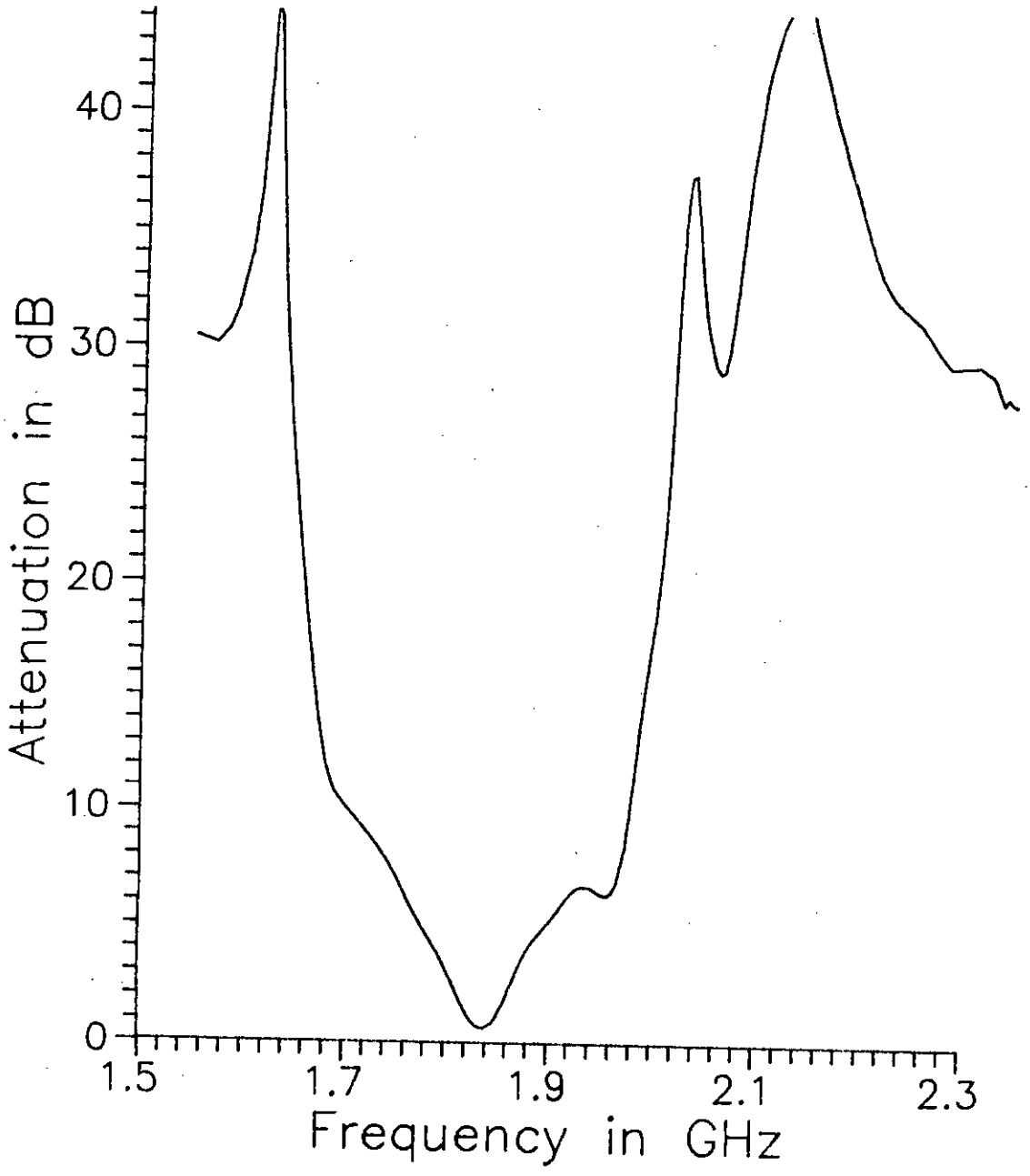

Fig 7.6 Insertion loss characteristics of the filter for a particular adjustment of ground plates

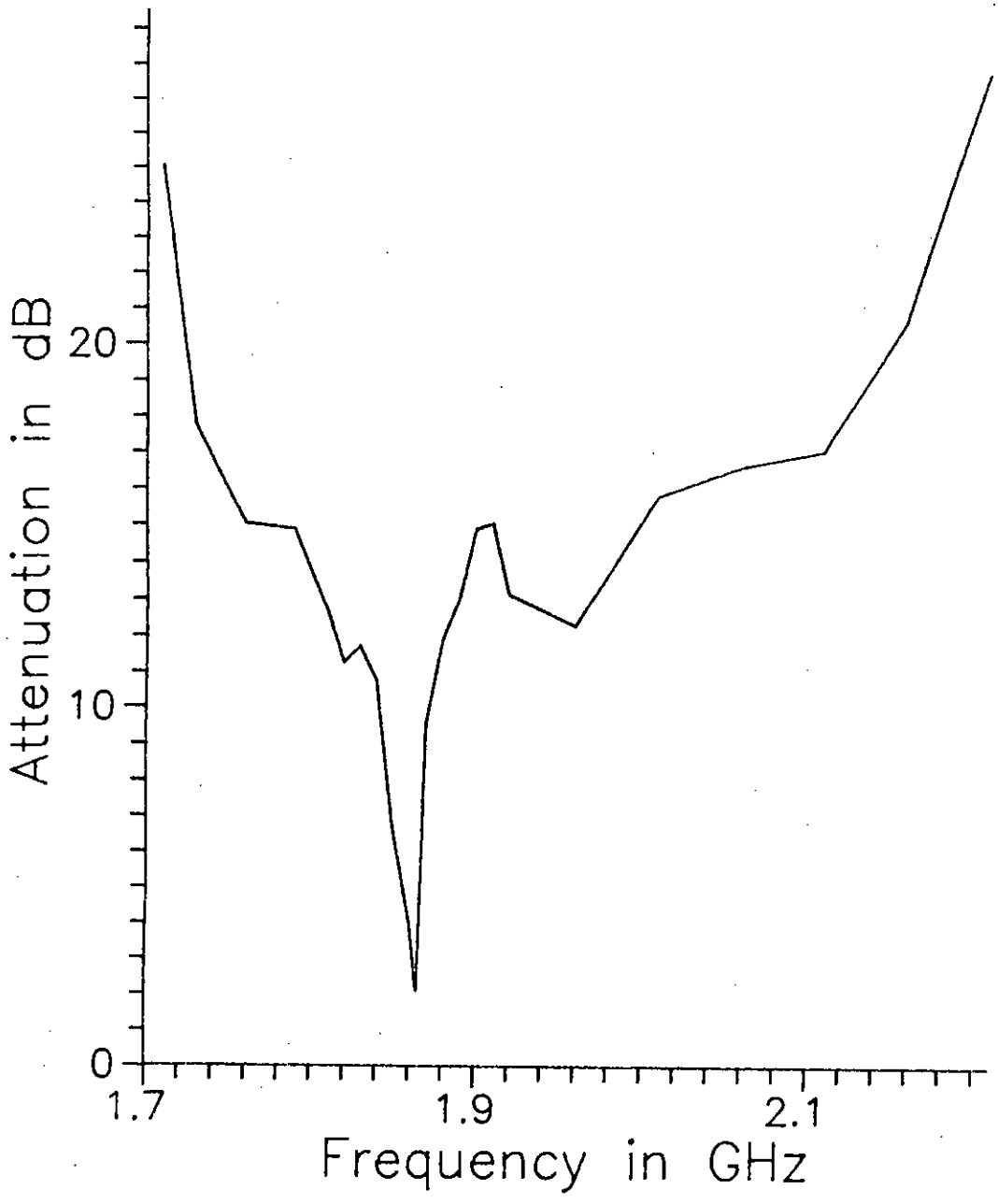

Fig 7.7(a) Experimentally obtained Insertion loss characteristics of the filter

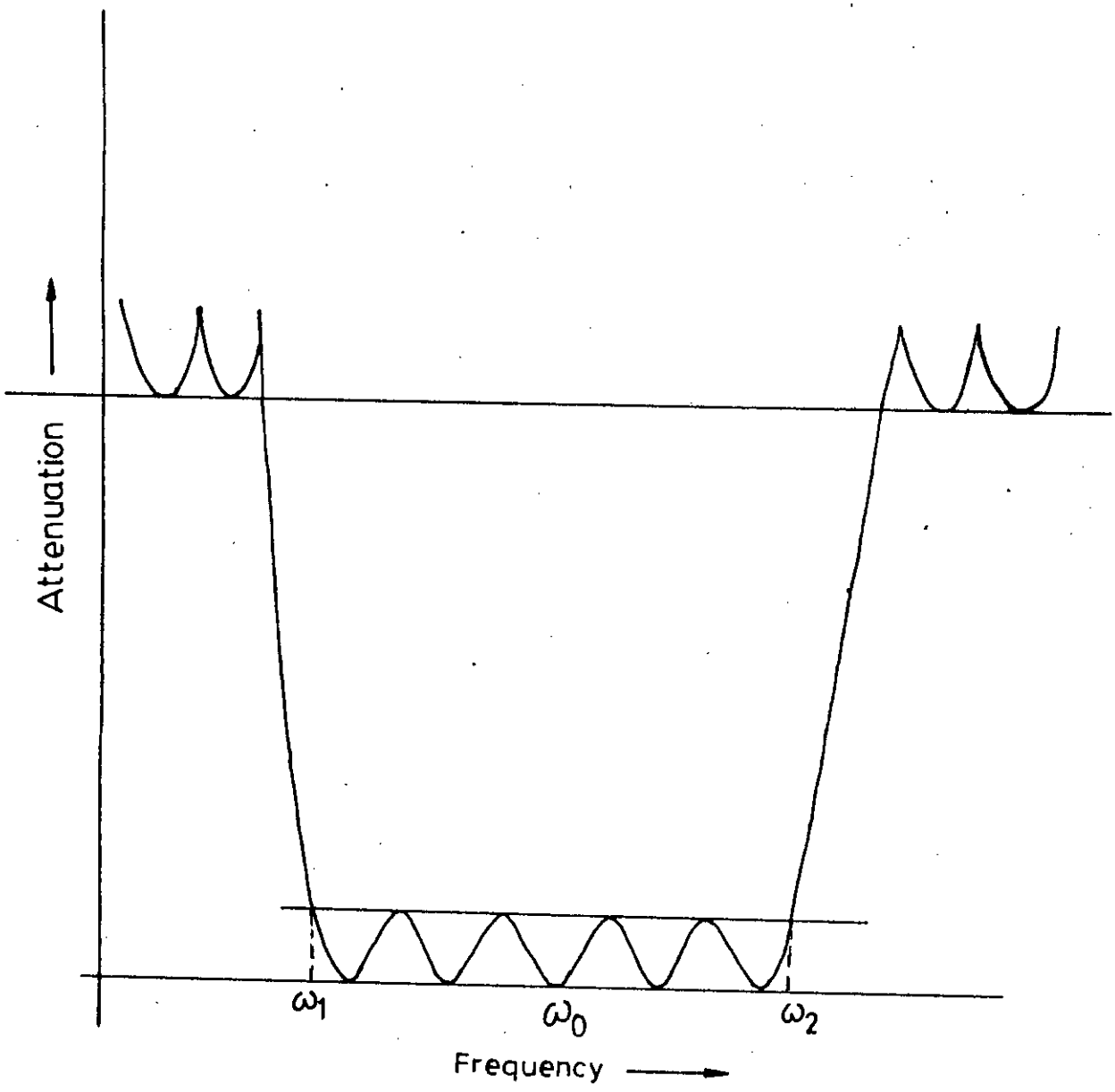

Fig. 7.7 (b) Theoretical curve for five element elliptical function band pass filter.

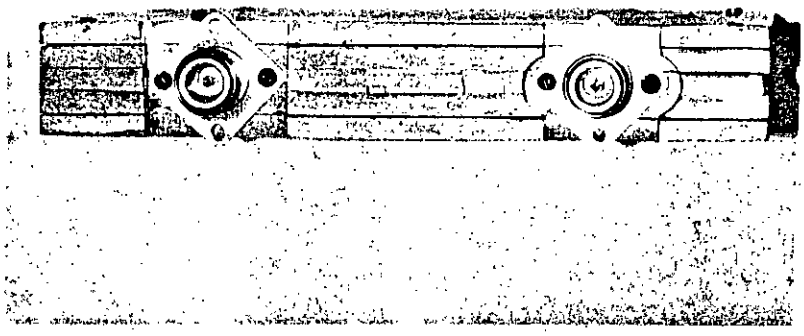

Fig 7.8(a) Top view of the constructed filter

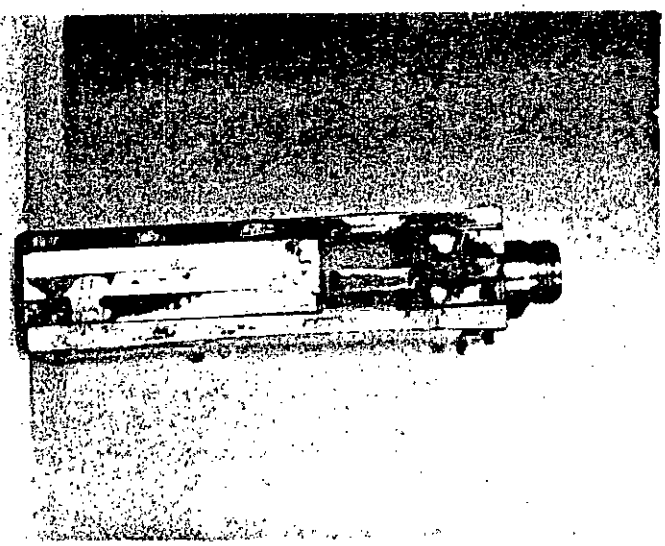

Fig 7.8(b) Side view of the constructed filter

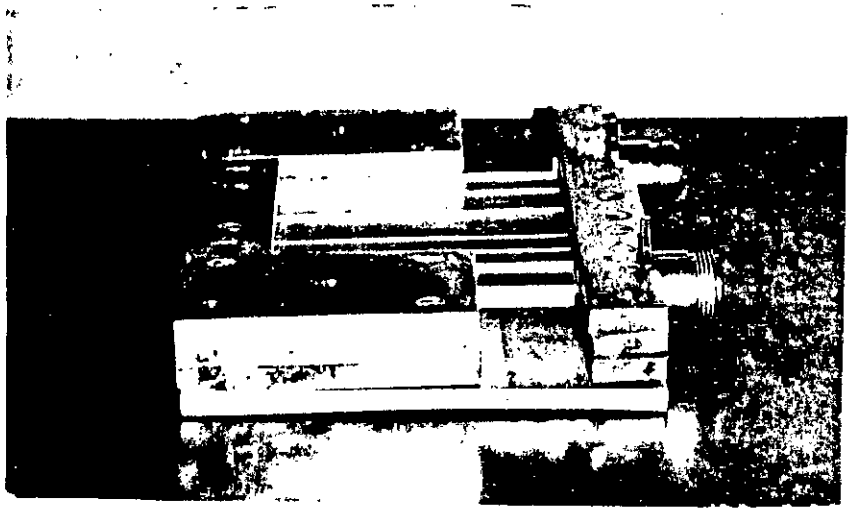

Fig 7.8(c) Lateral view of the constructed filter with top plate removed

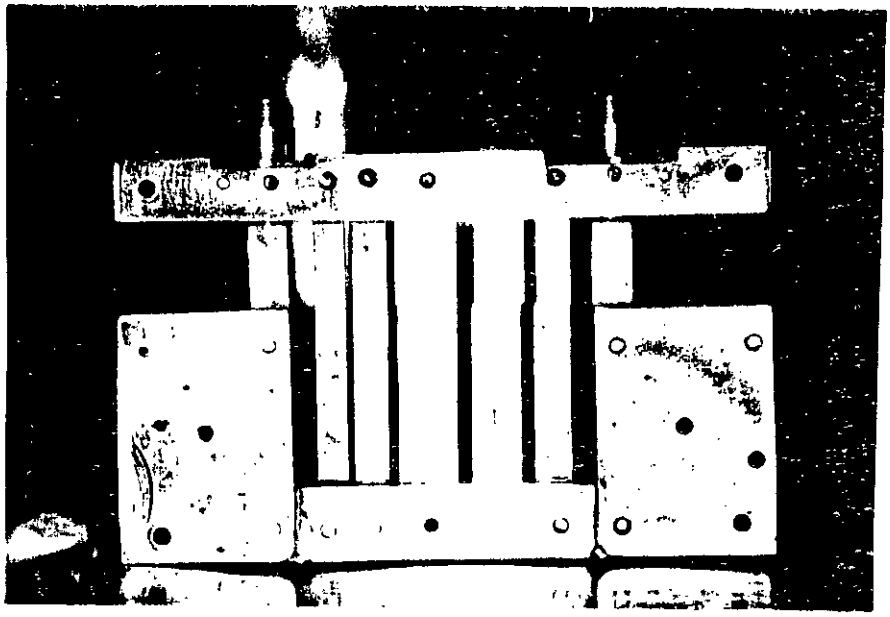

Fig 7.8(d) Front view of the constructed filter with top and bottom plates removed

This action causes the output from the oscillator inside the power meter to decrease to accomodate the external r.f. power through the thermistor element. The meter circuit inside the power meter measures the amount of this power decrease from the oscillator of the power meter and displays the results of measurement over a calibrated scale as the power increases due to the external r.f. source. This power is taken as the input power. Then the constructed filter is inserted in between the r.f. power source and the thermistor mount. The power now indicated by the power meter is taken as the output power. The above procedure was carried out repeatedly at different frequencies over the pass band. Finally the ratio of output power to input power was determined and the insertion loss was calculated in dB. Following the above procedure, a set of reading was taken with the experimental filter which has been given in appendix-D. The curve of attenuation vs. frequency is plotted using this set of reading in figure 7.7.

The insertion loss characteristics of the constructed filter was also obtained from hp-8510B network analyzer. The network analyzer gives directly the insertion loss characteristic curve in attenuation (dB) vs. frequency when the filter is connected between port 1 and port 2 of the network. The insertion loss characteristic curves as were obtained from the network analyzer are given in figures

(7.3(a), (b) and (7.4) Also figures (7.5) and (7.6) give the insertion loss characteristics of the same filter for different adjustments of the ground plates. So it is obvious that spacing of the ground plates from the center plate plays an important role in determining the characteristics of these types of filters.

7.4 **Summary**: The method of fabrication of the designed filter has been discussed in this chapter. Operation of the measuring devices has been described in short. The insertion loss characteristic curves of the filter have been obtained both from experimental data and from the network analyzer.

CHAPTER 8

Discussions and suggestions for future work

Discussions: A method of designing microwave band pass filter using half wave digital TEM lines have been presented in this work. In this method a low pass prototype filter has been transformed in to a distributed band-pass filter. The distributed band-pass filter has both series and shunt resonant elements. Using frequency transformation and static capacitance matrices these resonators have been converted to equivalent network of the band pass filter in the form of coupled half wave digital TEM lines. Using the design procedure developed, a band pass filter has been constructed for a center frequency of 2000 MHz with 1% bandwidth i.e. 20 MHz. The filter has been designed to have maximum pass band attenuation of 0.044 dB. The insertion loss characteristic curve as obtained from the network analyzer is given in figure (7.3(a). It was found that the center frequency has shifted to 1923.285 MHz and pass band width has increased to about 85 MHz. Figure (7.3(b) gives the same curve within a shorter span of frequency. Figure (7.4) shows the extended plot of the pass band to have a better look at the pass band ripples. The pass band attenuation as seen from figure (7.3(a) is about 1.1 dB. Figure (7.5) and (7.6) give the characteristic curves from the network analyzer for two different adjustments of the upper

ground plate of the filter. The center frequency in figure 7.5 has occured at about 1910 MHz but the bandwidth became much larger than expected. In figure 7.6, the center frequency has further shifted to a value of about 1850 MHz and bandwidth still larger than before. In figure 7.7(a) the characteristic curve has been obtained by plotting the experimental data. It was found from this curve that the center frequency has occured at around 1905 MHz and the bandwidth about 80 MHz. Maximum pass band attenuation was about 2 dB. So it is observed that the maximum pass band attenuation is more than the theoretically predicted value and the center frequency has increased by about 3.8% and the bandwidth has also increased substantially. Figure 7.7(b) shows the expected theoretical characteristic curve of an elliptic function band-pass filter.

The filter was constructed by cutting and machining brass plates. A high degree of accuracy in physical dimension is required for the construction of this type of filters. Introduction of inaccuracy to physical dimension of resonator or transformer element highly influences the overall performance of the filter characteristic. Also the position of the ground plate greatly influences the characteristics as was seen from the curves in figures 7.5 and 7.6 obtained from network analyzer. The length of the resonator elements influences the center frequency of the filter. If the length is increased the center frequency will decrease and vice versa. Probably this was the reason behind the shifting of the center frequency.

Another reason of introduction of error in dimensions is the reading of Getsinger's chart. Curves of ΔC vs. s/b in figure 5.2 shows that a change in the spacing between the lines causes considerable change in mutual capacitance between lines (ΔC). Moreover the curves are given for t/b=0, 0.025, 0.05, 0.10, 0.20, 0.40, 0.60, 0.80; whereas the present filter was designed for t/b=0.30 which was not supplied by Getsinger's chart. As a result the ΔC vs. s/b curve for t/b=0.30 has to be drawn by averaging the two curves for t/b=0.20 and t/b=0.40. All physical dimensions were then calculated using this newly drawn curve for t/b=0.30. It was very much likely that the readings taken from this curve were erroneous. On the other hand, lack of precision cutting, machining and joining the small parts together introduced some error in the interbar spacings. This causes a change in the value of mutual capacitance which in tern causes a change in the response of the filter.

Next, the setting of input and output connectors to the respective transformer elements was also a precision job. Due to the unavailability of two identical connectors to connect the filter to the network analyzer, two different types of connectors were used at the two ports of the filter which might have changed the characteristic impedance of 50 ohm of the filter. In fact, the difficulties faced in machining and setting made it almost impossible to maintain a high degree of accuracy at those connections. As a result impedance mismatch might have occured at the input and output ports. This type of impedance mismatch is

very much unwanted because it increases the loss in the pass band. At the same time loss of power in the connectors itself increases the attenuation in the pass band. Theoretically this type of filters should be constructed with materials having infinite conductivity. The brass plates were purchased from the local market which were not meant for this type of work. This impurity of material may cause some deviation in filter characteristics.

This type of elliptic function filter is constructed from resonator elements grounded at both ends which make this filter superior over the filters with resonators grounded at one end. Because the free ends of the resonators of the later type are prone to bend due to mechanical shock or rough handling. But the present filter is free from that problem because of its solid binding at both ends of the resonators.

REFERENCES

[1] *S. B. Cohn*, "**Microwave filters, an advancing art**", IEEE Transactions on Microwave Theory and Techniques, Vol. MTT-13, No. 5, September 1965, pp.487-488.

[2] *P. I. Richards*, "**Resistor-transmission-line circuits**", Proceedings of the IRE, Vol. 36, February 1948, pp. 217-220.

[3] *S. B. Cohn*, "**Dissipation loss in multiple-coupled-resonator filters**", Proceedings of the IRE, Vol. 47, August 1959, pp. 1342-1348.

[4] *E. G. Cristal*, "**Coupled circular cylindrical rods between parallel ground planes**", IEEE Transactions on Microwave Theory and Techniques, Vol. MTT-12, July 1964, pp. 428-439.

[5] *J. T. Bolljahn* and *G. L. Matthaei*, "**A study of the phase and filter properties of arrays of parallel conductors between ground planes**", Proceedings of the IRE, Vol. 50, March 1962, pp. 299-311.

[6] *G. L. Matthaei*, "**Interdigital band-pass filters**", IRE Transactions on Microwave Theory and Techniques, Vol. MTT-10, November 1962, pp. 479-491.

[7] *W. J. Getsinger*, "**Coupled rectangular bars between parallel plates**", IRE Transactions on Microwave Theory and Techniques, PGMTT-10, January 1962, pp. 65-72.

[8] *G. L. Matthaei*, "**Comb-line band-pass filters of narrow or moderate bandwidth**", Microwave Journal, Vol. 6, August 1963, pp. 82-91.

[9] *R. J. Wenzel*, "**Exact theory of interdigital band-pass filters and related coupled structures**", IEEE Transactions on Microwave Theory and Techniques, Vol. MTT-13, No. 5, September 1965, pp. 559-575.

[10] *R. J. Wenzel*, "**Theoretical and practical applications of capacitance matrix transformations to TEM network design**", IEEE Transactions on Microwave Theory and Techniques, Vol. MTT-14, No. 12, December 1966, pp. 635-647.

[11] *M. C. Horton* and *R. J. Wenzel*, "**The digital elliptic filter - a compact sharp-cutoff design for wide band-stop or band-pass requirements**", IEEE Transactions on Microwave Theory and Techniques, Vol. MTT-15, No. 5, May 1967, pp. 307-314.

[12] *R. Levy* and *I. Whiteley*, "**Synthesis of distributed elliptic-function filters from lumped-constant prototypes**", IEEE Transactions on Microwave Theory and Techniques, Vol. MTT-14, No. 11, November 1966, 506-517.

[13] *J. D. Rhodes*, "**The half-wave stepped digital elliptic filter**", IEEE Transactions on Microwave Theory and Techniques, Vol. MTT-17, No. 12, December 1969, pp. 1102-1107.

[14] *G. L. Matthaei, L. Young, E. M. T. Jones*, "**Microwave filters, impedance matching networks and coupling structures**", McGraw Hill, New York, 1964, pp. 38-39, 49-52, 83-84, 174-197.

[15] *S. B. Cohn*, "**Thickness corrections for capacitive obstacles and strip conductors**", IRE Transactions on Microwave Theory and Techniques, PGMTT-8, 6, November 1960, pp. 638-644.

[16] *R. Saal*, "**Der Entwarf Von Filtern Mit Hilfe Des Kataloges Normierter Tiefpasse**", Germany, Telefunken, Backnay/Wurtemberg, W., GmbH, 1964.

APPENDIX A

FORTRAN PROGRAM FOR COMPUTATION OF STATIC CAPACITANCE MATRICES FROM LOW-PASS PROTOTYPE ELEMENT VALUES

```
************************************************************************
*                        PROGRAM FOR                                   *
*      HALF WAVE STEPPED DIGITAL ELLIPTIC FILTER                       *
************************************************************************
      REAL L2P,L2M,L4P,L4M,M2,M4

      OPEN(9, FILE='FLTR')

      WRITE(9,*)'DETERMINATION OF CHARACTERISTIC ADMITTANCE '

      WRITE(9,*)'MATRICES FOR A 5 ELEMENT STEPPED DIGITAL'

      WRITE(9,*)'ELLIPTIC FILTER'

      WRITE(9,*)

      WRITE(9,*)'SPECIFICATIONS GIVEN ARE:'

      V=1.2222

      S=60.1

      WRITE(9,20) V,S

 20   FORMAT(/'VSWR= ',F10.3,2X,'STOPBAND LEVEL= ',F10.3)

************************************************************************
*                    MAXIMUM PASSBAND ATTENUATION                      *
************************************************************************
      RHO=(V-1.0)/(V+1.0)

      AMAX=-10.0*(ALOG10(1.0-RHO**2))

      WRITE(9,*)

      WRITE(9,30) AMAX

 30   FORMAT(/'MAX PASSBAND ATTN AS CALCULATED FROM VSWR IS',

     + F10.3,2X,'DB')

************************************************************************
*                    LOWPASS PROTOTYPE ELEMENT VALUES                  *
************************************************************************
      WRITE(9,*)
```

```
      WRITE(9,*)'LOWPASS PROTOTYPE ELEMENT VALUES ARE:'
      WRITE(9,*)
      C1=0.9265
      C2=0.05866
      C3=1.666
      C4=0.1607
      C5=0.8363
      M2=3.611883
      M4=2.303827
      WRITE(9,40)C1,C2,C3
 40   FORMAT(/'C1=',F7.4,2X,'C2=',F7.4,2X,'C3=',F7.4)
      WRITE(9,50)C4,C5
 50   FORMAT(/'C4=',F7.4,2X,'C5=',F7.4)
      WRITE(9,60)M2,M4
 60   FORMAT(/'M2=',F7.4,2X,'M4=',F7.4)
*************************************************************************
*      CENTER FREQUENCY, EDGE FREQUENCIES, PASSBAND, % BANDWIDTH        *
*************************************************************************
      F0=2000.0
      PB=20.0
      F1=(2.0*F0-PB)/2.0
      F2=(2.0*F0+PB)/2.0
      PBW=100.0*PB/F0
      WRITE(9,70)F0,PB,PBW,F1,F2
 70   FORMAT(/'CENTER FREQUENCY OF THE FILTER = ',F9.3,2X,'MHZ',
     + /'PASSBAND=',F9.3,2X,'MHZ ,',2X,'% BANDWIDTH=',F9.3,2X,'%',
     + /'PASSBAND EDGE FREQUENCIES ARE: F1=',F9.3,2X,'F2=',F9.3)
      WRITE(9,*)
```

```
*****************************************************************
*                  STEPPED IMPEDANCE PLANE (THETA0)             *
*****************************************************************
      PI=4.0*ATAN(1.0)

      THETA0=PI/3.0

      WRITE(9,80)THETA0

 80   FORMAT(/'CHOSEN STEPPED IMPEDANCE PLANE=THETA0=',F7.3,2X,'RAD')

      WRITE(9,*)

      X1=2.0*F0*SIN(2.0*THETA0)

      X2=4.0*THETA0*PB

      A=X1/X2

      WRITE(9,90)A

 90   FORMAT(/'CALCULATED BANDWIDTH SCALING FACTOR= ',F7.3)

*****************************************************************
*                     CALCULATION OF WAVELENGTH                 *
*****************************************************************
      B=2.0*A*THETA0*(ABS(TAN(THETA0)))/PI

      AB=M2*0.5/A

      BC=M4*0.5/A

      L2P=SQRT(AB**2+1.0)+AB

      L2M=SQRT(AB**2+1.0)-AB

      L4P=SQRT(BC**2+1.0)+BC

      L4M=SQRT(BC**2+1.0)-BC

      WRITE(9,*)

      WRITE(9,110)L2P,L2M,L4P,L4M

 110  FORMAT(/'LAMBDA2+=',F7.3,2X,'LAMBDA2-=',F7.3,2X,
     + 'LAMBDA4+=',F7.3,/'LAMBDA4-=',F7.3)

      WRITE(9,*)
```

```
*****************************************************************
*          CHARACTERISTIC ADMITTANCE MATRIX (NETWORK 1)         *
*****************************************************************
      Z=0.5*PI/THETA0

      Y11=1.0

      Y12=-1.0

      Y22=B*(C1+C2*(1.0+L2M**2+Z*(L2P**2-L2M**2)))

      Y23=Y22-B*C1

      Y33=B*C2*(2.0+L2M**2+L2P**2)

      Y34=B*C2*(1.0+L2P**2+Z*(L2M**2-L2P**2))

      Y45=B*C4*(1.0+L4M**2+Z*(L4P**2-L4M**2))

      Y44=B*C3+Y34+Y45

      Y55=B*C4*(2.0+L4M**2+L4P**2)

      Y56=B*C4*(1.0+L4P**2+Z*(L4M**2-L4P**2))

      Y66=B*(C5+C4*(1.0+L4P**2+Z*(L4M**2-L4P**2)))

      Y67=-1.0

      Y77=1.0

      Y=0.0

      WRITE(9,*)

      WRITE(9,*)'THE CHARACTERISTIC ADMITTANCE MATRIX'

      WRITE(9,*)'OF NETWORK 1 IS (WITHOUT SCALING):'

      WRITE(9,*)

      WRITE(9,100)Y22,-Y23,Y,Y,Y

      WRITE(9,100)-Y23,Y33,-Y34,Y,Y

      WRITE(9,100)Y,-Y34,Y44,-Y45,Y

      WRITE(9,100)Y,Y,-Y45,Y55,-Y56

      WRITE(9,100)Y,Y,Y,-Y56,Y66

  100 FORMAT(5(F8.4,2X))
```

```
*****************************************************************************
*       AUGMENTED CHARACTERISTIC ADMITTANCE MATRIX (NETWORK 1)              *
*****************************************************************************
      WRITE(9,*)
      WRITE(9,*)'THE AUGMENTED CHARACTERISTIC MATRIX OF NETWORK 1'
      WRITE(9,*)'AFTER ADDING A  UNIT ELEMENT TO EACH  END OF NETWORK
1:'
      WRITE(9,*)
      Y22=Y22+1.0
      Y66=Y66+1.0
      WRITE(9,10)Y11,Y12,Y,Y,Y,Y,Y
      WRITE(9,10)Y12,Y22,-Y23,Y,Y,Y,Y
      WRITE(9,10)Y,-Y23,Y33,-Y34,Y,Y,Y
      WRITE(9,10)Y,Y,-Y34,Y44,-Y45,Y,Y
      WRITE(9,10)Y,Y,Y,-Y45,Y55,-Y56,Y
      WRITE(9,10)Y,Y,Y,Y,-Y56,Y66,Y67
      WRITE(9,10)Y,Y,Y,Y,Y,Y67,Y77
   10 FORMAT(7(F8.4,1X))
*****************************************************************************
*            CHARACTERISTIC ADMITTANCE MATRIX (NETWORK 2)                   *
*****************************************************************************
      WRITE(9,*)
      WRITE(9,*)'CHARACTERISTIC ADMITTANCE MATRIX FOR NETWORK 2:'
      WRITE(9,*)'(WITHOUT SCALING)'
      WRITE(9,*)
      Z11=B*(C1+C2*(1.0+L2M**2))
      Z12=Z11-B*C1
      Z22=B*C2*(2.0+L2M**2+L2P**2)
      Z23=B*C2*(1.0+L2P**2)
```

```
      Z34=B*C4*(1.0+L4M**2)
      Z33=B*C3+Z23+Z34
      Z44=B*C4*(2.0+L4M**2+L4P**2)
      Z45=B*C4*(1.0+L4P**2)
      Z55=B*(C5+C4*(1.0+L4P**2))
      WRITE(9,*)
      WRITE(9,120)Z11,-Z12,Y,Y,Y
      WRITE(9,120)-Z12,Z22,-Z23,Y,Y
      WRITE(9,120)Y,-Z23,Z33,-Z34,Y
      WRITE(9,120)Y,Y,-Z34,Z44,-Z45
      WRITE(9,120)Y,Y,Y,-Z45,Z55
 120  FORMAT(5(F8.4,2X))
*************************************************************************
*        FIRST MODIFICATION OF ADMITTANCE MATRIX : NETWORK 1            *
*************************************************************************
      R=1.0/SQRT(B)
      Y22=Y22*R*R
      Y12=Y12*R
      Y23=Y23*R
      Y66=Y66*R*R
      Y67=Y67*R
      Y56=Y56*R
      WRITE(9,*)
      WRITE(9,*)'FIRST MODIFICATION OF ADMITTANCE MATRIX :
     + NETWORK 1'
      WRITE(9,*)
      WRITE(9,200)Y11,Y12,Y,Y,Y,Y,Y
      WRITE(9,200)Y12,Y22,-Y23,Y,Y,Y,Y
```

```
      WRITE(9,200)Y,-Y23,Y33,-Y34,Y,Y,Y
      WRITE(9,200)Y,Y,-Y34,Y44,-Y45,Y,Y
      WRITE(9,200)Y,Y,Y,-Y45,Y55,-Y56,Y
      WRITE(9,200)Y,Y,Y,Y,-Y56,Y66,Y67
      WRITE(9,200)Y,Y,Y,Y,Y,Y67,Y77
  200 FORMAT(7(F8.4,1X))
*****************************************************************
*        FIRST MODIFICATION OF ADMITTANCE MATRIX : NETWORK 2     *
*****************************************************************
      Z11=Z11*R*R
      Z12=Z12*R
      Z45=Z45*R
      Z55=Z55*R*R
      WRITE(9,*)
      WRITE(9,*)'FIRST MODIFICATION OF ADMITTANCE MATRIX :
     + NETWORK 2'
      WRITE(9,*)
      WRITE(9,210)Z11,-Z12,Y,Y,Y
      WRITE(9,210)-Z12,Z22,-Z23,Y,Y
      WRITE(9,210)Y,-Z23,Z33,-Z34,Y
      WRITE(9,210)Y,Y,-Z34,Z44,-Z45
      WRITE(9,210)Y,Y,Y,-Z45,Z55
  210 FORMAT(5(F8.4,2X))
*****************************************************************
*        SECOND MODIFICATION OF ADMITTANCE MATRIX : NETWORK 1    *
*****************************************************************
      F1=SQRT(Y22*1.2/Y33)
      B1=SQRT(Y66*1.2/Y55)
      Y33=Y33*F1*F1
```

```
      Y23=Y23*F1
      Y34=Y34*F1
      Y55=Y55*B1*B1
      Y56=Y56*B1
      Y45=Y45*B1
      F2=SQRT(Y33*1.2/Y44)
      Y44=Y44*F2*F2
      Y34=Y34*F2
      Y45=Y45*F2
      WRITE(9,*)
      WRITE(9,*)'SECOND MODIFICATION OF ADMITTANCE MATRIX :
     + NETWORK 1'
      WRITE(9,*)
      WRITE(9,300)Y11,Y12,Y,Y,Y,Y,Y
      WRITE(9,300)Y12,Y22,-Y23,Y,Y,Y,Y
      WRITE(9,300)Y,-Y23,Y33,-Y34,Y,Y,Y
      WRITE(9,300)Y,Y,-Y34,Y44,-Y45,Y,Y
      WRITE(9,300)Y,Y,Y,-Y45,Y55,-Y56,Y
      WRITE(9,300)Y,Y,Y,Y,-Y56,Y66,Y67
      WRITE(9,300)Y,Y,Y,Y,Y,Y67,Y77
  300 FORMAT(7(F8.4,1X))
*************************************************************************
*       SECOND MODIFICATION OF ADMITTANCE MATRIX : NETWORK 2            *
*************************************************************************
      F1=SQRT(Z11*1.2/Z22)
      Z22=Z22*F1*F1
      Z12=Z12*F1
      Z23=Z23*F1
```

```
      B1=SQRT(Z55*1.2/Z44)
      Z44=Z44*B1*B1
      Z34=Z34*B1
      Z45=Z45*B1
      F2=SQRT(Z22*1.2/Z33)
      Z33=Z33*F2*F2
      Z23=Z23*F2
      Z34=Z34*F2
      WRITE(9,*)
      WRITE(9,*)'SECOND MODIFICATION OF ADMITTANCE MATRIX :
     + NETWORK 2'
      WRITE(9,*)
      WRITE(9,400)Z11,-Z12,Y,Y,Y
      WRITE(9,400)-Z12,Z22,-Z23,Y,Y
      WRITE(9,400)Y,-Z23,Z33,-Z34,Y
      WRITE(9,400)Y,Y,-Z34,Z44,-Z45
      WRITE(9,400)Y,Y,Y,-Z45,Z55
  400 FORMAT(5(F8.4,1X))
*****************************************************************
*              STATIC CAPACITANCE MATRIX OF NETWORK 1           *
*****************************************************************
      E=377.7/50
      Y11=Y11*E
      Y12=Y12*E
      Y22=Y22*E
      Y23=Y23*E
      Y33=Y33*E
      Y34=Y34*E
```

```
      Y44=Y44*E
      Y45=Y45*E
      Y55=Y55*E
      Y56=Y56*E
      Y66=Y66*E
      Y67=Y67*E
      Y77=Y77*E
      WRITE(9,*)
      WRITE(9,*)'STATIC CAPACITANCE MATRIX OF NETWORK 1'
      WRITE(9,*)
      WRITE(9,500)Y11,Y12,Y,Y,Y,Y,Y
      WRITE(9,500)Y12,Y22,-Y23,Y,Y,Y,Y
      WRITE(9,500)Y,-Y23,Y33,-Y34,Y,Y,Y
      WRITE(9,500)Y,Y,-Y34,Y44,-Y45,Y,Y
      WRITE(9,500)Y,Y,Y,-Y45,Y55,-Y56,Y
      WRITE(9,500)Y,Y,Y,Y,-Y56,Y66,Y67
      WRITE(9,500)Y,Y,Y,Y,Y,Y67,Y77
  500 FORMAT(7(F8.4,1X))
*****************************************************************
*              STATIC CAPACITANCE MATRIX OF NETWORK 2           *
*****************************************************************
      Z11=Z11*E
      Z12=Z12*E
      Z22=Z22*E
      Z23=Z23*E
      Z33=Z33*E
      Z34=Z34*E
      Z44=Z44*E
```

```
      Z45=Z45*E
      Z55=Z55*E
      WRITE(9,*)
      WRITE(9,*)'STATIC CAPACITANCE MATRIX OF NETWORK 2'
      WRITE(9,*)
      WRITE(9,600)Z11,-Z12,Y,Y,Y
      WRITE(9,600)-Z12,Z22,-Z23,Y,Y
      WRITE(9,600)Y,-Z23,Z33,-Z34,Y
      WRITE(9,600)Y,Y,-Z34,Z44,-Z45
      WRITE(9,600)Y,Y,Y,-Z45,Z55
  600 FORMAT(5(F8.4,1X))
*************************************************************************
*            NORMALIZED CAPACITANCE VALUES OF NETWORK  1                *
*************************************************************************
      WRITE(9,*)
      WRITE(9,*)'NORMALIZED CAPACITANCE VALUES OF NETWORK 1'
      WRITE(9,*)
      WRITE(9,610)Y11+Y12
      WRITE(9,620)-Y12
      WRITE(9,610)Y22+Y12-Y23
      WRITE(9,620)Y23
      WRITE(9,610)Y33-Y23-Y34
      WRITE(9,620)Y34
      WRITE(9,610)Y44-Y34-Y45
      WRITE(9,620)Y45
      WRITE(9,610)Y55-Y45-Y56
      WRITE(9,620)Y56
      WRITE(9,610)Y66-Y56+Y67
```

```
      WRITE(9,620)-Y67
      WRITE(9,610)Y77+Y67
  610 FORMAT(F8.4)
  620 FORMAT(8X,F8.4)
*****************************************************************
*            NORMALIZED CAPACITANCE VALUES OF NETWORK 2         *
*****************************************************************
      WRITE(9,*)
      WRITE(9,*)'NORMALIZED CAPACITANCE VALUES OF NETWORK 2'
      WRITE(9,*)
      WRITE(9,710)Z11-Z12
      WRITE(9,720)Z12
      WRITE(9,710)Z22-Z12-Z23
      WRITE(9,720)Z23
      WRITE(9,710)Z33-Z23-Z34
      WRITE(9,720)Z34
      WRITE(9,710)Z44-Z34-Z45
      WRITE(9,720)Z45
      WRITE(9,710)Z55-Z45
  710 FORMAT(F8.4)
  720 FORMAT(8X,F8.4)
      STOP
      END
*****************************************************************
*****************************************************************
```

APPENDIX B

RESULT OF THE COMPUTER PROGRAM

DETERMINATION OF CHARACTERISTIC ADMITTANCE

MATRICES FOR A 5 ELEMENT STEPPED DIGITAL

ELLIPTIC FILTER

SPECIFICATIONS GIVEN ARE:

VSWR= 1.222 STOPBAND LEVEL= 60.100

MAX PASSBAND ATTN AS CALCULATED FROM VSWR IS 0.044 DB

LOWPASS PROTOTYPE ELEMENT VALUES ARE:

C1= 0.9265 C2= 0.0587 C3= 1.6660

C4= 0.1607 C5= 0.8363

M2= 3.6119 M4= 2.3038

CENTER FREQUENCY OF THE FILTER = 2000.000 MHZ

PASSBAND= 20.000 MHZ , % BANDWIDTH= 1.000 %

PASSBAND EDGE FREQUENCIES ARE: F1= 1990.000 F2= 2010.000

CHOSEN STEPPED IMPEDANCE PLANE=THETA0= 1.047 RAD

CALCULATED BANDWIDTH SCALING FACTOR= 41.350

LAMBDA2+= 1.045 LAMBDA2-= 0.957 LAMBDA4+= 1.028

LAMBDA4-= 0.973

THE CHARACTERISTIC ADMITTANCE MATRIX OF NETWORK 1

(WITHOUT SCALING):

50.3392	-6.1021	0.0000	0.0000	0.0000
-6.1021	11.2246	-5.1225	0.0000	0.0000
0.0000	-5.1225	100.8811	-16.2130	0.0000
0.0000	0.0000	-16.2130	30.7153	-14.5023
0.0000	0.0000	0.0000	-14.5023	54.4327

THE AUGMENTED CHARACTERISTIC MATRIX OF NETWORK 1

AFTER ADDING A UNIT ELEMENT TO EACH END OF NETWORK 1:

1.0000	-1.0000	0.0000	0.0000	0.0000	0.0000	0.0000
-1.0000	51.3392	-6.1021	0.0000	0.0000	0.0000	0.0000
0.0000	-6.1021	11.2246	-5.1225	0.0000	0.0000	0.0000
0.0000	0.0000	-5.1225	100.8811	-16.2130	0.0000	0.0000
0.0000	0.0000	0.0000	-16.2130	30.7153	-14.5023	0.0000
0.0000	0.0000	0.0000	0.0000	-14.5023	55.4327	-1.0000
0.0000	0.0000	0.0000	0.0000	0.0000	-1.0000	1.0000

CHARACTERISTIC ADMITTANCE MATRIX FOR NETWORK 2: (WITHOUT SCALING)

49.6045	-5.3674	0.0000	0.0000	0.0000
-5.3674	11.2246	-5.8572	0.0000	0.0000
0.0000	-5.8572	100.3328	-14.9300	0.0000
0.0000	0.0000	-14.9300	30.7153	-15.7853
0.0000	0.0000	0.0000	-15.7853	55.7157

FIRST MODIFICATION OF ADMITTANCE MATRIX : NETWORK 1

1.0000	-0.1447	0.0000	0.0000	0.0000	0.0000	0.0000
-0.1447	1.0752	-0.8831	0.0000	0.0000	0.0000	0.0000
0.0000	-0.8831	11.2246	-5.1225	0.0000	0.0000	0.0000
0.0000	0.0000	-5.1225	100.8811	-16.2130	0.0000	0.0000
0.0000	0.0000	0.0000	-16.2130	30.7153	-2.0988	0.0000
0.0000	0.0000	0.0000	0.0000	-2.0988	1.1610	-0.1447
0.0000	0.0000	0.0000	0.0000	0.0000	-0.1447	1.0000

FIRST MODIFICATION OF ADMITTANCE MATRIX : NETWORK 2

1.0389	-0.7768	0.0000	0.0000	0.0000
-0.7768	11.2246	-5.8572	0.0000	0.0000
0.0000	-5.8572	100.3328	-14.9300	0.0000
0.0000	0.0000	-14.9300	30.7153	-2.2845
0.0000	0.0000	0.0000	-2.2845	1.1669

SECOND MODIFICATION OF ADMITTANCE MATRIX : NETWORK 1

1.0000	-0.1447	0.0000	0.0000	0.0000	0.0000	0.0000
-0.1447	1.0752	-0.2994	0.0000	0.0000	0.0000	0.0000
0.0000	-0.2994	1.2903	-0.2152	0.0000	0.0000	0.0000
0.0000	0.0000	-0.2152	1.5484	-0.4278	0.0000	0.0000
0.0000	0.0000	0.0000	-0.4278	1.3932	-0.4470	0.0000
0.0000	0.0000	0.0000	0.0000	-0.4470	1.1610	-0.1447
0.0000	0.0000	0.0000	0.0000	0.0000	-0.1447	1.0000

SECOND MODIFICATION OF ADMITTANCE MATRIX : NETWORK 2

1.0389	-0.2589	0.0000	0.0000	0.0000
-0.2589	1.2467	-0.2384	0.0000	0.0000
0.0000	-0.2384	1.4960	-0.3893	0.0000
0.0000	0.0000	-0.3893	1.4003	-0.4878
0.0000	0.0000	0.0000	-0.4878	1.1669

STATIC CAPACITANCE MATRIX OF NETWORK 1

7.5540	-1.0932	0.0000	0.0000	0.0000	0.0000	0.0000
-1.0932	8.1224	-2.2617	0.0000	0.0000	0.0000	0.0000
0.0000	-2.2617	9.7469	-1.6254	0.0000	0.0000	0.0000
0.0000	0.0000	-1.6254	11.6963	-3.2314	0.0000	0.0000
0.0000	0.0000	0.0000	-3.2314	10.5240	-3.3765	0.0000
0.0000	0.0000	0.0000	0.0000	-3.3765	8.7700	-1.0932
0.0000	0.0000	0.0000	0.0000	0.0000	-1.0932	7.5540

STATIC CAPACITANCE MATRIX OF NETWORK 2

7.8480	-1.9555	0.0000	0.0000	0.0000
-1.9555	9.4176	-1.8006	0.0000	0.0000
0.0000	-1.8006	11.3011	-2.9405	0.0000
0.0000	0.0000	-2.9405	10.5778	-3.6846
0.0000	0.0000	0.0000	-3.6846	8.8148

NORMALIZED CAPACITANCE VALUES OF NETWORK 1

6.4608

1.0932

4.7674

2.2617

5.8598

1.6254

6.8395

3.2314

3.9161

3.3765

4.3003

1.0932

6.4608

NORMALIZED CAPACITANCE VALUES OF NETWORK 2

5.8924

1.9555

5.6614

1.8006

6.5600

2.9405

3.9527

3.6846

5.1302

APPENDIX C

EXPERIMENTAL DATA OF THE FILTER CHARACTERISTICS

f in GHz	P_{in} in mW	P_{out} in mW	Attn. in dB
1.75	0.32	0.001	-25.05
1.77	0.30	0.005	-17.78
1.80	0.32	0.01	-15.05
1.83	0.31	0.01	-14.91
1.85	0.28	0.015	-12.71
1.86	0.27	0.02	-11.30
1.87	0.30	0.02	-11.76
1.88	0.30	0.025	-10.79
1.89	0.28	0.06	-6.69
1.90	0.26	0.10	-4.15
1.905	0.26	0.16	-2.11
1.91	0.27	0.03	-9.54
1.92	0.31	0.02	-11.9
1.93	0.30	0.015	-13.01
1.94	0.31	0.01	-14.91
1.95	0.32	0.01	-15.05
1.96	0.31	0.015	-13.15
2.00	0.35	0.02	-12.30
2.05	0.38	0.01	-15.80
2.10	0.46	0.01	-16.63
2.15	0.51	0.01	-17.07
2.20	0.58	0.005	-20.64
2.25	0.60	0.001	-27.78